Optimal and Adaptive Stimulation Design

Xu Zhang[1,2,3] and Sabato Santaniello[1,2,3*]

[1]*Biomedical Engineering Department, University of Connecticut;* [2]*CT Institute for the Brain and Cognitive Sciences, University of Connecticut;* [3]*Brain Research Imaging Center, University of Connecticut*

ABSTRACT

Successful stimulation therapies of the central nervous system for chronic neurological disorders have been based so far on electric pulses that have equal amplitude and are delivered at constant intervals. Recent advancements, however, have shown that irregular and time-varying sequences of pulses may be equally effective in treating chronic disease conditions. This suggests that both the temporal arrangement and the waveform of the pulses are important factors in determining the therapeutic merit of a stimulation protocol in the treatment of neurological disorders and can be used to address the tradeoff between therapeutic effectiveness, amount of charge delivered per unit of time, and efficiency of neural stimulators. Accordingly, a wide range of computational approaches have been developed to optimize this tradeoff, and novel nonregular pulse trains have been designed. Optimization, adaptive control, and machine learning have been rapidly integrated into the design process of stimulation therapies, leading to highly efficient solutions but also dramatically increasing the complexity of the design process. This chapter will review the most significant advancements in optimization-based design for neural stimulation, along with the computational challenges, methodological innovations, and the most promising clinical applications for the treatment of the central nervous system.

KEYWORDS (10 keywords)

Optimal Control, Adaptive Control, Machine Learning, Optimization, Neural Control, Computational Modeling, Deep Brain Stimulation, Movement Disorders, Epilepsy, Brain-Machine Interface.

***CORRESPONDENCE:**

Sabato Santaniello

260 Glenbrook Road, Unit 3247
University of Connecticut
Storrs, CT 06269-3247 (USA)
Tel.: +1 (860) 486-4701
Email: sabato.santaniello@uconn.edu

INTRODUCTION

Neuromodulation of the central nervous system via electrical impulses and implantable devices is a well-established therapeutic approach to treat chronic neurological conditions such as movement disorders, psychiatric disorders, epilepsy, and sensory impairment [1-4]. Despite numerous innovations introduced over the past thirty years pertaining to the technology of the implantable devices, the design of the stimulation protocol, and the selection of anatomical targets, all clinically recognized neurostimulation therapies share three common traits, i.e., they (*i*) use trains of charge-balanced pulses that are equal in duration and shape, (*ii*) aim to keep the amplitude of the electric pulses during anodic and cathodic phases as constant as possible, and (*iii*) arrange the electric pulses according to a predetermined temporal sequence that is repeated periodically. Historically, these traits originate from a common design principle, which focuses on ensuring that the pulse trains can evoke strong, periodic responses in a critical mass of neurons or axons around the location where the electrodes of the implantable device are placed [5]. Evoking a strong and repetitive response over time is expected to induce a prolonged and consistent modulation of the activity along nerves and neural ensembles, which would eventually help mitigate one or more symptoms of a chronic condition.

As converging evidence, e.g., [6-8], has recently pointed out, though, the span of stimulation protocols that can evoke a prolonged and consistent modulation of the neural activity while being safe (i.e., within regulatory safety guidelines for clinical use [9, 10]) far exceeds the set of stimulation protocols that strictly exhibit traits (*i*)-(*iii*). Furthermore, several studies have shown that significant advantages, both technologically and clinically, may be gained from relaxing traits (*i*)-(*iii*) in the design of stimulation protocols while still maintaining the therapeutic merit of the treatment via electric stimulation, e.g., see [11] for a review. Hence, interest has grown in recent years on how to design stimulation protocols that relax traits (*i*)-(*iii*).

Relaxing traits (*i*)-(*iii*), though, poses significant methodological challenges, as the admissible combinations of pulse amplitudes, shapes, and temporal patterns to be explored dramatically increase. Accordingly, a need has emerged for novel design techniques that may explore a vast space of stimulation parameter settings in a smart, efficient, and yet thorough way. Such design techniques should also provide tools to identify surely and timely the clinical merits of a stimulation protocol and to rank several stimulation protocols according to quantitative criteria, as this would steer the selection of the most promising stimulation settings. A stimulation protocol obtained as the outcome of one of these novel design techniques is defined "*optimal*" as it combines two traits, i.e., it is *feasible* (i.e., safe, and effective) and the *best* possible option according to the assigned criteria. This chapter will present the mathematical framework and several design techniques that have been recently introduced to design optimal stimulation protocols, both open loop and closed loop (i.e., adaptive).

The concept of optimality is appealing to the design of neural prostheses, especially neurostimulation systems, because it determines a significant paradigm shift in how the stimulation settings are investigated and stimulation protocols are ultimately defined. A schematic of the conceptual transition to optimal stimulation is depicted in **Figure 1**. For sake of graphical visualization, it is assumed that a stimulation protocol is uniquely defined by selecting two parameters, which are generically called x_1 and x_2. Symbols Ω and Ω_t denote the space of all pairs (x_1, x_2) that would result in viable stimulation settings, i.e., settings within established safety constrains (Fig. 1A), and the subset of parameter values that would lead to regular stimulation protocols (*inset* in Fig. 1A), respectively. Current guidelines and algorithms to program neurostimulation protocols

typically consist of (1) sampling the subset Ω_t, with the selection of samples being informed by one or more criteria derived from clinical studies, (2) testing the sampled settings in a patient to determine the resultant clinical outcomes, and (3) choosing the specific settings (e.g., *red star* in Fig. 1A) among the tested ones that may produce the most effective therapeutic outcomes.

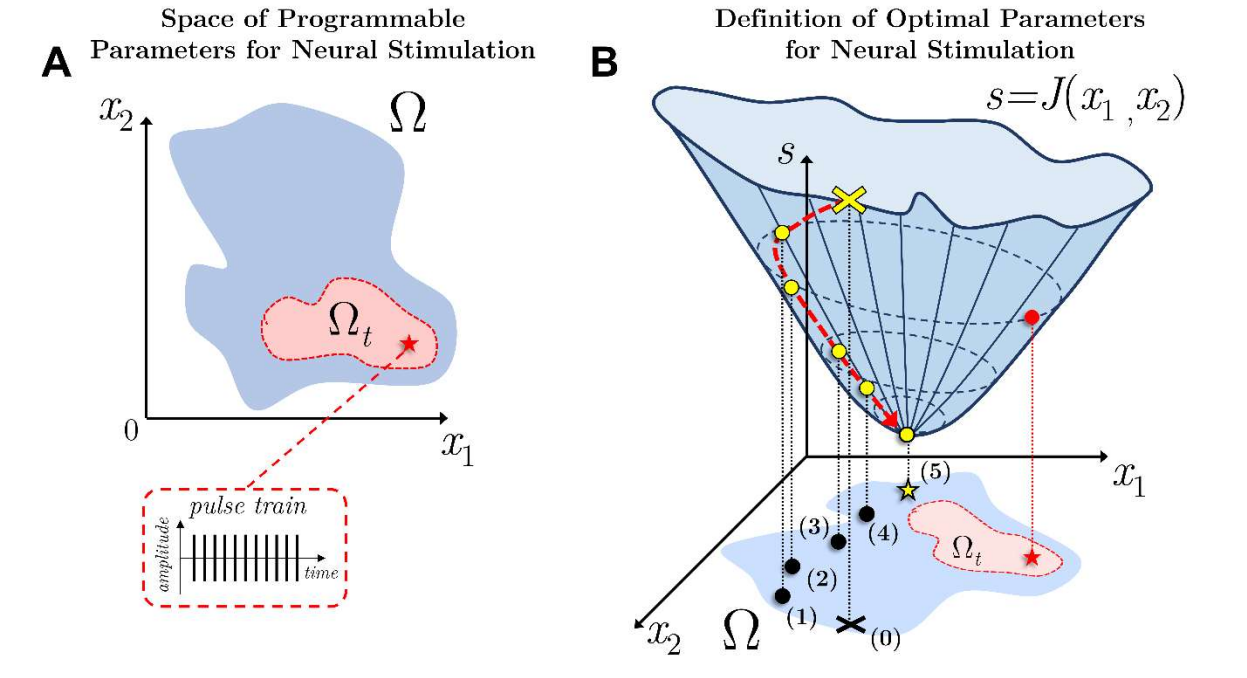

Figure 1. ***Schematic of the framework for optimal stimulation protocol design.*** **A)** Pulse sequences identify neurostimulation protocols. For sake of visualization, sequences are assumed to depend on two parameters x_1 and x_2, with Ω and Ω_t denoting the space of parameters that define viable sequences (*blue* area) and the subset of parameters that define regular sequences (*red* area), respectively. Current programming protocols sample the subset Ω_t differently for every patient according to a trial-and-error paradigm. For every patient, these protocols eventually settle on one set of parameters (e.g., *rest star*) that shows some effect on the patient's symptoms. *Inset*: Pulse sequence defined by the parameters indicated by the red star, with anodic and cathodic phases shown together. **B)** Schematic of the design process for optimal stimulation: A convex cost function $J(x_1, x_2)$ is introduced to assign a merit value to every pair of parameters in Ω, with the merit being inversely related to the cost associated with the pulse sequence univocally identified by the parameters, i.e., better pulse sequences have lower cost. According to J, the pulse sequence chosen in A) (*red star*) has suboptimal cost (*red circle*) and is outperformed by other sequences outside Ω_t. The optimal pulse sequence minimizes $J(x_1, x_2)$ and can be reached using a gradient-descent-based algorithm [12] from an initial guess (*black cross marker*, labelled as (0)), which is associated with an initial cost (*yellow cross marker*). A sequence of intermediate parameter values (*black dots*, sequentially labelled as (1) through (4)) is iteratively formed moving away from the initial guess and following the direction of maximum descend along J until the optimal solution, *yellow star*, labelled as (5), is achieved. The sequence of parameters (0), (1), …, (5) corresponds to cost values (*yellow dots*) forming the steepest descending trajectory (*red dashed curve*) from the initial cost along J and is the only subset of parameters in Ω that is explored to converge onto the optimal solution.

While the scenario depicted in Fig. 1A mainly follows a heuristic approach, optimal stimulation protocols are designed by introducing a mathematical function of the stimulation parameters, which is defined as $J(x_1, x_2)$ in Fig. 1B (see a description in section 2) and is known as *cost function*. This function is defined on the entire set of viable parameters, Ω, and assigns a value or "*cost*" to every pair of parameters (x_1, x_2) based on the expected impact of the resultant stimulation protocol. The cost function, in fact, quantifies the value that a stimulation protocol may have when clinically used, and the optimal solution is defined as the stimulation protocol that minimizes the value of the cost function over the entire set Ω, e.g., *yellow star* in Fig. 1B. The following sections will present several techniques that have been proposed to determine the optimal solution, either mathematically, i.e., in closed form, or numerically, given the set Ω, a formulation of the cost function $J(\cdot)$, and, eventually, a mathematical model of the neural ensembles or nervous fibers that are stimulated.

As discussed in detail in this chapter, designing stimulation protocols by solving a mathematical problem that involves a parameter set Ω and a cost function is a paradigm shift from established heuristic approaches because it allows to systematically pursue two major goals. First, it makes the entire design process less empirical and allows to identify stimulation protocols that may be applicable to a wider class of conditions than those determined by heuristic programming guidelines. Secondly, an approach based on optimization facilitates the identification of stimulation protocols that can have therapeutic effects on multiple patients, despite the intrinsic variability that exists across patients.

1. THE PATH TO OPTIMAL STIMULATION

The first embodiments of electrical stimulation of the central nervous system (CNS), that eventually led to clinical applications, trace back to the late 1960s [13, 14], and it is since 1997 that the electrical stimulation of deep brain structures (deep brain stimulation, DBS) has been approved by the US Food and Drug Administration (FDA) to treat movement disorders, including Parkinson's disease, tremor, and dystonia [15]. In addition, implantable devices for electrical stimulation have been approved by the US FDA over the years to target nerves outside the CNS, including the vagus nerve for the treatment of epilepsy (vagus nerve stimulation, VNS) [16] and the sacral nerve for the treatment of urinary voiding dysfunctions [17, 18]. Finally, neuromodulation therapies based on implantable stimulation devices are currently investigated for the treatment of severe psychiatric disorders [3].

A 2018 survey of public regulatory databases [19] reported that over 150 neuromodulation embodiments, i.e., implantable devices or therapies, had received some level of premarket approval by the US FDA. A follow-up review of the regulatory databases (URL: https://www.fda.gov/medical-devices/device-advice-comprehensive-regulatory-assistance/medical-device-databases, last accessed on July 15, 2020) showed that 30 unique stimulation devices had received pre-market approval (PMA) for 22 distinct clinical applications (i.e., unique product codes) at the date of July 1, 2020, see **Table 1**. A full list of these devices is reported in **Table 2**. Moreover, 167 products for the electrical stimulation of the spinal cord had received 501(k) clearance, of which 17 are implantable neurostimulators, and one of the PMA systems in **Table 2**, i.e., Medtronic Active®, had received humanitarian exemption for the treatment of behavioral and psychiatric disorders. Four additional stimulation devices were listed as recipient of an exemption for the treatment of incontinence and apnea, but did not eventually reach pre-market approval, see **Table 1**.

Indication or Disease	*US FDA Product Code*	*Description*	*No. of PMA*	*No. of 501(k)*	*No. of HDE*
Incontinence	EZW	Stimulator, Electrical, Implantable, for Incontinence	3	-	2
Respiration / Apnea	GZE	Implanted Diaphragmatic/Phrenic Nerve Stimulator	1	-	-
	MNQ	Stimulator, Hypoglossal Nerve, Implanted, Apnea	1	-	-
	OIR	Diaphragmatic/Phrenic Nerve Laparoscopically Implanted Stimulator	-	-	2
	PSR	Implanted Phrenic Nerve Stimulator for Central Sleep Apnea	1	-	-
Pain	GZB	Stimulator, Spinal-Cord, Implanted (Pain Relief)	1	138 (16)	-
	GZF	Stimulator, Peripheral Nerve, Implanted (Pain Relief)	-	29 (1)	-
	LGW	Stimulator, Spinal-Cord, Totally Implanted for Pain Relief	6	-	-
	PMP	Dorsal Root Ganglion Stimulator for Pain Relief	1	-	-
Hearing Loss	MCM	Implant, Cochlear	7	-	-
	PGQ	Hybrid Cochlear Implant	1	-	-

Movement Disorders	MHY	Stimulator, Electrical, Implanted, for Parkinsonian Tremor	2	-	-
	MRU	Implanted Subcortical Electrical Stimulator (Motor Disorders)	-	-	1
	NHL	Stimulator, Electrical, Implanted, for Parkinsonian Symptoms	2	-	-
	PJS	Stimulator, Electrical, Implanted, for Essential Tremor	1	-	-
Epilepsy	LYJ	Stimulator, Autonomic Nerve, Implanted for Epilepsy	1	-	-
	PFN	Implanted Brain Stimulator for Epilepsy	1	-	-
Behavior / Depression	MFR	Stimulator, Brain, Implanted, for Behavior Modification	-	-	1
	MUZ	Stimulator, Autonomic Nerve, Implanted (Depression)	1	-	-
	OLM	Deep Brain Stimulator for Obsessive Compulsive Disorder	-	-	1
Obesity	PIM	Neuromodulator for Obesity	1	-	-
Unspecified	GZC	Stimulator, Neuromuscular, Implanted	1	-	-

Table 1. Number (No.) of Implantable Neural Stimulation Devices Approved by the US FDA for Use in Human Subjects.
Devices are grouped according to the product code assigned by the US Food and Drug Administration (FDA) and the indication of use for which US FDA clearance was obtained. Legend: *PMA*: Pre-Market Approval; *501(k)*: Granted 501(k) clearance; *HDE*: Humanitarian Device Exemption. The number of devices granted 501(k) clearance is reported according to the format **X** (**Y**), where **X** is the total number of cleared devices under each product code and **Y** is the subset of devices that are neural stimulators. Information is current as of July 1, 2020.

PMA ID	*Applicant*	*First Approval*	*Product / Device Name*	*Latest Approval*	*FDA Product Code*
P860026	AVERY BIOMEDICAL DEVICES, INC.	01/05/1987	DIAPHRAGMATIC PACEMAKER PHRENIC NERVE STIMULATOR	11/04/2019	GZE
P080025	MEDTRONIC NEUROMODULATION	03/14/2011	MEDTRONIC INTERSTIM SACRAL NERVE STIMULATION THERAPY SYSTEM	10/04/2016	EZW
P180046 P190006	AXONICS MODULATION TECHNOLOGIES, INC.	11/13/2019	AXONICS SACRAL NEUROMODULATION SYSTEM	07/10/2020	EZW
P970004	MEDTRONIC NEUROMODULATION	09/29/1997	MEDTRONIC INTERSTIM THERAPY SYSTEM FOR URINARY CONTROL	02/06/2017	EZW
P950035	BIOCONTROL TECHNOLOGY, INC.	08/15/1997	NEUROCONTROL FREEHAND SYSTEM(R)	01/18/2002	GZC
P010032	ABBOTT MEDICAL	11/21/2001	GENESIS AND EON FAMILY NEUROSTIMULATION (IPG) SYSTEMS	07/29/2019	LGW GZB
P030017	BOSTON SCIENTIFIC CORP.	04/27/2004	PRECISION SPINAL CORD STIMULATION(SCS) SYSTEM	11/14/2017	LGW
P130022	NEVRO CORPORATION	05/08/2015	NEVRO SENZA SPINAL CORD STIMULATION (SCS) SYSTEM	01/04/2018	LGW
P130028	NUVECTRA CORPORATION	11/20/2015	ALGOVITA SPINAL CORD STIMULATION SYSTEM	05/05/2020	LGW
P800040	CORDIS CORP.	04/14/1981	CORDIS PROGRAMMABLE NEURAL STIMULATOR MODELS 900A	03/22/1988	LGW
P840001	MEDTRONIC NEUROMODULATION	11/30/1984	ITREL(R) TOTALLY IMPLANTABLE SPINAL CORD STIM. SYS	07/29/2019	LGW
P970003	LIVANOVA USA, INC.	07/16/1997	VNS THERAPY SYSTEM	05/13/2020	LYJ
P000025	MED-EL CORP.	08/20/2001	COMBI 40+ COCHLEAR IMPLANT SYSTEM	10/15/2019	MCM
P830069	COCHLEAR AMERICAS	11/26/1984	3M BRAND COCHLEAR IMPLANT SYSTEM/HOUSE DESIGN	05/22/1986	MCM
P840024	COCHLEAR AMERICAS	10/31/1985	NUCLEUS MULTICHANNEL IMPLANTABLE HEARING PROSTHESIS	03/29/1991	MCM

P890027	COCHLEAR AMERICAS	06/27/1990	NUCLEUS 22 CHANNEL COCHLEAR IMPLANT SYS / CHILDREN	05/07/1999	MCM
P940022	ADVANCED BIONICS CORP.	03/22/1996	CLARION(TM) MULTI-STRATEGY COCHLEAR IMPLANT	09/23/2002	MCM
P960058	ADVANCED BIONICS	06/26/1997	CLARION MULTI-STRATEGY COCHLEAR IMPLANT	09/23/2002	MCM
P970051	COCHLEAR AMERICAS	06/25/1998	NUCLEUS 24 COCHLEAR IMPLANT SYSTEM	07/02/2020	MCM
P140009	ABBOTT MEDICAL	06/12/2015	BRIO NEUROSTIMULATION SYSTEM	11/19/2019	MHY NHL PJS
P960009	MEDTRONIC INC.	07/31/1997	MEDTRONIC ACTIVA TREMOR CONTROL SYSTEM	07/29/2019	MHY
P130008	INSPIRE MEDICAL SYSTEMS	04/30/2014	INSPIRE II UPPER AIRWAY STIMULATOR	03/02/2020	MNQ
P970003	LIVANOVA USA, INC.	07/16/1997	VNS THERAPY SYSTEM	05/13/2020	MUZ
P150031	BOSTON SCIENTIFIC CORP.	12/08/2017	VERCISE DEEP BRAIN STIMULATION (DBS) SYSTEM	06/29/2020	NHL
P100026	NEUROPACE INC	11/14/2013	NEUROPACE RNS SYSTEM	04/06/2020	PFN
P130016	COCHLEAR AMERICAS	03/20/2014	NUCLEUS HYBRID L24 COCHLEAR IMPLANT SYSTEM	02/21/2020	PGQ
P130019	RESHAPE LIFESCIENCES, INC.	01/14/2015	MAESTRO RECHARGEABLE SYSTEM	02/15/2019	PIM
P150004	ABBOTT MEDICAL	02/11/2016	AXIUM NEUROSTIMULATOR SYSTEM	07/01/2020	PMP
P160039	RESPICARDIA	10/06/2017	REMEDE® SYSTEM	12/23/2019	PSR

Table 2. List of Implantable Neurostimulation Systems with Pre-Market Approval from the US FDA.

Systems are reported along with the unique ID assigned by the US Food and Drugs Administration (FDA) to the Pre-Market Approval (PMA), the date of the first granted PMA, the approved FDA product code, and the company filing the PMA application. Since a revised PMA must be sought after amendments or modifications, the date of the most recently granted PMA is also reported for every system in the list. Information is current as of July 1, 2020.

Altogether, this evidence suggests that the electrical stimulation of nerves and neurons, especially in the CNS, is perceived as a mature and safe option. A major contributor to this scenario is the fact that the primary safety-related concern about neural stimulation is tissue damage [20], which, despite a few exceptions discussed in [19], can be efficiently mitigated by adopting short, charge-balanced pulsatile stimuli with strict limitations on the amount of charge density and charge per phase of every pulse [9, 10].

Electrical stimulation-based therapies that have successfully translated into clinical applications thus far abide to the safety guidelines determined in [9, 10] and share a common design principle, i.e., they are designed to evoke strong, periodic responses in a critical mass of neurons or neural fibers around the location where the probes are implanted [21]. This response can be either a supra-threshold depolarization or a prolonged hyperpolarization of the cells, depending on the frequency of stimulation (e.g., see differences in [22, 23] between high- and low-frequency stimulation) and the ion channel expression of the neuronal membranes [24-26]. Regardless of the polarity, though, the response is always expected to be strong enough and sufficiently consistent over time to produce a prolonged effect. This effect is then expected to modulate the activity along nerves, cells, and neural ensembles and eventually mitigate one or more symptoms of a chronic condition. An extended review of the relationship between the modulatory effects of electrical stimulation on neurons in deep brain structures and behavioral outcomes can be found in [27].

Interestingly, all neurostimulation therapies that use implantable devices to reach some level of clinical merit exhibit three common traits, i.e.,

(i) The stimulation paradigm must involve trains of charge-balanced pulses, with pulses having equal duration and shape.

(ii) The amplitude of the electric pulses during each phase (i.e., anodic, or cathodic) must change as little as possible and remain constant across all pulses.

(iii) The electric pulses must be arranged in a predetermined temporal sequence that is repeated periodically over time [28, 29].

A typical embodiment of these traits is the stimulation protocol approved for DBS, which is reported in **Figure 2** and used to treat both movement disorders and psychiatric disorders ("*regular*" open-loop DBS profile in Fig. 2A, panel a). Overall, these traits identify a subset of the larger group of stimulation protocols that satisfy the safety guidelines established for neural stimulation [9, 10]. Protocols in this subset are characterized by regularity in the temporal arrangement of the pulses, uniformity in shape and duration across consecutive pulses, and low programming complexity, as these protocols can be uniquely defined by manually selecting a handful of programming parameters in the neurostimulation devices, i.e., inter-pulse interval, pulse duration, and pulse amplitude [30, 31].

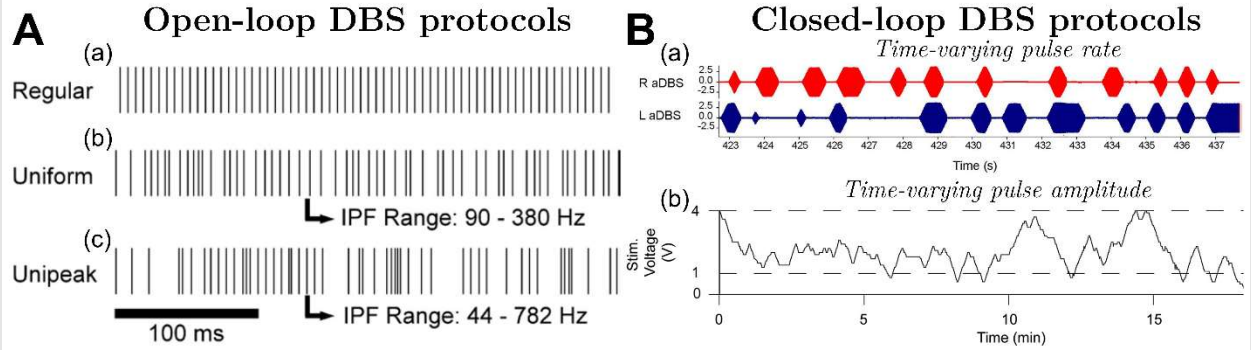

Figure 2. ***Examples of pulse arrangement in electrical stimulation protocols for DBS.*** **A)** Pre-programmed (i.e., *open loop*) pulse arrangements for DBS. Panel a) shows the regular DBS protocol, which is approved by the US FDA to treat movement disorders. Panels b-c) show two experimental protocols that were tested in (Brocker *et al*., 2013) and improved the motor symptoms of patients with Parkinson's disease (PD). Pulses in b) and c) are equal in amplitude and drawn from a uniform distribution and a log-uniform distribution, respectively, thus resulting in irregular pulse arrangements (*IPF*: instantaneous pulse frequency). **B)** Time-varying stimulation protocols for DBS obtained via closed-loop control (*closed loop* DBS). Panel a) shows the stimulation profiles applied to a PD patient in (Little *et al*., 2016) via a bilateral closed loop DBS device (*red*: right hemisphere [*R aDBS*]; *blue*: left hemisphere, [*L aDBS*]). The closed-loop scheme in a) measures a neural proxy of PD and decides in real time when the stimulation is ON or OFF, thus resulting in irregularly spaced bursts of pulses and a time-varying pulse rate. Panel b) shows the time-varying profile of the pulse amplitude in a PD patient treated with a closed loop DBS protocol from (Velisar *et al*., 2019). The control scheme in b) measures a neural proxy of PD and decides the amplitude of the next voltage-controlled pulse while keeping the pulse rate constant over time. *Panels a)-c) in A) and panel b) in B) are reproduced with permission from* [7] and [32], respectively, *© 2013 and 2019 Elsevier. Panel a) in B) is reproduced from* [33] *under the terms of the Creative Commons CC BY 4.0 license, © 2016 BMJ Publishing Group Ltd*.

1.1. The Emerging Merit and Challenges of Irregular Stimulation Protocols

The range of viable stimulation protocols that can evoke strong, consistent, and repeatable responses in neurons and neural fibers while satisfying the safety guidelines in [9, 10] encompasses and far exceeds the set of stimulation protocols that strictly exhibit traits (i)-(iii). This has become evident in recent years, as new software interfaces have been introduced to program sophisticated time-varying pulse trains in new and existing implantable neurostimulators, e.g., see [34].

By using these interfaces, several studies have investigated whether stimulation protocols that relax traits (i)-(iii) may still be effective in treating neurological conditions while providing some

advantage over existing, US FDA-approved regular stimulation protocols. For instance, studies [7, 35, 36] introduced stimulation protocols in open loop for DBS that, differently than the regular protocols depicted in Fig. 2A, panel a, involve the periodic repetition of finite sequences of irregularly arranged pulses, Fig. 2A, panels b-c. These protocols were tested in patients with severe movement disorders and demonstrated promising therapeutic outcomes despite the temporal irregularity while using, on average, just 30% of the electric pulses used by regular DBS (average pulse rate: 45 pulses per second in [7, 35, 36] versus 130-180 pulses per second for regular DBS protocols in [30, 31]). Similarly, phase-locked stimulation protocols [8, 37] and adaptive DBS protocols for Parkinson's disease [6, 32, 33, 38] have provided proof-of-principle evidence of the fact that abrupt, non-periodic variations in the instantaneous frequency and amplitude of the electric pulses (Fig. 2B, panels a-b, respectively) may result in therapeutic effects as relevant as clinically accepted regular DBS. As for irregular open-loop DBS, the pulse arrangements obtained under closed-loop DBS protocols [6, 8, 32, 33, 37, 38] are time-varying and can use fewer pulses per unit of time than regular DBS, thus resulting more energetically efficient, safer, and long-term manageable.

Altogether, the investigation of time-varying and irregular stimulation patterns has suggested that traits (i)-(iii) may pose unnecessary limitations to the span of neural stimulation with therapeutic merit. It has also suggested that more advantageous stimulation protocols may be obtained by relaxing traits (ii) and (iii). However, expanding the range of eligible stimulation patterns poses remarkable methodological challenges regarding the design of actual stimulation protocols.

1.1.1. *Challenges in Designing Irregular Stimulation: A Wide Parameter Space*

The combination of traits (i), (ii), and (iii) in section 1 has the important advantage of dramatically reducing the space of parameters that can be considered to program a stimulation protocol. A train of regularly spaced, equal-amplitude pulses, in fact, is uniquely identified by three parameters, i.e., the pulse amplitude (A, either in voltage or current, depending on the technology of the stimulator), the pulse width, PW, and the interval between consecutive pulses, IPI. Moreover, even though there are thousands of different triplets (A, PW, IPI) that meet the safety requirements in [9, 10] and can be programmed in clinically used implantable neurostimulators (e.g., 12,964 distinct triplets were estimated in [39] for the Medtronic DBS neurostimulators), the boundaries of the subset of parameter values that can actually result in positive therapeutic outcomes are well characterized for most applications, e.g., see [30, 40, 41]. Finally, depending on the application, reliable procedures and practical guidelines have been developed to assist clinicians and technicians in probing the space of admissible parameters and personalize the parameter values to every patient, e.g., see [28, 29, 31, 42].

Relaxing requirements (ii) and/or (iii), instead, increases the number of parameters that must be chosen to program an implantable device, which translates into a combinatorial expansion of the space of admissible stimulation settings to be investigated. With more viable options to be considered, the time and effort devoted to programming a stimulation protocol may significantly increase, without necessarily guaranteeing convergence to stimulation protocols that improve over the existing regular ones. This has led to the need for new ways of probing the space of parameters.

1.1.2. *Challenges in Designing Irregular Stimulation: Lack of Practical Guidelines*

Practical guidelines and algorithms established in [28, 29, 31, 42] for regular stimulation protocols were derived from clinical studies such as [30, 40, 41]. These studies tested several combinations of parameters A, PW, and IPI empirically to extrapolate an input-output relationship between these parameters and the clinical outcomes of the stimulation. As the arrangement of electric pulses is varied over time, though, this relationship loses predictive value and hardly applies to the response evoked by irregular stimulation patterns. Accordingly, guidelines and algorithms derived for regular stimulation hardly generalize to irregular and time-varying stimulation patterns, thus creating a need for new approaches to the design of effective stimulation protocols.

These challenges are further amplified by recent innovations in the design of the hardware for implantable neurostimulation, which have introduced directional neuromodulation devices and electrode leads consisting of hundreds of contacts [43-45]. These innovations have added further degrees of freedom to the design of effective stimulation protocols, including the possibility of selecting the configuration of electrodes to be activated at any time.

Altogether, these innovations, along with the relaxation of requirements (ii)-(iii) in section 1, have contributed to define a novel and challenging set of requirements:

a) A stimulation protocol must be designed by exploring a vast space of parameter settings, which is larger than the space created by constraints (i)-(iii) in section 1. The exploration of this space must be smart, efficient, and yet thorough.

b) Stimulation settings that have some clinical merit must be identified surely within a reasonable amount of time.

c) As numerous stimulation settings are explored, quantitative criteria are needed to sort the explored settings objectively and rapidly, thus steering the selection of the most promising settings in a deterministic and repeatable way.

These requirements can hardly be addressed by the protocols and guidelines set in [28, 29, 31, 42] and have led to the need for novel design methodologies. The bulk of new methodologies introduced in recent years to address requirements a), b), and c) consists of approaches based on optimal control and optimization methods. Accordingly, in this chapter, an *optimal* stimulation protocol is the outcome of anyone of the design processes that have been proposed to simultaneously satisfies conditions a), b), and c). Here, the term "*optimal*" means that the stimulation is not just a feasible option with some level of expected therapeutic outcome – which are traits obtained by addressing requirements a) and b) – but it is the *best possible option* according to the criteria defined in c).

1.2. Optimality and Cost Functions Can Aid Irregular Stimulation Design

The notion of optimality defined by condition c) above is achieved by introducing a cost function (Fig. 1 and Introduction) as the cost functions, when paired with minimum-seeking numerical routines [12], can steer the search among several stimulation protocols, reduce the number of candidate protocols to be assessed, and contribute to the definition of deterministic, repeatable procedures to select an optimal stimulation protocol. Accordingly, cost functions are an important factor towards the definition of a paradigm shift regarding how stimulation settings are investigated and ultimately chosen.

This occurs because the notion of "cost function", whose implications in neuroscience are

discussed in further details in [46], is more general than the measures of therapeutic outcome used in practical guidelines [28, 29, 31, 42]. The cost function summarizes the overall value that a stimulation protocol may have with respect to several conflicting objectives, where an "objective" is a goal that is desired for the stimulation protocol. Examples of objectives may include:

- Suppressing a specific, measurable symptom of the neurological condition for which the stimulation protocol is designed,
- Reducing the amount of stimulation delivered at any time, or
- Restoring specific statistical characteristics of the neural activity in and around the site of stimulation.

Table 3 exemplifies how objectives are typically formulated mathematically and reports common examples of cost functions that combine competing objectives and are used for the design of optimal stimulation protocols. Examples of these cost functions in clinical applications are then discussed in section 5.

Cost Function	***Application***	***Reference***
$$J(x) = \int_0^x \mathcal{P}(t)dt + w\delta(x).$$ The function is defined for a pulse train and is used to choose the best pulse width ($x = PW$). The function weights two competing objectives, i.e., (i) to minimize the instantaneous power of the pulse train, $\mathcal{P}(t)$, and (ii) avoid the penalty, w, which applies if the pulse train fails to elicit action potentials ($\delta(x) = 1$) in the target neural ensemble.	DBS, movement disorders	[47]
$$J(x) = \int_0^T x^2(t)dt.$$ The function is defined for a single pulse, whose shape, $x(t)$, over an assigned interval $[0, T]$ must be chosen. The function weights a single objective, i.e., to minimize the pulse energy.	No specific application	[48, 49]
$$J(\boldsymbol{x}) = \sum_{i=1}^{n} w_i \left(\sum_{k=1}^{U} H(\max(C_{i,k}\boldsymbol{x}) - \alpha) \right).$$ The function is used to find the optimal combination of contacts on a multi-contact electrode probe that must be activated to evoke a response in axons in an assigned volume. The vector $\boldsymbol{x}$ contains the pulse amplitudes assigned at the contacts, and n is the count of competing objectives that must be satisfied, which are weighted according to weights w_i. An objective in this function consists of maximizing (or minimizing) the predict number of axons activated by the stimulation in one of n distinct anatomical regions. For each region, the predict number is given by counting how many estimated axons (i.e., 1, 2, …, U) receive a stimulus high enough to evoke action potentials, where the number of estimated axons is derived from CT scans. $H(\max(C_{i,k}\boldsymbol{x}) - \alpha)$ is a binary indicator saying whether axon k in the anatomical region i is activated, where H is the Heaviside function, $C_{i,k}$ projects the electrode configuration onto the activation function of axon k in region i, and α is an activation threshold.	DBS, Parkinson's disease	[50, 51]
$$J(x) = \frac{1}{2\pi} \int_0^{2\pi} \left[x(\theta)\left(x(\theta) - \lambda Z(\theta + \varphi_+)\right) - \lambda\, \Delta\, \omega \right] d\theta.$$ The function is used to find a periodic stimulus $x(\theta)$, which is defined in the phase space $\theta \in [0,2\pi[$ and then repeats, that can entrain an ensemble of spiking neurons. Neurons in the ensemble spike periodically according to a natural frequency, which is different than the frequency, ω^*, of the desired entrainment. Hence, $\Delta\omega$ is the difference between the natural spiking frequency and ω^*. Also, $Z(\cdot)$ is the phase response curve (PRC, see definition in section 3.2) of the spiking neurons, λ is a Lagrange multiplier [12], and φ_+ is the phase that maximizes the mean value (computed with respect to θ) of $Z(\theta + \varphi)x(\theta)$. The cost function addresses the trade-off between (i) minimizing the energy of the stimulus (i.e., the integral of $x^2(\theta)$) and (ii) minimizing the distance, $\Delta\,\omega$, between the natural frequency of the spiking neurons and the desired frequency of entrainment.	No specific application	[52-54]

Table 3. Examples of Cost Functions Used to Design Optimal Stimulation Protocols in Clinical Applications.

This collection exemplifies how competing objectives are mathematically formulated in cost functions. Variations of the cost functions reported in this table are found in additional studies beyond those cited in this table. These studies, along with the examples in this table, are discussed in this chapter. *Legend*: "*No specific application*" means that the cost function was used in a study that was not directly applied to a clinical application.

The combination of multiple objectives quantifies the overall, multifaceted impact that a stimulation protocol is expected to carry and, in doing so, objectives assist with the fulfillment of requirement b) (section 1.1.2) and help define the geometrical shape of the cost function (e.g., the shape of $J(\cdot)$ in Fig. 1B), thus constraining the search for an optimal solution.

The importance of cost functions in designing irregular stimulation protocols is twofold. First, cost functions provide a mathematical formulation for the tradeoff between objectives and, even though costs may be informed by clinical data, cost functions are not limited to input-output empirical relationships as those established in [30, 40, 41]. Hence, design methods for neurostimulation based on cost functions may have a practical advantage over traditional heuristic approaches because, under mild constraints, the cost function may be changed (i.e., the objectives and/or the tradeoff among objectives may be varied) without affecting how the optimal solution is computed, which makes the entire stimulation design process more flexible and easier to translate across applications.

Secondly, by carefully designing the cost function (e.g., by making it convex), the optimal solution can be obtained using one of many well-established numerical algorithms drawn from the theory of optimization, e.g., see [12] for an introduction to the most common algorithms. A graphical intuition of the advantage that may stem from using convex cost functions is depicted in Fig. 1B: because of the convexity of the cost function $J(\cdot)$, the search for optimal parameters can start from any initial combination of values (*black cross-shaped marker*) and, by using a gradient-descent-based algorithm [12], different parameter settings (*black dots*) will be sequentially identified along the direction of maximum reduction of the cost function (*yellow dots*) until a global minimum (*yellow star*) is achieved. Interestingly, in this example, the minimization of the cost function leads to selecting parameter settings along a specific trajectory (*red dashed curve* in the figure), which provides a strong guidance on how stimulation settings must be chosen and lowers the number of settings to be considered during the search, thus satisfying requirement a) in section 1.1.2

Finally, it should be emphasized that the notion of optimality discussed here has a precise mathematical interpretation (see section 2) and is relative to the definition of the cost function and the support set Ω. Accordingly, a stimulation protocol may be "optimal" and yet result ineffective in the treatment of a specific neurological condition. This would happen if the solution were obtained using a cost function that does not explicitly account for the effects of stimulation on the neurological condition of interest. This indicates the importance of using problem-specific cost functions (e.g., disease-specific, or patient-specific), which will be further discussed in the rest of the chapter through specific examples.

2. A THEORETICAL FRAMEWORK FOR OPTIMAL STIMULATION

The definition of *optimality* provided by conditions a-c) in section 1.1.2 is aligned with the definition given in Mathematical Programming [12] and formalizes a scenario where one or more decisions must be taken based on the decisions' expected effects. A common representation is:

$$\begin{aligned} &\min_{\boldsymbol{x}\in\Omega} J(\boldsymbol{x}) \\ &\text{subject to} \quad f_i(\boldsymbol{x}) \leq b_i, \qquad i = 1, 2, 3, \dots, m \end{aligned} \tag{1}$$

where the objective of the decision-making process is to select a specific vector $\boldsymbol{x}^*$ (e.g., in Fig. 1B, $\boldsymbol{x} = [x_1, x_2]^T$ is a set of stimulation parameters) that minimizes a certain cost function $J(\boldsymbol{x})$.

The cost is a mathematical expression quantifying the effect of an undesirable outcome [12], while the mathematical expressions $f_i(\boldsymbol{x}) \leq b_i$ provide a set of $m > 0$ constraints that must be simultaneously satisfied by the optimal solution. The number m, the functions $f_i(\boldsymbol{x})$, and the bounds b_i depend on the application and help capture the conditions that would make solutions feasible and of any practical value, i.e., they contribute to define the support set Ω. In case of neural stimulation, constraints are typically used to impose that the stimulation is pulsatile and to keep the amount of charge per stimulation phase below a safety threshold [55]. Hence, the solution of the optimization problem is a vector $\boldsymbol{x}^*$ such that $J(\boldsymbol{x}^*) \leq J(\boldsymbol{x})$ for any $\boldsymbol{x}$ satisfying the constraints $f_i(\boldsymbol{x}) \leq b_i$.

Depending on the specific problem, a single decision might be required, and the vector $\boldsymbol{x}$ will be kept constant at the optimal value $\boldsymbol{x}^*$ thereafter, or several decisions must be taken sequentially. In the latter case, the vector $\boldsymbol{x}$ is rather a collection of values that a certain variable w must take at the time of consecutive decisions, i.e., we have $\boldsymbol{x} = [w_0, w_1, w_2, \dots, w_k, \dots, w_{N-1}]^T$, where N is the number of decisions and $N \to \infty$ in case decisions must be taken continuously over time.

If a sequence of decisions must be made, the formulation of the problem may require additional constraints. This would occur because the outcome of each decision may not be fully predictable and must be anticipated to some extent before the next decision is made. Also, the cost function must be reformulated to ponder the cost of every decision, and each decision may need to balance the desire for low present cost with the undesirability of high future costs. To account for these additional conditions, the problem is typically reformulated as follows [56]:

$$\begin{aligned} \min_{\boldsymbol{x} \in \Pi} J(\boldsymbol{x}) &= E\left\{ g_N + \sum_{k=0}^{N-1} g_k(w_k) \right\} \\ \text{subject to} \quad & \boldsymbol{x} \in \Pi, \end{aligned} \tag{2}$$

where $E\{\cdot\}$ indicates the expected value, $g_k(w_k)$ denotes the cost associated with the k-th decision, w_k, g_N is the final cost associated to the condition reached when an entire sequence of decisions $\boldsymbol{x} = [w_0, w_1, w_2, \dots, w_{N-1}]^T$ has been completed, and Π is the set of admissible sequences $\boldsymbol{x}$, with Π being defined by boundary conditions as in (Eq. 1). The symbol Π is used here instead of Ω to emphasize the fact that $\boldsymbol{x}$ is a sequence of decisions, with every decision being constrained to a specific feasibility set Ω. The cases of optimal stimulation discussed in the following sections can all be casted according to (Eq. 1) or (Eq. 2).

Algorithms of increasing complexity and computational efficiency are available to solve problems defined as in (Eq. 1) numerically and have been used to design optimal stimulation protocols. See [12, 57] for a presentation of the most effective algorithms for convex cost functions and nonconvex functions, respectively. A solution to problems defined as in (Eq. 2), instead, is found by applying the Bellman's principle of optimality [56], and Dynamic Programming (DP) is an efficient technique to compute the solution. To use DP, though, the space of admissible decisions at any time k must be known to some extent. This condition is typically formalized by introducing a state variable $\boldsymbol{z}$ and an evolutionary model of the state $\boldsymbol{z}_{k+1} = F_k(\boldsymbol{z}_k, w_k)$, i.e., the problem defined in (Eq. 2) is recast as

$$\begin{aligned} \min_{\boldsymbol{x} \in \Pi} J(\boldsymbol{x}) &= E\left\{ g_N(\boldsymbol{z}_N) + \sum_{k=0}^{N-1} g_k(\boldsymbol{z}_k, w_k) \right\} \\ \text{subject to} \quad & \boldsymbol{z}_{k+1} = F_k(\boldsymbol{z}_k, w_k), \qquad \boldsymbol{x} = [w_0 \; w_1 \dots w_{N-1}]^T \in \Pi \end{aligned} \tag{3}$$

Here the state variable $\boldsymbol{z}_k$ accounts for the possible evolution leading to those feasible options

that are available at time k, and the mathematical function $F_k(.)$ estimates the next state value that will be reached from the state $\boldsymbol{z}_k$ because of the decision w_k.

Altogether, by formulating the stimulation design problem as an optimization problem of one of the types reported in (Eq. 1), (Eq. 2), or (Eq. 3), three major goals are pursued, i.e.,

(i') To make the entire design process less empirical.

(ii') To derive solutions that may be applicable to a wider class of conditions than those covered by current programming guidelines [28, 29]. This is a consequence of the modular nature of the optimization procedure.

(iii') To identify stimulation protocols that may have therapeutic effects on multiple patients, despite the intrinsic variability that exists across patients. This can be pursued by selecting cost functions and state evolution models that focus on the average effects of stimulation over multiple patients.

Finally, this optimization framework is insensitive to the nature of the evoked response (i.e., excitation or inhibition) that is expected by stimulating the nervous tissue. Hence, depending on the clinical applications, the same framework may be used to define electrical stimulation that aims to block the activity of nerves, as in the treatment of bladder oversensitivity [58, 59], modulate the response of nerves to exogenous stimuli, as in the treatment of neuropathic pain [60], or evoke a tonic response in neurons, as in the treatment of movement disorders via DBS [24, 25]. The optimization framework would remain invariant to the type of evoked response because different neural responses would be translated into specific sets of constraints in the formulations (Eq. 1), (Eq. 2), or (Eq. 3), i.e., the framework would not change even if further conditions of the form $f_i(\boldsymbol{x}) \leq b_i$ were added to account for the expected type of response or additional constraints.

For instance, blocking the nerve conductance or the modulatory effect of mechanosensory stimuli on neural fibers can be translated into lower bounds on the stimulation frequency, as shown in [58, 59] and [60] in case of peripheral nerve stimulation and spinal cord stimulation, respectively. This means that tools and procedures available to solve an optimization problem remain valid and applicable with minimum changes as the specific therapeutic domain varies.

Despite the generality of the framework, though, most optimal stimulation problems considered in the neuromodulation community thus far have primarily dealt with evoking patterned responses in neurons and neural ensembles. Accordingly, the approaches presented in the following sections mainly resulted in sequences of depolarizing electrical stimuli, while little effort has been devoted thus far to extending these approaches to the design of inhibitory stimuli.

3. OPTIMAL STIMULATION FOR SINGLE NEURONS

Neurons encode sensory stimuli and higher order information by modulating the discharge of action potentials [61, 62]. Depending on the information value, the response to a stimulus such as a sound or a visual cue may be a brief burst of action potentials fired at high frequency or a sequence of spikes arranged according to a recurrent temporal pattern. The neuronal response depends on the presynaptic stimuli reaching the neuron as well as the neuron's own intrinsic dynamics and can be altered by adding external stimuli such as optical and electric pulses [63, 64].

This has led to a fundamental question: *how to drive a neuron to output a desired spike train with temporal precision, given existing physiological constraints?* This problem naturally falls into

the realm of constrained optimization, as the solution would be an exogenous stimulus that maximizes the neuron's precision in tracking a desired firing pattern.

The problem may have modest practical relevance because of the limited span of applications (mostly *in vitro* but see ref. [65] for *in vivo* optogenetic applications using optical stimuli) requiring direct stimulation of single neurons. Nonetheless, the problem has been intensively investigated in recent years, as it has both theoretical and translation relevance. From a strictly theoretical viewpoint, solutions to this problem have established the mathematical foundations and algorithmic tools that were later instrumental to find optimal stimulation protocols for more complex scenarios, such as scenarios involving large ensembles of neurons and neural tissues. From a translation viewpoint, the problem deals with the manipulation of the encoding abilities of individual neurons [66], and the solutions to this problem may therefore directly inform the design of rehabilitative technologies for brain-machine interface. The rationale for using optimal stimulation of individual neurons to restore encoding capabilities is illustrated in **Figure 3**.

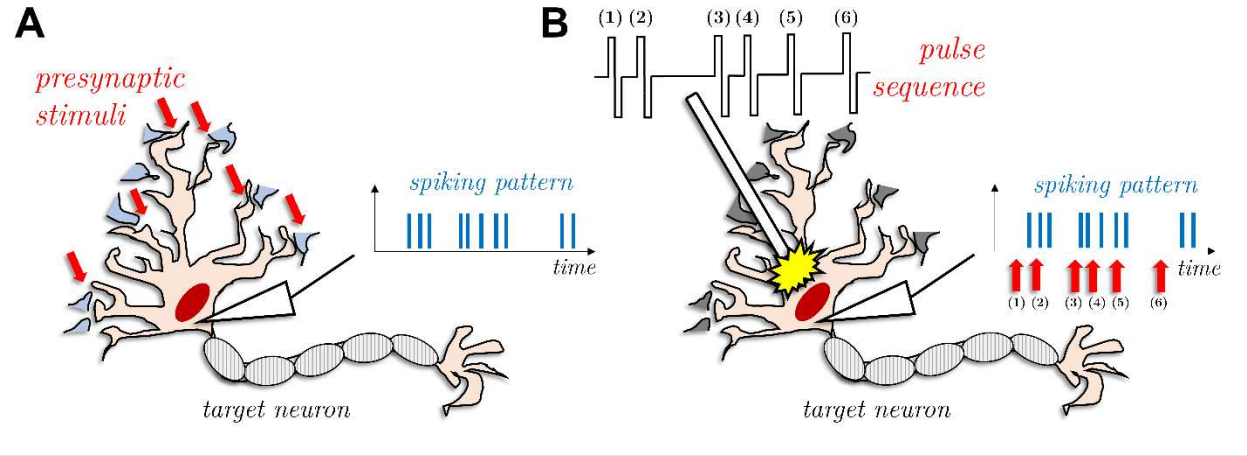

Figure 3. ***Schematic of the optimal stimulation problem for single neurons.*** **A)** Exogeneous stimuli and commands can be encoded via sequences of action potentials in a neuron, and action potentials are transmitted between neurons via synapses (*red arrows*). Synapses are formed between the terminal buttons of transmitting neurons (*blue area*) and the dendrites of the target neuron. A target neuron may respond to presynaptic stimuli (*red arrows*) with a sequence of action potentials, i.e., a "spiking pattern" (*inset*), that is measured at the soma or at the axon. Statistical properties of the temporal arrangement of spikes in a spiking pattern can be univocally related to the synaptic input and can be used to encode/decode stimuli. **B)** Neurological conditions may affect the encoding capability of a neuron by altering the spiking pattern due to presynaptic stimuli. For instance, postsynaptic activity may be lacking (*gray* terminal buttons) in the target neuron because of a neurological condition. If so, a sequence of charge-balanced electric pulses may be delivered to the neuron via an electrode probe (*white bar*) to restore the neuron's encoding capability. An optimization problem is often solved to select the timing of the pulses in the sequence. In this problem, the objective is to ensure that, by delivering pulses (1), (2), …, (6) (*red arrows*), the target neuron will generate a spiking pattern that is as close as possible (in a specific mathematical or statistical sense) to the original pattern in A).

Neurons naturally translate presynaptic stimuli into precise sequences of action potentials (i.e., spiking patterns, Fig. 3A) and, since these stimuli bear critical bits of information about higher order inputs such as sensory stimuli, cognitive states, or commands, it is commonly accepted that the statistical and temporal properties of a neuron's spiking pattern responding to presynaptic stimuli contribute towards a reliable representation of higher order inputs. See [67] for an introduction to the most common techniques of neural decoding.

Neural injuries and synaptic dysfunctions can impair the ability of neurons to respond to synaptic stimuli and therefore deteriorate the representation of higher order inputs [67]. In this case, electric pulses can be delivered concurrently with higher order inputs to elicit spiking patterns that exhibit more naturalistic statistical and temporal properties (Fig. 3B), which help restore the proper encoding of these inputs. Duration, amplitude, and timing of the electric pulses must be designed

to enforce the desired spiking patterns while satisfying several constraints, which usually account for safety requirements and limitations to the neuron's actual response, e.g., refractoriness and ion channel dynamics may pose limitations to the slope and firing rate of the response that is evoked.

Optimization methods appear a natural option to explicitly address the tradeoff between restoration of neural representation and constraints on neural response. The solutions discussed in Section 3.2-3.5 summarize the ample range of formulations that have been introduced over the years to account for the tradeoff. These solutions usually rely on conductance-based models of neurons to constrain the optimal stimulation to the dynamics of ion channels and transmembrane voltages, and the resultant optimal pulse sequences are either determined offline and applied with no adaptation over time (i.e., *open loop* solutions, section 3.2-3.4) or updated periodically online based on real-time feedback about the neuron's ongoing behavior (i.e., *closed loop* solutions, section 3.5).

3.1. Steps to Solve the Optimal Stimulation Problem: A Case Study

A formalization of the problem depicted in Fig. 3B was first provided in ref. [68]. In this study, the objective is to control the firing rate of a neuron over time by enforcing that the interval between any two consecutive spikes is as close as possible to a predetermined value $T_f > 0$. The sequence of steering pulses is applied at the presynaptic terminals and is expected to interact with the ongoing presynaptic stimuli, which are unknown and must be characterized stochastically. Under these assumptions, the problem must determine the sequence of steering pulses to be applied right after an action potential to maximize the chance of evoking another action potential T_f milliseconds after the first one. Denoted with $t = 0$ the time of the first action potential and using the notation introduced in Section 2, the variable to be optimized is the rate $\lambda(t)$ of the steering pulses over the interval $(0, T_f)$, i.e., $\boldsymbol{x}(t) = \lambda(t)$. The function $\boldsymbol{x}(t)$ is then repeated after every action potential to control the firing rate. **Figure 4** provides a schematic of the design problem.

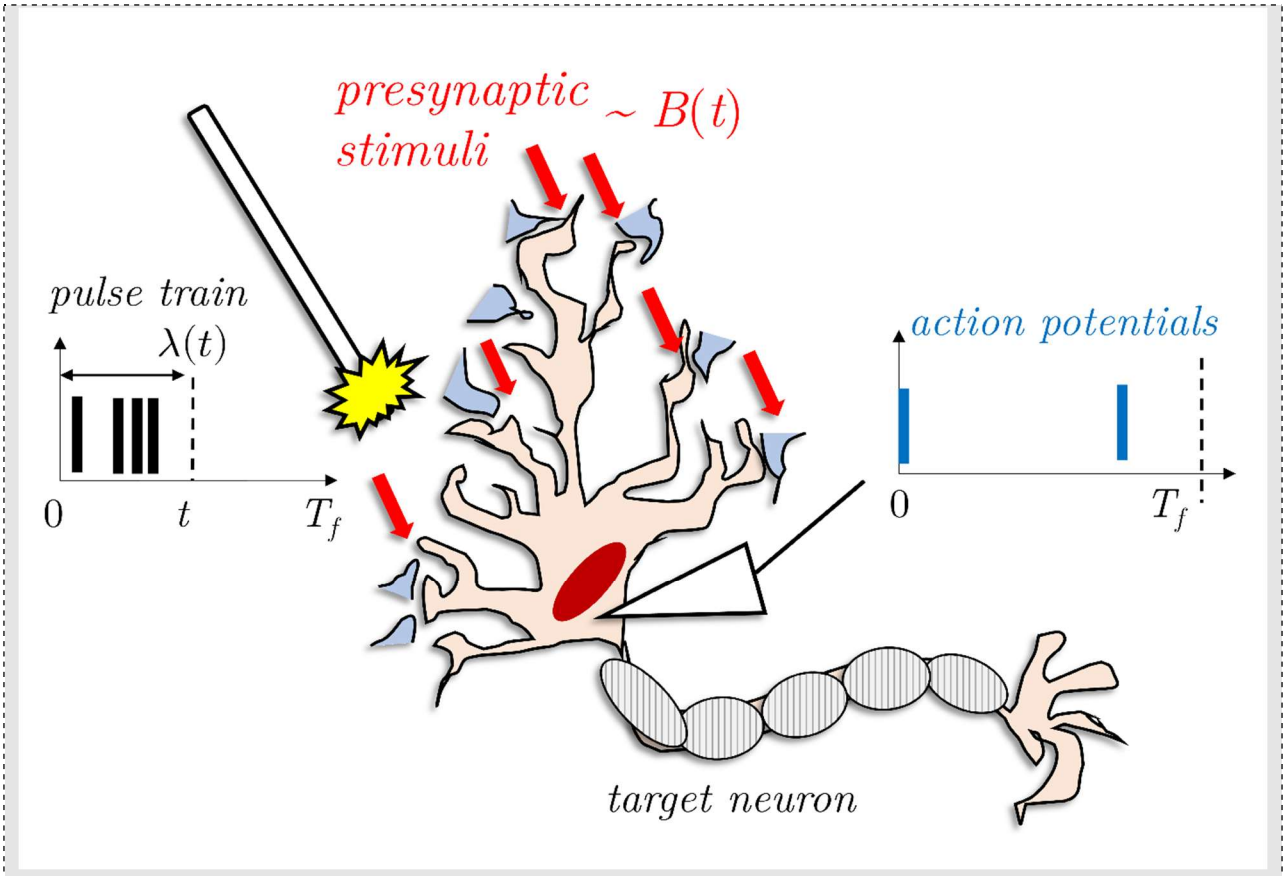

Figure 4. ***Schematic of the optimal stimulation problem in ref.*** [68]. A train of pre-synaptic electric pulses with instantaneous rate $\lambda(t)$ must be designed over an assigned interval $(0, T_f)$ to guarantee that the post-synaptic neuron (target) fires one action potential right at the end of the interval. The rate $\lambda(t)$ must be designed under the assumption that the neuron also receives concurrently pre-synaptic stimuli from neighbor neurons. The timing and amplitude of these pre-synaptic stimuli are unknown but the resultant cumulative input to the target neuron is hypothesized to be standard (mean zero, variance t at time t) Brownian motion $B(t)$.

Although the mathematical formulation in ref. [68] is simplistic from a neurophysiologic standpoint, the solution offers useful insights about the steps of the optimization procedure and the potential benefits of this approach to design stimulation protocols. Hence, the main steps in ref. [68] are discussed here to clarify the procedure leading to an optimal stimulation protocol.

First, the solution to the optimization problem must be constrained. Constrains are required here to account for the important fact that the response of a neuron to presynaptic pulses varies over time, depending on the dendritic arborization, the ion concentration in the extracellular environment, and the amount of synaptic release [69-71], see Fig. 4. Since these factors can be elusive and challenging to track individually, the approach proposed in [68] constrains the optimal solution by introducing a stochastic model for the generation of action potentials. Specifically, the impact of elusive factors is lumped into a Brownian model describing the synaptic currents to the neuron:

$$dI_{syn} = a(1-r)\lambda(t)dt + a\sqrt{1+r^{2\alpha}}\lambda^{\alpha}(t)dB(t) \tag{4}$$

where I_{syn} is the synaptic current to the neuron, $dB(t)$ is standard Brownian motion (i.e., zero mean and variance equal to t at time t), $a > 0$ is the magnitude of every excitatory postsynaptic potential, which typically measured *in vitro*, $0 < r < 1$ is the ratio between inhibitory and excitatory synaptic inputs, $\lambda(t)$ is the rate of pulses to be applied, and $\alpha > 0$ is a parameter to be determined, i.e., a parameter that depends on the specific type of neuron to be controlled.

The synaptic current I_{syn} is then applied to a leaky integrate-and-fire (LIF) model [72] of the neuronal transmembrane voltage:

$$dV(t) = -\frac{V(t) - V_{rest}}{\gamma} dt + dI_{syn} \tag{5}$$

where V is the transmembrane voltage, V_{rest} is the transmembrane voltage at rest, and γ is the decay time constant. The LIF neuron is a hybrid model, i.e., (Eq. 5) holds for $V < V_{thrd}$, where V_{thrd} is the threshold for the generation of an action potential, and $t > 0$. Once V crosses the threshold V_{thrd} from below, a spike is generated, and V is reset to V_{rest}.

As a result of the stochastic representation in (Eq. 4)-(Eq. 5), V is a random variable, and the objective of evoking an action potential at $T_f > 0$ can be translated into the constraint $E\{V(T_f)\} = V_{thrd}$, which follows the general form of constraints in (Eq. 1), and the cost $J(\boldsymbol{x}) = \mathrm{var}\{V(T_f)\}$, where $E\{\cdot\}$ and $\mathrm{var}\{\cdot\}$ denote mean and variance operators, respectively, $V(T_f)$ is the transmembrane voltage at time $t = T_f$, and $V(T_f)$ depends on the sequence $\boldsymbol{x}(t) = \lambda(t)$. Accordingly, the optimization problem is a special case of the general form given in (Eq. 1) in Section 2, i.e.,

$$\begin{aligned} &\min_{\lambda \in \Omega} \mathrm{var}\{V(T_f)\} \\ &\text{subject to} \quad E\{V(T_f)\} = V_{thrd}, \end{aligned} \tag{6}$$

where Ω the set of admissible rate functions $\lambda(t)$, and the optimal solution is the function $\lambda^*(t) = \arg\min_{\lambda} \mathrm{var}\{V(T_f)\}$. Interestingly, the solution to the problem in (Eq. 6) does not ensure that an action potential will be generated exactly at time $t = T_f$, as this would be unfeasible, given the presynaptic arrangement of the applied pulses and the stochastic nature of the synaptic current. However, the solution guarantees that, on average over time, the conditions for an action potential at time $t = T_f$ will be satisfied, and the chance of having $V(T_f) < V_{thrd}$ (i.e., no action potential) will be minimal.

Second, the combination of the model and objective in (Eq. 4), (Eq. 5), and (Eq. 6) leads to a convex optimization problem, whose solution is determined analytically and results in (Eq. 7) below, where $\delta(t)$ is Dirac's delta function.

$$\lambda^*(t) = \begin{cases} \dfrac{2(\alpha-1)V_{thr} \ \exp\left(\dfrac{T_f - t}{\gamma(2\alpha-1)}\right)}{(2\alpha-1)a\gamma\left(1 - \exp\left(\dfrac{2T_f(\alpha-1)}{\gamma(2\alpha-1)}\right)\right)} & \alpha > 1/2\,, \alpha \neq 1 \\ \dfrac{V_{thrd}}{aT_f} \exp\left(\dfrac{T_f - t}{\gamma}\right) & \alpha = 1 \\ \delta(t) & \alpha = 1/2 \\ \delta(t-\tau), \tau \in [0, T_f] & \alpha < 1/2 \end{cases} \tag{7}$$

While the mathematical derivation of (Eq. 7) is beyond the scope of this presentation and can be found in [68], the existence of an analytical solution clarifies the important role that mathematical models have in optimization. Although simplistic, the model in (Eq. 4), (Eq. 5) allows to derive an explicit formula for the solution $\lambda^*(t)$ and, more importantly, to express $\lambda^*(t)$ as a function of known parameters of neuronal activity, i.e., V_{thrd}, a, and γ. These parameters, in fact, have a clear biophysical interpretation and are typically estimated for neurons from recordings either *in vitro*

or *in vivo*.

Altogether, the steps leading to the solution $\lambda^*(t)$ emphasize an important benefit of the optimization framework, i.e., *the solution to an optimization problem can result in a parametric stimulation protocol that can be rapidly adjusted to the properties of the recipient neurons*. Moreover, the solution in (Eq. 7) provides useful insights about the dynamics of the neuron under stimulation. Specifically, parameter α in (Eq. 4) determines the randomness of the presynaptic inputs to the neuron, with larger values of α indicating more randomness [73]. For $\alpha = 1/2$, the input dI_{syn} is derived from a Poisson process, while the cases $\alpha > 1/2$ and $\alpha < 1/2$ lead to processes with larger variance and lower variance than a Poisson process, respectively. Accordingly, (Eq. 7) indicates that the optimal pulse rate has a smooth, time-varying profile when $\alpha > 1/2$, which is easily programmed in current neurostimulation devices. Larger values of α would indicate higher randomness in the presynaptic input, and this would require a faster presynaptic stimulation to better control the response of the neuron, i.e., the average value of $\lambda^*(t)$ grows with α, when $\alpha > 1/2$. As the value of α decreases, instead, (Eq. 7) indicates a degeneration of the optimal stimulation. In fact, as α approaches $\frac{1}{2}$, the optimal stimulation concentrates at the onset of the stimulation interval, i.e., $t = 0$, and becomes purely impulsive for $\alpha = 1/2$. More importantly, as the synaptic inputs become sub-Poisson (i.e., $\alpha < 1/2$), the optimal solution is not unique, as the application of a Dirac's function at any time $\tau \leq T_f$ would reduce the variance of $V(T_f)$ to zero. The interpretation of the case $\alpha \leq 1/2$ is straightforward from a physiological standpoint, i.e., as the noise (i.e., randomness) of the presynaptic inputs decreases, it becomes possible to elicit an action potential with a single pulse, provided that the pulse's amplitude is sufficiently high, and therefore the optimal stimulation protocol consists in delivering one single impulse.

Altogether, these results indicate that *an optimal solution aims to adapt the stimulation protocol to the expected dynamics of the target neuron*, i.e., an optimal solution accounts for the limitations that a neuron may have in responding to exogenous stimuli and determines stimuli that can maximally exploit the underlying dynamics of the neuron.

3.2. Solutions in Open Loop with State-Space Representation

The solution in [68] controls the firing rate of a neuron by modulating the instantaneous rate of presynaptic pulses. However, no boundaries were set on the amplitude of these pulses, and this led to an impulsive rate function (i.e., a Dirac's delta function) when the neuron is excited by Poisson and sub-Poisson processes. Since the intensity of the applied stimuli is a critical factor in determining the feasibility of a stimulation protocol [9, 10, 20], numerous variations to the problem defined in (Eq. 6) have been considered in recent years to explicitly limit the amount of stimulation delivered over time.

Studies [48, 74, 75] focus on stimulating a neuron by injecting a current directly into the neuron's soma and formulate the optimization problem using the amplitude $I(t)$ of this current as the control variable, i.e., $\boldsymbol{x}(t) = I(t)$, while the cost function to be minimized is the total energy of the injected current over an assigned horizon $T > 0$, i.e., $J(\boldsymbol{x}) = \int_0^T I^2(t)dt$.

In [48], the optimization problem deals with finding a minimum-energy stimulus waveform that surely evokes an action potential within an assigned temporal interval $[0, T]$, with no specific constraints on the exact onset time of the action potential. Accordingly, authors formulated the problem using non-stochastic conductance-based neuron models (i.e., FitzHugh-Nagumo and

Hodgkin-Huxley models) and proposed an iterative algorithm derived from the gradient-descent formula to compute the optimal waveform.

The interest in the approach proposed in [48] is twofold. Firstly, the proposed solution provided an efficient way to search a large, nonparametric body of supra-threshold current waveforms and identify non-pulsatile, charge-balanced stimulation profiles, which indicates a potential advantage of using optimization methods instead of more empirical approaches. **Figure 5** reports an example of non-pulsatile optimal waveform obtained in [48].

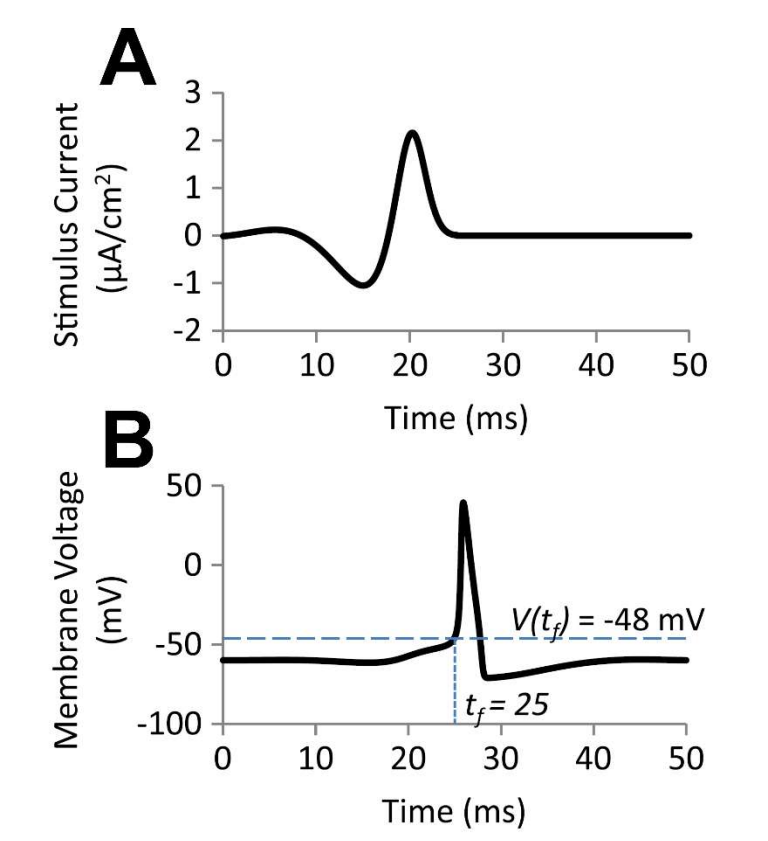

Figure 5. ***Optimization of stimulus waveforms.*** **A)** An optimal pulse waveform is proposed in (Chang & Paydarfar, 2014) by solving a minimum-energy stimulation problem. Waveforms are constrained to be suprathreshold for an assigned conductance-based neuron model. **B)** Action potential generated by the neuron model in response to the optimal pulse in A). The pulse smoothly changes over several milliseconds before the threshold for an action potential (*dashed blue line*) is met at time t_f. *Image reproduced with permission from* [48]*, © 2014 Springer Nature.*

As shown in Fig. 5A, these optimal profiles smoothly vary the amount of charge delivered over time to avoid tissue damage during pulse phase transitions [20]. The charge modulation lowers the slope of the phase transition, thus enhancing the safety of the stimulation while evoking an action potential. Secondly, conduction-based models introduce a state vector $\boldsymbol{z}_k$ in the problem, where $\boldsymbol{z}_k$ gathers all the model's variables, i.e., transmembrane voltage and ion channel gating variables. The presence of a state vector leads to state-based constraints of type $\boldsymbol{z}_{k+1} = F_k(\boldsymbol{z}_k, \boldsymbol{x})$ (or the continuous-time counterpart, i.e., $\dot{\boldsymbol{z}} = F(\boldsymbol{z}, \boldsymbol{x})$) to the problem, as discussed in Section 2, and these constraints result in the optimal solution being expressed as a function of the state vector $\boldsymbol{z}_k$.

Altogether, the solution in [48] emphasizes an important aspect of the optimal stimulation problems involving a state-space representation, which is that *optimal solutions aim to estimate the internal state of the neuron to better anticipate the underlying dynamics and modulate the profile*

of stimulation accordingly. In [48], for instance, the optimal stimulus waveform follows the estimated evolution of the ion gating variables, i.e., it slowly depolarizes the neuron during the opening stage of sodium channels (Fig. 5A) well before the threshold for an action potential is met (*dashed line*, Fig. 5B). Then, it rapidly changes polarity in anticipation of the repolarization phase, thus maintaining charge neutrality. This waveform uses the minimum amount of charge per phase that is necessary to reach the threshold for an action potential within the assigned time window.

3.3. Solutions in Open Loop with Phase Representation

The notion of state is used in a slightly different way in ref. [74, 75]. In these studies, the neuron is assumed to fire action potentials periodically at rest, and the evolution of the neuron's transmembrane voltage is subsumed in a phase model, i.e., a differential state-space model whose state variable $\boldsymbol{z}$ is confined to the interval $[0, 2\pi[$ and represents the instantaneous phase of the transmembrane voltage during the time window. The values $\boldsymbol{z}(0) = 0$, $\boldsymbol{z}(T) = 2\pi$ denote the phase values at which action potentials are fired, and the injected stimulus $I(t)$ over the interval $(0, T)$ must be chosen to enforce an action potential at time T. The model is typically formulated as:

$$\dot{\boldsymbol{z}} = \omega + Z(\boldsymbol{z})I(t) \tag{8}$$

where ω is the natural frequency of the neuron's oscillations and $Z(\boldsymbol{z})$ is the phase response curve (PRC) [76], which is a function modeling the sensitivity of the neuron to exogenous stimuli. Studies [74, 75] exploit the regularity properties of the phase model in (Eq. 8) and, using a variational framework, demonstrate that, for any choice of $T > 0$, an optimal current $I^*(t)$ exists, is unique, and is provided by an analytical formula as a function of the PRC $Z(\boldsymbol{z})$, i.e., $I^*(t) = I^*\big(\boldsymbol{z}(t)\big)$. Since the PRC is a sensitivity function and can be estimated offline based on the neuron's oscillation at rest, the optimal current $I^*(t)$ was computed offline for all $t \in (0, T)$ by mapping the sequence of desired phases $\boldsymbol{z}(t)$ onto the interval $[0, 2\pi]$. The optimal current was then applied in open loop to neuron models of increasing complexity and nonlinearities.

Interestingly, since the optimal current depends on the instantaneous phase, the values $I^*(t)$ can be mapped onto any time interval $(0, T)$, which means that the optimal solution $I^*(t)$ can be repeated over consecutive nonoverlapping intervals of different lengths to enforce an irregular spiking pattern. In case a regular spiking pattern must be followed, instead, a minimum energy stimulus can be achieved by envisioning the desired spiking pattern as the output of a reference phase model

$$\dot{\boldsymbol{z}}_{ref} = \omega_{ref} + Z_{ref}(\boldsymbol{z}_{ref})I(t), \tag{9}$$

with ω_{ref} and $Z_{ref}(\boldsymbol{z}_{ref})$ assigned. In this case, the optimal stimulus can be chosen to minimize both the energy of the stimulus and the distance between the actual phase $\boldsymbol{z}(t)$ of the neuron, which follows (Eq. 8), and the desired phase $\boldsymbol{z}_{ref}(t)$ for all t. This problem was first formulated in [77] for neurons and resulted in an open loop optimal solution $I^*(t)$ that depends on both the desired PRC $Z_{ref}(\boldsymbol{z}_{ref})$ and an upper bound on the mismatch $\big\|Z_{ref}(\boldsymbol{z}) - Z(\boldsymbol{z})\big\|$, where the upper bound can be set conservatively offline without prior knowledge about the neuron's activity.

3.3.1. *From "Minimum-Energy" to "Minimum-Time" Stimulation.*

The problem formulated in (Eq. 6) with the phase model in (Eq. 8) aims to minimize the energy of the stimulus over the interval of interest (minimum-energy stimulation). A variation to this problem is the so-called "*minimum time*" problem and was proposed in refs. [78, 79]. In this case,

the phase model in (Eq. 8) is retained but the goal is to determine the optimal current $I^*(z(t))$ that minimizes the arrival time T of an action potential under the constraint that the current must be charge-balanced over $[0, T]$ and bounded at all times, i.e., $|I| \leq I_{max}$, with I_{max} being a known finite value. As in [74, 75], a variational approach can be used to derive the optimal solution $I^*(z(t))$, which is expressed as a function of the PRC $Z(z)$. Further developments for the minimum time problem were later given in [80], where an optimal presynaptic stimulus was determined, and the optimization was constrained on an estimated model of the phase portrait of the neuron.

3.3.2. *Experimental Validation of Phase-based Optimal Stimulation Protocols.*

Minimum-energy and minimum-time solutions developed in [74, 75, 77-79] have demonstrated a direct translational potential when tested *in vitro* in hippocampal slices from rats. **Figure 6** is reported from [77], which provides a proof-of-concept validation of the phase-based methods.

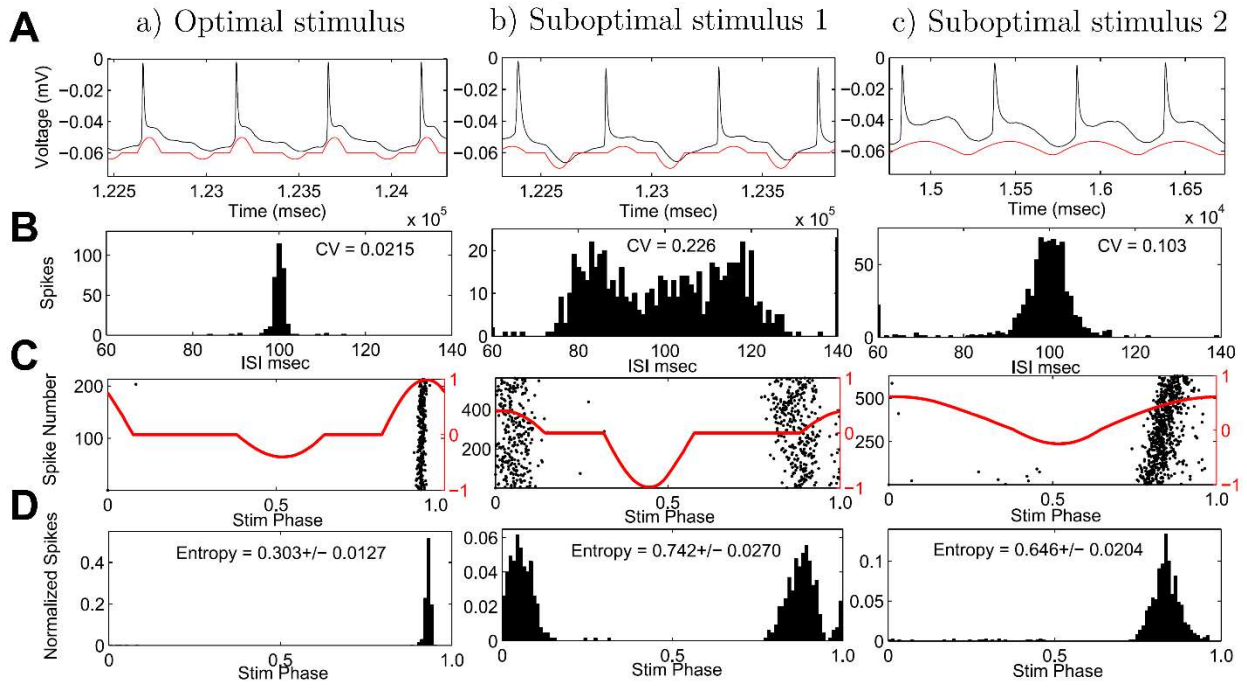

Figure 6. ***Phase-based optimal stimulation in vitro.*** Response of a pyramidal neuron *in vitro* to a minimum energy stimulus (a) and two suboptimal stimuli, i.e., stimulus 1 (b) and stimulus 2 (c) reported in (Wilson *et al*., 2015). **A)** Voltage traces (*black lines*) and applied stimulus waveform (*red lines*). **B)** Histograms of inter-spike-intervals for the neuron under stimulation. Coefficient of variation (CV) values are reported. **C)** Instantaneous phase of the applied stimulus at the time of each action potential (*black dots*). The stimulus waveform is overlapped (*red line*). **D)** Histograms of the stimulus phase at the time of action potentials. Entropy values are reported as mean ± SEM. *Image reproduced from* [77] *under the terms of the Creative Commons Attribution License (CC BY 4.0). © 2015 Wilson, Holt, Netoff and Moehlis.*

In this study, the optimal open-loop stimulation protocol was shown to enforce a regular firing pattern in pyramidal neurons (*black line*, Fig. 6A) with small differences between consecutive inter-pulse intervals (Fig. 6B). Also, the shape of the optimal current (*red line*, Fig. 6A) was shown to modulate the amount of charge delivered to the neuron over time to enforce a small, fixed lag between the stimulus and the neuron's action potentials (Fig. 6C-D). Finally, the optimal solution was shown to outperform non-optimal stimuli (compare panel a) versus panels b-c) in Fig. 6) both in terms of precision of the enforced spiking pattern (Fig. 6B) and lag between the stimulus and the evoked action potentials (Fig. 6D). In a similar *in vitro* preparation, ref. [53] compared the

performance of minimum energy stimuli from [74, 75] to standard pulsatile stimulation protocols and demonstrated that the optimal solutions offered higher efficiency and a more precise control of the spiking pattern of pyramidal neurons than pulsatile stimulation protocols while requiring significantly less energy.

Overall, solutions [74, 75, 77-79] are relevant because a clear rationale is provided to determine the waveform of the applied currents. Specifically, the optimal current $I^*(\boldsymbol{z}(t))$ is proportional to the PRC $Z(\boldsymbol{z})$, and this results in the amplitude of $I^*(\boldsymbol{z}(t))$ rapidly increasing as the PRC is compressed onto short time intervals, i.e., as the time T is moved closer to zero. Accordingly, it is demonstrated that a bang-bang stimulation protocol (i.e., a controlled alternation between the values $+I_{max}$ and $-I_{max}$) is necessary to minimize the arrival time of an action potential, whereas for values $T \gg 0$ (i.e., for small perturbations), the intensity of $I^*(\boldsymbol{z}(t))$ decreases with the frequency of the oscillations of the neuron's transmembrane voltage and can be modulated dynamically at different phases according to the sensitivity of the neuron to perturbations.

3.4. Solutions in Open Loop with Stochastic Modeling of Neural Spiking

A limitation to the formulations proposed in [53, 74, 75, 77-80] lies in the assumption that either neurons fire periodically on their own or the neuronal activity in a time window bears no impact on the activity during the next window. Spiking history, however, has a pivotal role in shaping the propensity of a neuron to future spikes [81, 82]. Hence, studies [83, 84] developed a more general formulation of the optimal stimulation problem, where the objective is to control the timing of several, irregularly spaced action potentials in a sequence rather than the arrival time of a single action potential at the time. To achieve this goal, the cost function is modified to explicitly penalize the mismatch between the entire spiking pattern $\boldsymbol{r}$ fired by the neuron over an assigned time horizon and a desired pattern $\hat{\boldsymbol{r}}$, while the control variable is the current $I(t)$ to be injected in the neuron, i.e., $\boldsymbol{x}(t) = I(t)$ and $J(\boldsymbol{x}) = E\{c(\boldsymbol{r}, \hat{\boldsymbol{r}})|I\}$, where $c(\cdot)$ is a measure of the cost incurred because of the mismatch (e.g., a negative Dirac's delta function) and the conditional expected value $E\{\cdot\,|I\}$ is computed across all admissible spike trains $\boldsymbol{r}$ that the neuron could fire.

The use of a conditional cost function requires an estimation of the conditional probability of the spiking pattern $\boldsymbol{r}$, given the input current $I(t)$, i.e., $p(\boldsymbol{r}|I)$. To estimate this probability for any train $\boldsymbol{r}$, a stochastic model was developed, where the arrival time of an action potential is given by an integrate and fire (IF) model with a soft stochastic threshold. Similar to the LIF model in (Eq. 5), the IF model aims to capture physiological constraints that may limit the evolution of the neuronal transmembrane voltage, including refractoriness and rate saturation, while the stochastic threshold accounts for the fact that the firing rate of a neuron may fluctuate over time because of presynaptic stimuli and noise. The combination of the IF model and the soft stochastic threshold results in a point-process representation of the neuron's spike arrival times, which is then used to estimate the probability $p(\boldsymbol{r}|I)$. Finally, the combination of the stochastic neuron model and the cost function $J(\boldsymbol{x}) = E\{C(\boldsymbol{r}, \hat{\boldsymbol{r}})|I\}$ results in a convex optimization problem, whose solution is unique and can be calculated numerically using a gradient-based algorithm.

Figure 7 reproduces numerical simulations reported in ref. [83]. In these simulations, a neuron model was stimulated to track a reference spike train $\hat{\boldsymbol{r}}$ over 20 consecutive trials, while the intensity of the applied current $I(t)$ was constrained.

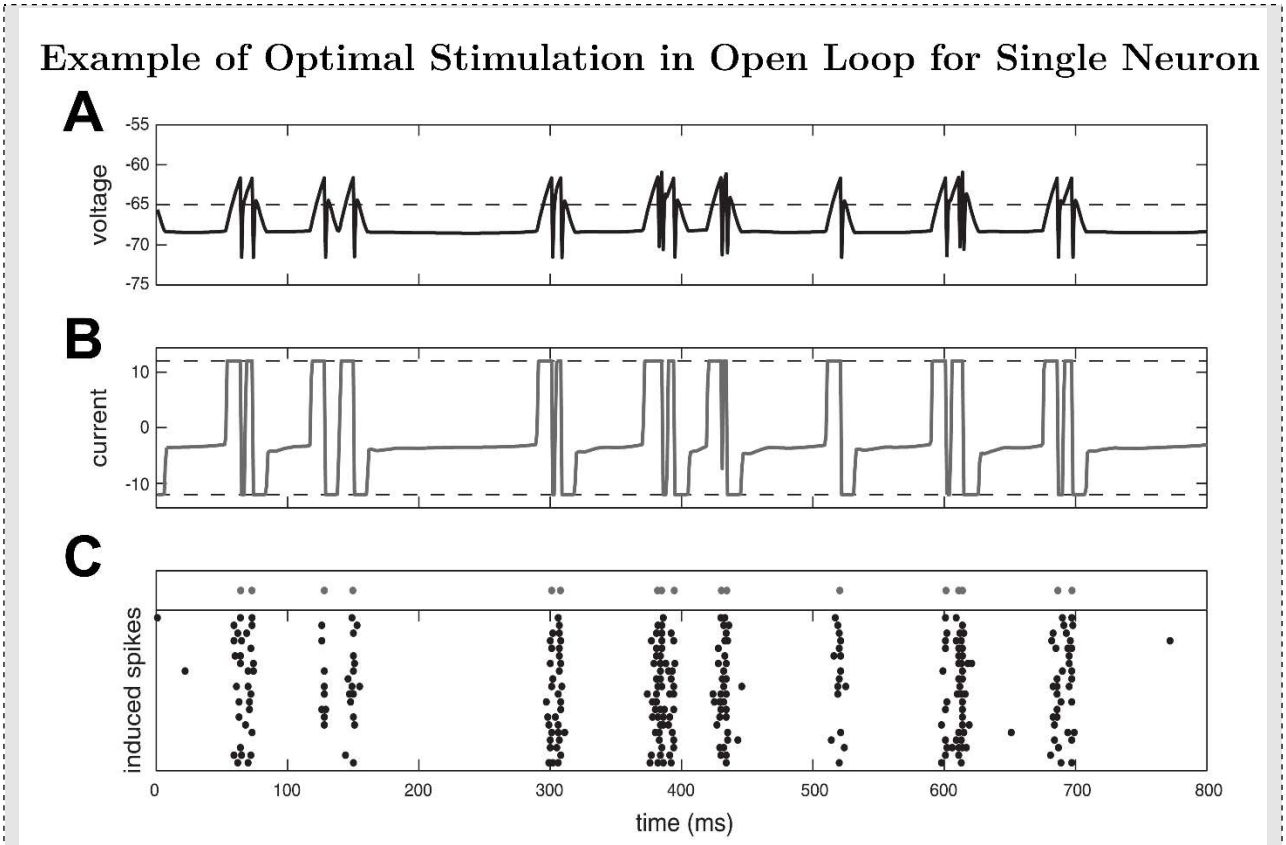

Figure 7. ***Stochastic optimal stimulation of single neuron.*** Example of optimal stimulus proposed in (Ahmadian *et al*., 2011) to track a spiking pattern. **A-B)** Predicted voltage trace of a neuron model (A) responding to the optimal stimulus (B). *Dashed lines* in B) indicate the amplitude constraints on the optimal stimulus. **C)** Arrival times of the desired spike train (*gray dots*) and the actual spike train (*black dots*) of a neuron model under the optimal stimulus reported in B) over 20 trials. *Image reproduced with permission from* [83]*, © 2011 American Physiology Society.*

Fig. 7A reports the transmembrane voltage of the neuron model during one trial in response to the optimal stimulus I^*, and Fig. 7B shows the temporal pattern of I^* along with applied constraints (*dashed lines*). The optimal stimulus rapidly changes around the time of each spike in the desired pattern $\hat{\boldsymbol{r}}$ (*gray dots* in Fig. 7C) to elicit an action potential and then hyperpolarize the neuron right after. This optimal stimulus results in consistent spiking patterns across multiple trials and limits the jitter between the time of the desired spikes and the time of the actual spikes (Fig. 7C), thus increasing the precision in tracking $\hat{\boldsymbol{r}}$.

Interestingly, the optimal stimulus in Fig. 7B is applied in open loop, which indicates that the optimal design encompassed the desired spiking pattern $\hat{\boldsymbol{r}}$ and a model of the neuron's evolution but does not rely on any feedback observation about the current state of the neuron or actual pattern $\boldsymbol{r}$. Also, Fig. 7A-B indicate that the optimal stimulus is not a sequence of suprathreshold impulses delivered at the time of the desired spikes in $\hat{\boldsymbol{r}}$. Because of the model predictions, in fact, changes in the stimulus' shape aim to anticipate the desired spikes and last several milliseconds beyond the spikes, which contribute to make the response robust against trial-to-trial fluctuations.

3.5. Solutions in Closed Loop

A potential limitation to the solutions presented in section 3.2-3.4 is that high levels of noise, unforeseen dynamics in the neuronal activity, and abrupt events such short-term synaptic stimuli

may corrupt the effects of the optimal stimulation protocol and result in a deterioration of the overall performance. Lack of precision in evoking action potentials at the expected time and rising jitter across trials between the desired spiking and the actual spiking are common indicators of a performance deterioration and are often observed when optimal stimulation protocols are implemented in loosely controlled environments [85].

The lack of robustness of these optimal stimulation protocols stems from the open loop implementation and is well studied in systems theory, e.g., see [86] for a general presentation. Although solving different problems, phase-based optimal stimuli in [53, 74, 75, 77-80] and stochastic model-based optimal stimuli in [83, 84] share a common trait, i.e., they both rely on a state variable (i.e., the phase and the spiking pattern $\boldsymbol{r}$, respectively) in the cost function or in the final formula of the optimal solution. Accordingly, these solutions estimate the state variable offline and determine the optimal stimulus as a function of the estimated values. As substantial mismatches appear between the neuron's estimated state and the neuron's actual behavior, though, the optimal stimulus remains unchanged and therefore becomes unable to guarantee the expected spiking patterns. These limitations have motivated the development of optimal solutions in closed loop. The key idea for a transition to closed loop optimal stimulation protocols is depicted in **Figure 8**.

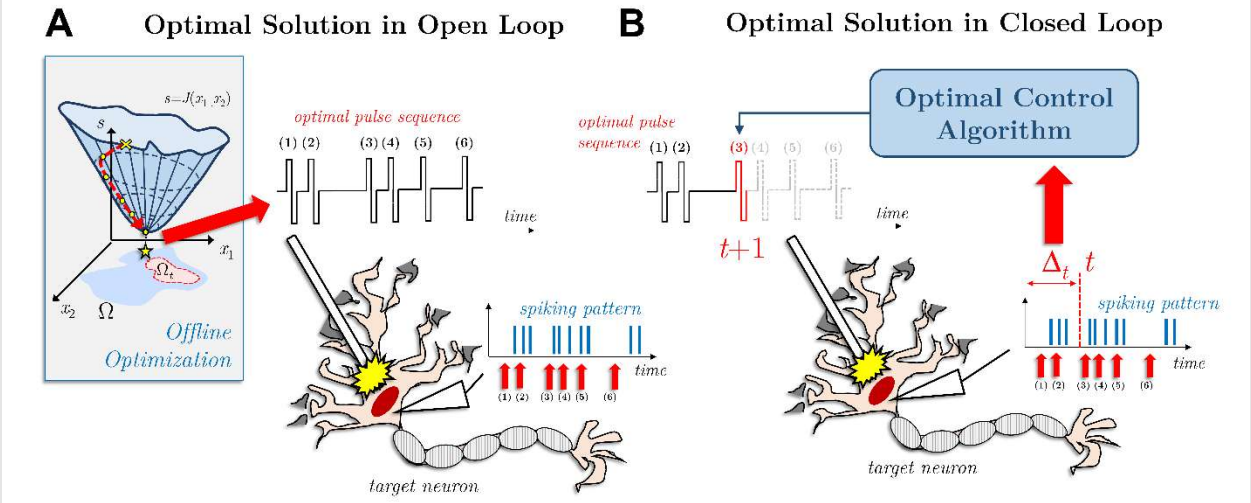

Figure 8. ***Optimal stimulation protocols in open loop versus closed loop.*** **A)** Schematic of optimal stimulation in *open loop*. An optimization problem is solved offline to determine the combination of parameters, e.g., $\boldsymbol{x}^* = (x_1^*, x_2^*)$, in a set Ω that minimizes a cost function $J(x_1, x_2)$ (*yellow star*). The optimal stimulus is programmed using $\boldsymbol{x}^*$ and results in a precomputed pulse sequence that is delivered regardless of the neuron's actual evolution over time. **B)** Schematic of optimal stimulation in *closed loop*. Differently than A), the optimal solution is a time-varying function of a state variable $\boldsymbol{z}$ that accounts for the neuron's evolution, i.e., $\boldsymbol{x}^*(t) = f^*(\boldsymbol{z}(t))$. At any time $t > 0$, $\boldsymbol{z}(t)$ accounts for the activity of the neuron up to t and is estimated by an algorithm (*Optimal Control Algorithm*) using measurements of the neuron's activity over an interval Δ_t up to t. The algorithm then implements the formula $\boldsymbol{x}^*(t) = f^*(\boldsymbol{z}(t))$ to determine the stimulus that must be applied at time $t + 1$ (e.g., pulse (3) in *red*).

While open loop stimulation protocols rely on solving an optimization problem offline and apply the resultant optimal stimulus (e.g., a pulse sequence) regardless of the neuron's evolution over time (Fig. 8A), closed loop protocols adjust the timing and/or amplitude of the applied stimuli to the actual, i.e., current, state of the neuron, as estimated from measurements that are directly collected from the neuron online (Fig. 8B).

From a theoretical viewpoint, the transition from open loop to closed loop stimulation requires minimal changes to the optimization framework and ultimately results from using an online estimation of the state variable $\boldsymbol{z}(t)$ in the formula of the optimal solution. For instance, studies in [87, 88] introduced a mathematical formulation based on the phase model (Eq. 8) where the value of

the PRC $Z(\boldsymbol{z})$ is updated over time as the actual phase $\boldsymbol{z}(t)$ is measured. Accordingly, the phase-based optimal current $I^*(\boldsymbol{z}(t))$ discussed in section 3.3 is determined in closed-loop. In [87, 88], the resultant optimal stimulus resulted in a bimodal protocol, i.e., the stimulus switches between a minimum and a maximum value (bang-bang stimulation), and the phase $\boldsymbol{z}(t)$ is estimated to determine the switching time between the minimum value and the maximum value, thus resulting in a time-varying irregular stimulation pattern.

Iolov *et al*. in [85], instead, noted that the minimum-energy current $I^*(t)$ that makes a neuron fire at a given time $T > 0$ abides the Bellman's principle of optimality, i.e., the optimal solution over the interval $(0, T]$ must be also optimal over any partition of the interval $(0, t_1]$ and $(t_1, T]$, with $0 < t_1 < T$. Specifically, the original minimum-energy problem is defined with cost function

$$J(\boldsymbol{x}) = E\left\{\epsilon \int_0^{\tau} \boldsymbol{x}^2(s)ds + (\tau - T)^2\right\}, \tag{10}$$

which trades off the energy associated with the control variable $\boldsymbol{x}(t) = I(t)$ and the mismatch between the desired onset time T of the evoked action potential and the actual onset time τ (i.e., $\tau \neq T$ but $\tau \to T$) using the coefficient $\epsilon > 0$.

Authors defined the minimum *remaining* cost as

$$w^*(t) = \min_{\boldsymbol{x}(s), s \geq t} E\left\{\epsilon \int_t^{\tau} \boldsymbol{x}^2(s)ds + \big((\tau - t) - (T - t)\big)^2\right\}, \tag{11}$$

to represent the cost associated with the optimal stimulus from a time $t < \tau$ to the onset time τ of the evoked potential, and solved the recursive problem

$$\min_{\boldsymbol{x}(s), s < t} E\left\{\epsilon \int_0^{t} \boldsymbol{x}^2(s)ds + w^*(t)\right\} \tag{12}$$

using the Hamilton-Jacobi-Bellman equation [56]. The revised minimization problem in (Eq. 12) was constrained on a LIF neuron model, which describes the evolution of the neuron's transmembrane voltage V, and the optimal solution was unique and analytically derived as a function of V, i.e., $\boldsymbol{x}^* = I^*(V, t)$. Accordingly, $V(t)$ was measured at any time t to inform the optimal current and led to a closed loop implementation. The exact formula for the optimal solution in closed loop $I^*(V, t)$ can be found in [85]. **Figure 9** reports numerical simulations of a LIF model that responds to $I^*(V, t)$ under the effects of standard Brownian motion noise.

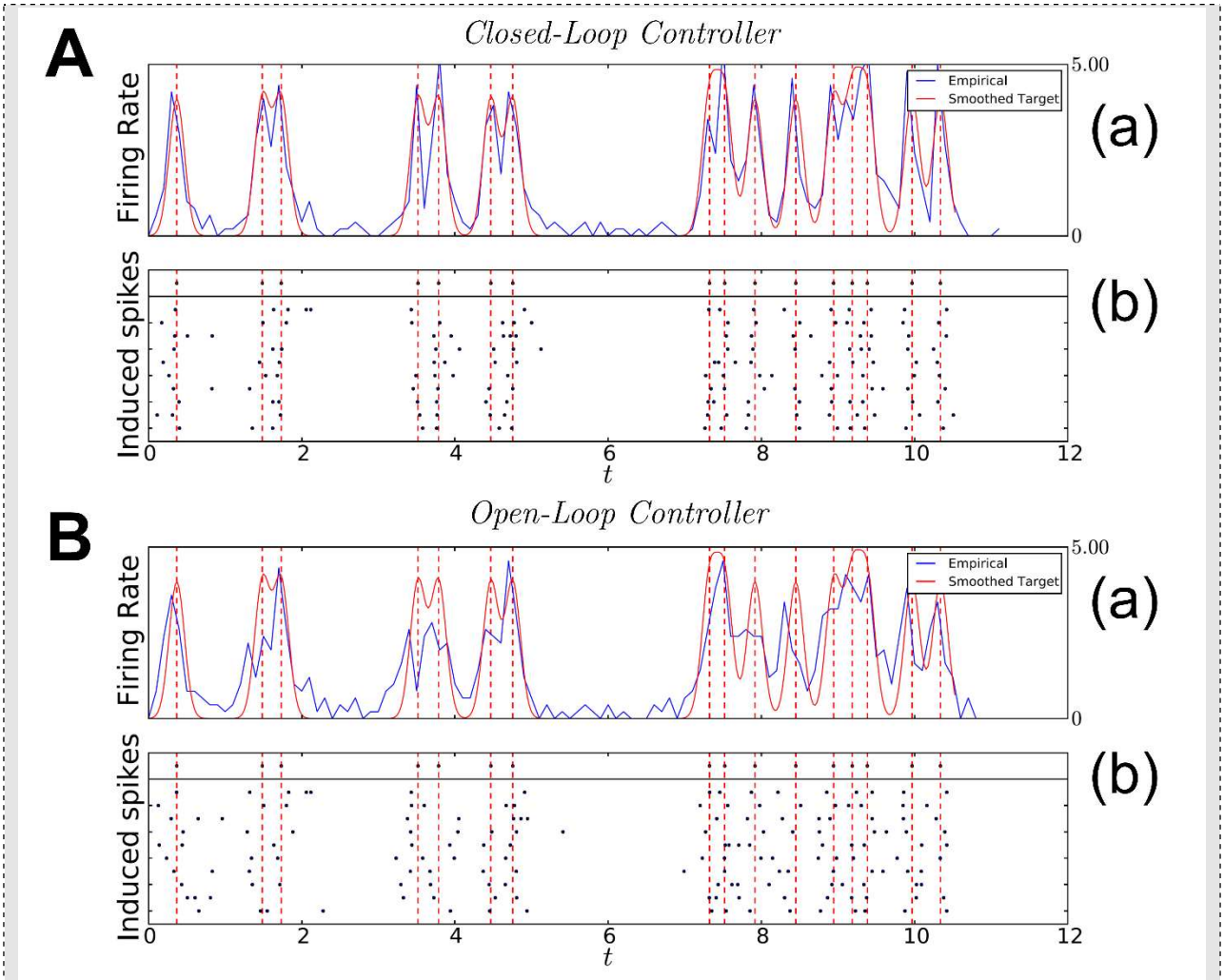

Figure 9. ***Optimal stimulation of neurons in closed loop.*** Example of closed-loop minimum-energy stimulation proposed in (Iolov *et al*., 2014) to control the spiking pattern of a neuron model in a high-noise regime. **A-B)** The optimal stimulus is obtained by applying the optimality principle (A) and the maximum principle (B), respectively. Solution in A) is an adaptive function of the neuron's transmembrane voltage (closed loop) while solution B) is computed offline and applied in open loop. Panels a) in A-B) show the empirical firing rate averaged across 50 spike trains generated by the neuron under optimal stimulation (*blue line*) and a smoothed version of the desired spike train (*red line*). Panels b) in A-B) show the target times of the desired spike train (*dashed red lines*) and the actual spike train of the neuron model under optimal stimulation over 50 trials (*blue dots*). *Image reproduced from* [85] *under the terms of the Creative Commons Attribution (CC-BY) 3.0 license, © 2014 IOP Publishing Ltd.*

To assess the merit of the closed-loop formula $I^*(V,t)$, the original minimum energy problem with the cost function in (Eq. 10) was also solved using the maximum principle, which resulted in an open-loop analytical formula for the optimal current with no explicit dependency on the neuron's transmembrane voltage, i.e., $I^* = I^*(t)$. Fig. 9A and Fig. 9B compare simulation results for the closed-loop formula $I^* = I^*(V,t)$ obtained solving (Eq. 12) and the open-loop formula $I^* = I^*(t)$ obtained using the maximum principle, respectively. A comparison between the estimated firing rates (Fig. 9A, panel a versus Fig. 9B, panel a) and the jitter among spike arrival times across multiple trials (Fig. 9A, panel b versus Fig. 9B, panel b) for the two formulations indicate that, in presence of strong Brownian noise, the closed-loop solution steers the neuron to elicit action potentials at the desired times (*dashed red lines*) with higher temporal precision and less inter-trial jitter than the open-loop solution.

Altogether, these studies provide a rich body of mathematical methods and numerical solutions that enable the control of the neurons' spiking with maximum temporal precision and minimum

energy. The existence of such solutions is critical to the decoding and the enhancement of sensory stimuli, e.g., [64, 67, 89], as well as the encoding of neural information for brain-machine interface applications. Moreover, these solutions are instrumental to take full advantage of the potential for neuromodulation offered by the latest technological developments, which include optogenetics, high-density electrode arrays, programmable interfaces, and closed-loop neural stimulators [45, 90-92]. Finally, these solutions provide the opportunity to precisely target individual neurons and small groups of neurons.

4. OPTIMAL STIMULATION FOR ENSEMBLES OF NEURONS

Despite successful proof-of-concept *in vitro* applications [53, 77], the optimal stimuli discussed in section 3 have largely been confined to the status of theoretical contributions thus far. They have a remarkable merit, though, as they have contributed to establish core mathematical foundations and tools for the optimal stimulation framework. The lack of empirical applications for these optimal solutions, instead, likely depends on the limited range of preclinical problems where a single neuron must be controlled via dedicated inputs, where these problems are mostly confined to the regulation of the firing rate and synchrony of neurons against exogenous insults, e.g., [65, 93, 94].

Most neural stimulation-based applications of clinical interest, instead, involve the modulation of large populations, i.e., ensembles, of neurons. Hence, extensive investigation has been devoted in recent years on *how to extend the optimal stimulation framework from controlling a single neuron to controlling an ensemble of neurons.* A straightforward answer to this question would involve adding as many terms to the cost function as the number of neurons in the ensemble, as the solution should trade off the precision of the spiking pattern of every neuron in the ensemble. As well, the number of constraints to the optimal solution should grow linearly with the size of the ensemble, as one model per neuron should be added, see **Figure 10**.

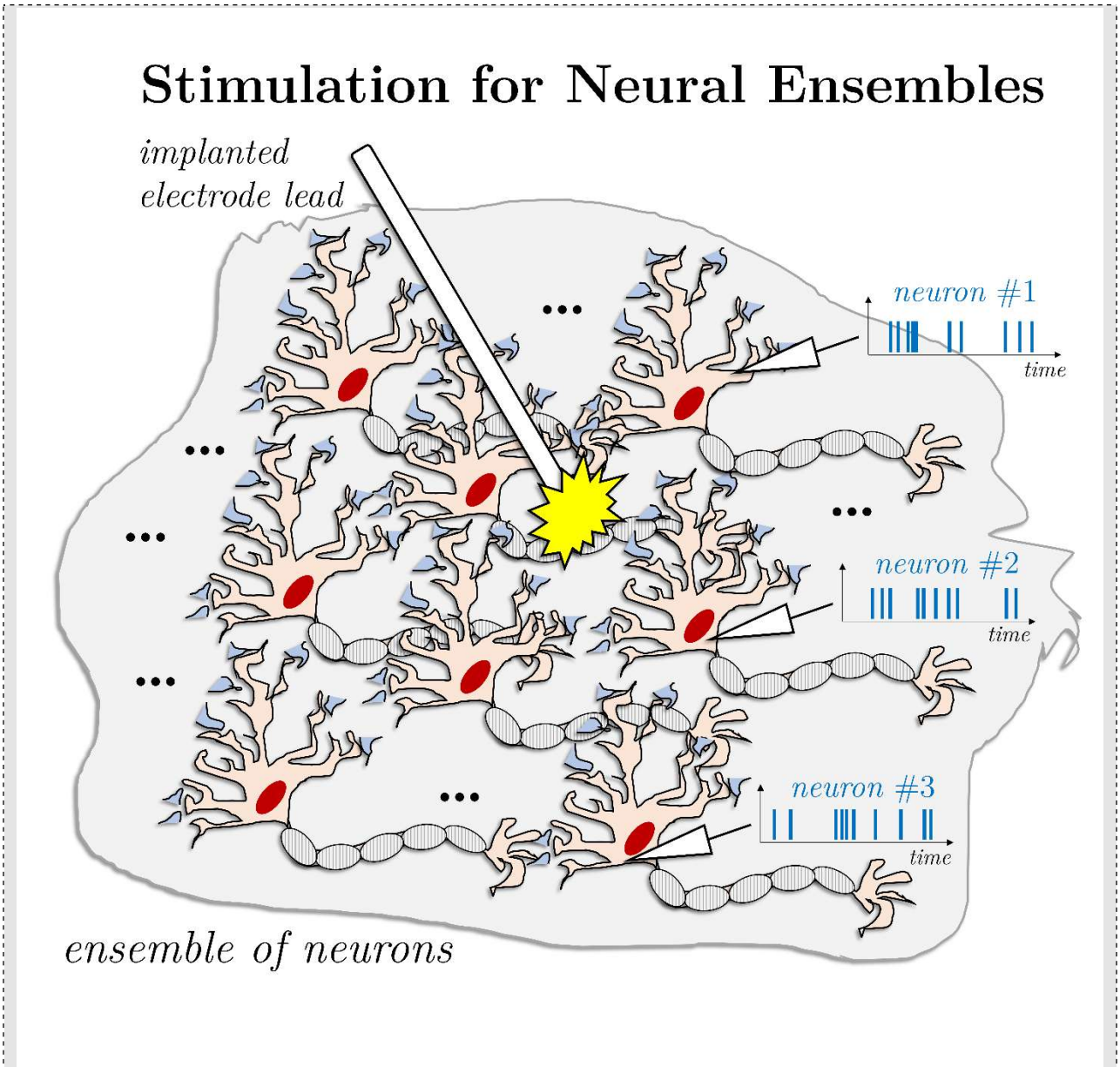

Figure 10. ***Challenges affecting the design of optimal stimuli for neural ensembles.*** An ensemble of $N > 0$ neurons (*gray box*) can be represented as a system with N output channels, i.e., one per neuron, where each output is the neuron's spiking pattern (*blue raster plots*). A challenge is that the interactions between neurons are difficult to model, and this affects the ability to solve optimization problems for large ensembles. Another challenge is that the ensemble is underactuated because, despite N outputs, a single electrode is typically inserted in the ensemble (*white bar*). A common electric stimulus is delivered through the electrode and must therefore modulate the spiking pattern of all neurons simultaneously. Hence, limitations may arise on the number of distinct spiking patterns that can be simultaneously imposed on groups of neurons in the ensemble.

As indicated in Figure 10, this solution poses significant challenges and rapidly loses feasibility as the number of neurons increases. Altogether, the following challenges must be considered when the regulation of the spiking activity in a neural ensemble is investigated:

1. Remarkable technical challenges arise from scaling-up neuron models, regardless of whether these models are simple LIF models or stochastic models. Challenges emerge because these models are expected to describe both the concurrent evolution of neurons and the interactions that are formed among neurons, even though these interactions are often difficult to ascertain [95]. Accordingly, it becomes difficult to properly constrain the optimization problem.

2. As the number of state variables increases with the number of neuron models, challenges are posed by the numerical optimization routines. The computational time of these routines grows significantly as more variables and more complex cost functions are considered [12], which reduces the chance of calculating a solution to an optimization problem in a reasonable time.
3. The stimulation of an ensemble of neurons is intrinsically underactuated because the number of neurons is remarkably larger than the number of applicable stimuli [96]. As the problem presents more outputs than inputs, neurons cannot be driven to distinct spiking patterns, and the optimal stimuli must rather aim to synchronize all neurons to a common pattern or disrupt a common pattern (i.e., desynchronize) by resetting all neurons to their spontaneous activity.

Hence, besides a few case studies involving very small ensembles, e.g., two-neuron ensembles in [97], these challenges have prevented from generalizing the framework discussed in section 3. To address issue 1), a common approach has rather consisted of the following three steps [98]:

a) Envision an ensemble of $N > 1$ neurons as a complex network [99], where the evolution of the individual neurons is modelled simplistically (e.g., via LIF models) and often driven by stochastic inputs.

b) Assume that the interactions among neurons contribute linearly to the neuron models, i.e., the contribution $g_{k\to j}$ of any neuron k on any neuron j in the ensemble is an additional term in the model of neuron j and depends on the state $\boldsymbol{z}_k$ of neuron k. Since $g_{k\to j} \neq 0$ for pairs (k, j) of interacting neurons and $g_{k\to j} = 0$ otherwise, the entire set of connections will be given by a matrix function $\mathcal{G} = \{g_{k\to j}\}_{1\leq k,j\leq N}$, whose actual structure may be partially unknown.

c) Design optimal control solutions that remain valid for a large set of functions $\mathcal{G}$, thus guaranteeing that the optimality is maintained even though specific connections $g_{k\to j}$ are unknown.

The general idea behind steps a), b), and c) is to embrace the issue at point 1) and shift the focus from constraints derived from the neuron models to constraints derived from a characterization of the uncertainty associated with these models. This means that the optimal solution can no longer be obtained through a variational formula as in [53, 74, 75, 78-80, 87, 88] for single neurons. The optimal solution, instead, must be obtained using a robust control approach, where the term "*robust*" is according to the mathematical sense defined in [100] and means that the optimal solution must account for an explicit characterization of the uncertainty associated with the neuron models, i.e., the solution must be robust against uncertainty coming from simplistic model assumptions.

4.1. Robust Stimulation Protocols and Network Connectivity

The shift towards robust design methods addresses both issue 1) and issue 2) indicated in section 4 above, as it leads to constraints that focus on the ensemble as a whole unit rather than individual neurons. The shift also results in fewer constraints overall, which make the computation of an optimal solution more easily attainable. The shift, however, has limited impact on issue 3), i.e., under-actuation [96]. The introduction of robust design methods rather brought additional emphasis on one critical aspect of controlling neural ensembles, which is that *the connectivity properties of neurons influence the formation of collective behaviors across the ensemble in response to applied stimuli* [101]. Specifically, the topology of the network formed by neurons can result in a scenario where stimulating certain neurons (a.k.a. "*drivers*") is more effective than stimulating other neurons to elicit a common pattern. This would occur because perturbations applied to

drivers can propagate more easily throughout the entire ensemble.

Altogether, (i) the shift towards robust design methods and (ii) the link between control objectives in a neural ensemble and ensemble connectivity are investigated in [102-109] and organized around two main problems, i.e.,

P1) ***Identification of drivers in a neural ensemble.*** The problem deals with finding the neurons in the ensemble that should be primarily stimulated to control the entire ensemble. Studies [102, 103] focus on this problem and follow steps a), b), and c) outlined above to define an optimal set of drivers that should be stimulated to recruit the entire ensemble into one common trajectory. Authors use an established relationship between controllability of networks and eigenvalues of $\mathcal{W} \triangleq [\mathcal{G}\ \boldsymbol{x}]$, where $\mathcal{G}$ denotes the connectivity matrices associated with the ensemble (see section 4) and $\boldsymbol{x}$ is a binary vector indicating the neurons that will receive stimulation in the ensemble. Note that $\boldsymbol{x}$ is the vector to be chosen, and the eigenvalues of $\mathcal{W}$ determine the trajectories that the ensemble can reach under stimulation, see [98, 110, 111] for details. Also, depending on the value of $\boldsymbol{x}$, the eigenvalues of $\mathcal{W}$ can be modified, thus determining the span of trajectories that the ensemble may reach. Accordingly, authors first formulate boundaries on the eigenvalues of $\mathcal{W}$ within which the desired common trajectory would be reachable. Then, an evolutionary algorithmic procedure is derived to select the drivers whose stimulation would maximize the enforcement of the desired common trajectory while guaranteeing that the controlled ensemble has a matrix $\mathcal{W}$ with eigenvalues within the assigned boundaries. Studies [104-106], instead, focus on a variation of the optimal driver selection problem and investigate how to alternate the stimulation among subsets of drivers while maintaining synchronization across the ensemble. These studies follow steps a), b), and c) above to derive adaptive solutions that optimize the switching times from one subset to the next.

Physiologically, the studies addressing problem P1 are relevant because they demonstrate, under mild assumptions that are consistent with the structure of most neuronal networks, that wide synchronization across a neural ensemble can be achieved by randomly delivering stimuli to those neurons in the network that, on average, have the largest degree of centrality (DoC), where DoC is a measure of how many connections a neuron has in the ensemble [99]. This suggests that neurons with high DoC, e.g., neurons located in dense regions of the ensemble, can serve as drivers for the entire ensemble.

P2) ***Definition of optimal stimulation protocols for drivers***. The problem deals with finding optimal sequences of stimuli that, when applied to an assigned set of drivers, will synchronize the entire ensemble. Tang *et al*. solved this problem in [107-109] via the Lyapunov function method [112]. Specifically, authors first select target drivers by combining evolutionary search algorithms from [102, 103] and then introduce local state-feedback stimulation strategies for the target drivers. Each stimulation strategy has a time-varying gain and results in a sequence of pulses with varying amplitude and duration. Finally, the Lyapunov function method is used to determine boundaries on the control gains that would guarantee the synchronization of the ensemble in the mean square sense, and a constrained optimization problem with relaxation is solved to determine the set of gain values that best satisfy these boundaries while minimizing the energy of the stimuli to the drivers.

Beyond the technical merits of the proposed solutions, studies addressing problem P2 are relevant because they provide useful insights into the mechanisms of synchronization within

neural ensembles. It is shown, in fact, that synchronous behaviors can be elicited by stimulating drivers in a staggered way, i.e., one driver at the time instead of all drivers at once. Also, it is shown that information about the connectivity within the ensemble, such as notions of neuroanatomy and information derived from tractography studies, can be explicitly used in the stimulation protocols to elicit collective behaviors efficiently while limiting the total amount of delivered stimulation, which is appealing for clinical applications.

Finally, the wealth of stimulation protocols investigated in refs. [104-109] to address problems P1 and P2 is relevant because it provides a decentralized approach to the control of neural ensembles. All protocols devised in [104-109], in fact, *adjust the timing and amplitude of pulses separately for each target driver based on the local mismatch between the activity of the driver and the activity of the most immediate neighbors*. The notion of decentralized stimulation is appealing for applications where multielectrode arrays are used to stimulate and record the neural activity in multiple ensembles. Examples of such applications include retinal prostheses [113] and multiresolution DBS [45]. In these applications, a decentralized protocol can be translated into an efficient algorithm that sequentially activates one electrode contact at the time, thus preserving the safety of the stimulation and reducing the average amount of stimulation delivered at each electrode.

4.2. Optimal Stimulation for Stochastic Ensembles

The major contribution of the methods discussed above consists of decentralized stimulation protocols for neural ensembles, where the protocols are designed based on local information and assumptions about the structure of the ensemble. These protocols can synchronize the entire ensemble while being selectively applied to a subset of neurons in the ensemble, which is a relevant trait to be used in applications that involve multielectrode arrays and multi-site stimulation.

However, the assumptions underlying these methods (i.e., steps a), b), and c) described in section 4) are nontrivial, and several technical challenges may arise from pursuing robust solutions [98]. Hence, alternative approaches have been pursued in recent years. Among these alternatives, methods that consider neural ensembles as multi-input multi-output (MIMO) stochastic processes have drawn significant interest, e.g., [96, 114, 115].

The central idea of a stochastic representation is that the *evolution of a neuron can be subsumed in the neuron's spiking pattern, and the spiking patterns of many locally clustered neurons share similar statistical properties* [82]. Accordingly, the mechanisms of spike generation for a cluster of neurons in an ensemble can be subsumed into a single generative stochastic model that is fitted on spike trains from the entire cluster and is often constructed nonparametrically [81, 82]. The schematic in **Figure 11** depicts the construction of generative models in case of multielectrode arrays and multi-site stimulation.

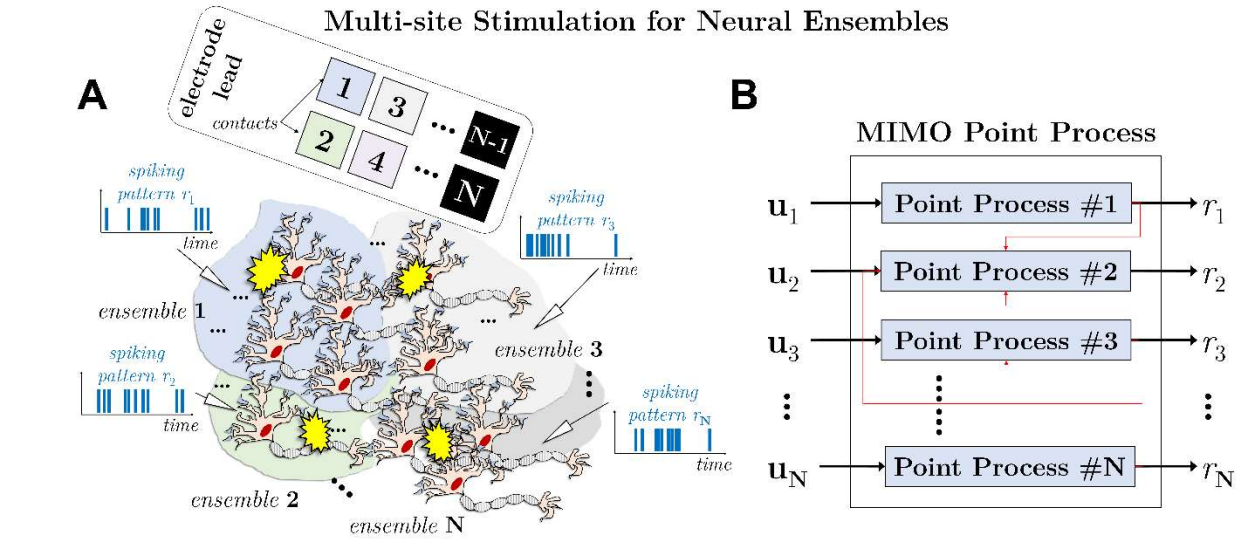

Figure 11. ***Multi-site stimulation and stochastic modeling for neural ensembles.*** **A)** A neural ensemble stimulated with a multielectrode array can be represented as a multi-input multi-output (MIMO) system, where stimulating electrodes are input channels and the multiunit activity recorded at each electrode is a distinct output channel. Output channels capture the activity of subsets of neurons in the ensemble (e.g., sub-ensembles 1, 2, …, N). The spiking pattern $\boldsymbol{r}_k$ at any channel $1 \leq k \leq N$ over a given temporal interval is influenced by the sequence of stimuli $\mathbf{u}_k$ applied at channel k and partially overlaps with the spiking patterns at adjacent channels over the same interval. **B)** A stochastic model (e.g., a point process model) can be estimated for every input-output channel from A), e.g., by using maximum-likelihood methods. For any channel k, the stochastic model (*blue box*) provides the likelihood of the pattern $\boldsymbol{r}_k$ as a function of the stimuli $\mathbf{u}_k$ (*black arrows*) and the neighbor patterns $\boldsymbol{r}_j$, $j \neq k$ (*red arrows*). The stochastic model is often chosen nonparametric to facilitate the fitting on available spiking data.

As shown in Figure 11, recordings from a single electrode contact may capture the cumulative spiking pattern of a cluster of neurons (Fig. 11A), and the spiking pattern of a cluster can be influenced by stimuli delivered through the electrode contact as well as the spiking patterns of neighbor clusters. Hence, the neural activity at a single electrode contact can be represented as a multivariate stochastic process. As recordings at multiple electrode contacts become available, efficient algorithms, e.g., [116-118], have been introduced to estimate nonparametric models for the stochastic processes at all electrodes simultaneously and retain significant interactions between the activities at adjacent electrode contacts, thus leading to a MIMO model of neural ensembles (Fig. 11B).

As discussed in section 3.4 for individual neurons, the introduction of a purely stochastic framework, requires a probabilistic formulation of the control objectives used to determine an optimal stimulus. Refs. [96, 115] address this issue for a scenario where all neurons in an ensemble receive dedicated stimulation, e.g., via optical probes. In these studies, authors determine the conditions under which neurons can be concurrently driven to a set of desired spiking patterns (one pattern per neuron) and the likelihood of this event. Then, denoted with $\boldsymbol{r}_n$, $\hat{\boldsymbol{r}}_n$, and $\boldsymbol{u}_n$ the actual spiking pattern, a desired spiking pattern, and a stimulus sequence for the generic neuron n, respectively, in an ensemble of size $N > 1$ authors demonstrate that the optimal input $\mathbf{U}^* = [\boldsymbol{u}_1^* \; \boldsymbol{u}_2^* \ldots \boldsymbol{u}_n^* \ldots \boldsymbol{u}_N^*]$ that maximizes the likelihood of enforcing the desired patterns $\hat{\boldsymbol{r}} = [\hat{\boldsymbol{r}}_1 \; \hat{\boldsymbol{r}}_2 \ldots \hat{\boldsymbol{r}}_n \ldots \hat{\boldsymbol{r}}_N]$ is obtained by solving the problem

$$\min_{\mathbf{U}} J(\mathbf{U}) = E\{c(\boldsymbol{r}, \hat{\boldsymbol{r}}) | \mathbf{U}\}, \tag{13}$$

where the cost function has a similar structure as the function used in Figure 7 and $c(\boldsymbol{r}, \hat{\boldsymbol{r}})$ is a measure of mismatch between the desired patterns and the actual patterns $\boldsymbol{r}$ obtained under $\mathbf{U}$.

The significance of the stochastic framework discussed in [96, 115] is twofold. First, *optimal*

stimulation protocols derived in this framework have a precise probabilistic sense, which better reflects the performance limitations that may stem from uncertainty about the activity of individual neurons in the ensemble. Second, it is shown that *the performance of the optimal stimulation protocol depends on whether the ensemble is controllable to the desired pattern* $\hat{\boldsymbol{r}}$. This means that the controllability of an ensemble, which can be determined *a priori*, will inform the stimulation design process. Based on controllability information, in fact, it becomes possible to decide whether a desired set of spiking patterns is attainable via stimulation and, depending on the application, it becomes possible to predict the likely therapeutic value of stimulation.

Refs. [95, 119] further develop the MIMO stochastic framework by introducing a kernel-based representation of the neurons' spiking patterns. Specifically, authors observed that, in neural ensembles of practical relevance (e.g., cortical columns), the spiking patterns of N neurons (or neuron clusters) can be described as a linear combination of M parametric stochastic processes (i.e., kernels), with $M \ll N$. The spiking patterns of N neurons can therefore be expressed as $\boldsymbol{r} = \mathbf{W}\boldsymbol{\Phi}$, where $\boldsymbol{\Phi} = [\phi_1 \ \phi_2 \ \phi_3 \ldots \phi_M]^T$ is the array of kernel functions and $\mathbf{W}$ is an $N \times M$ matrix of weights to be estimated offline from neural recordings. Depending on the desired patterns $\hat{\boldsymbol{r}}$, matrices $\mathbf{W}$ and $\boldsymbol{\Phi}$ can then be used to design an adaptive, closed-loop stimulation protocol that drives the ensemble to $\hat{\boldsymbol{r}}$. As before, the protocols stemming from using $\mathbf{W}$ and $\boldsymbol{\Phi}$ are optimal in the sense that the resultant inputs to the ensemble minimize the mismatch between the neurons' actual spiking patterns and $\hat{\boldsymbol{r}}$.

4.3. Optimal Stimulation for Ensemble Desynchronization

Approaches discussed in section 4.1-4.2 aim to design stimulation protocols that can elicit a set of desired spiking patterns in a neural ensemble. Depending on the controllability of the ensemble, action potentials in these patterns can be arranged at constant intervals or irregularly [115]. Also, distinct patterns can be imposed on different clusters of neurons in the ensemble (e.g., via multisite stimulation) or all neurons can be synchronized to a common pattern.

In the study of the CNS, though, neural synchronization is often associated with pathological conditions and chronic diseases, e.g., [120-123], and stimulation protocols are rather investigated to desynchronize neurons. Hence, several studies have focused on optimization methods that may lead to a desynchronization of neural ensembles.

A few aspects of neural desynchronization are well-suited for using optimization techniques. First, the objective of desynchronization is to disrupt a common pattern. Several metrics quantify the degree of synchrony across a neural ensemble, e.g., see [124] for an overview, which means that the desynchronization of an ensemble can be mathematically posed as the problem of minimizing the degree of synchrony in the ensemble. Second, while synchronization may require continuous and region-specific inputs to the ensemble [106-108] to preserve a high level of synchrony among neurons, desynchronization does not require the enforcement of any pattern to the ensemble, and therefore stimuli do not need to be region-specific nor continuous in time. Hence, a desynchronizing stimulation protocol can be derived by trading off two objectives, i.e., minimizing the degree of synchrony in the ensemble and minimizing the amount of stimulation delivered over time. This trade-off can be easily posed as part of an optimization problem.

Consistently with the mathematical tools introduced in Section 3.3, neurons can be represented as oscillators with similar phase portraits that are entrained into a common pattern because of the

mutual interconnections or a common noise [52, 125, 126]. Accordingly, a desynchronizing stimulus works by resetting all neurons at once to a common resting state, from which neurons eventually escape by following different trajectories because of their own internal conditions and exogenous inputs [127].

Refs. [128, 129] formulate the desynchronization problem using the ensemble-averaged transmembrane voltage as a proxy for synchrony within the ensemble, i.e., the average voltage $\bar{V}(t)$ is a periodic signal in case of a fully synchronized ensemble and progressively loses regularity as neurons desynchronize. A phase portrait of $\bar{V}(t)$ is derived from numerical simulations of conductance-based models of individual neurons in the ensemble, and the optimal stimulus is designed as the minimum-energy input that can drive $\bar{V}(t)$ to an unstable fixed point. $\bar{V}(t)$ reflects the field potential activity in the ensemble, and an unstable fixed point for $\bar{V}(t)$ defines a condition in which neurons are utmost sensitive to noise and easily desynchronized by local perturbations [129].

Altogether, the approach developed in [128, 129] consists of two steps: (1) developing a representation of the ensemble activity, e.g., a mean-field model of $\bar{V}(t)$, and (2) using tools devised for the control of individual neurons (see section 3.2-3.3) to solve a minimum energy problem for the ensemble, e.g., for the mean-field model of $\bar{V}(t)$. **Figure 12** depicts the results of ensemble desynchronization by reproducing numerical simulations from ref. [129].

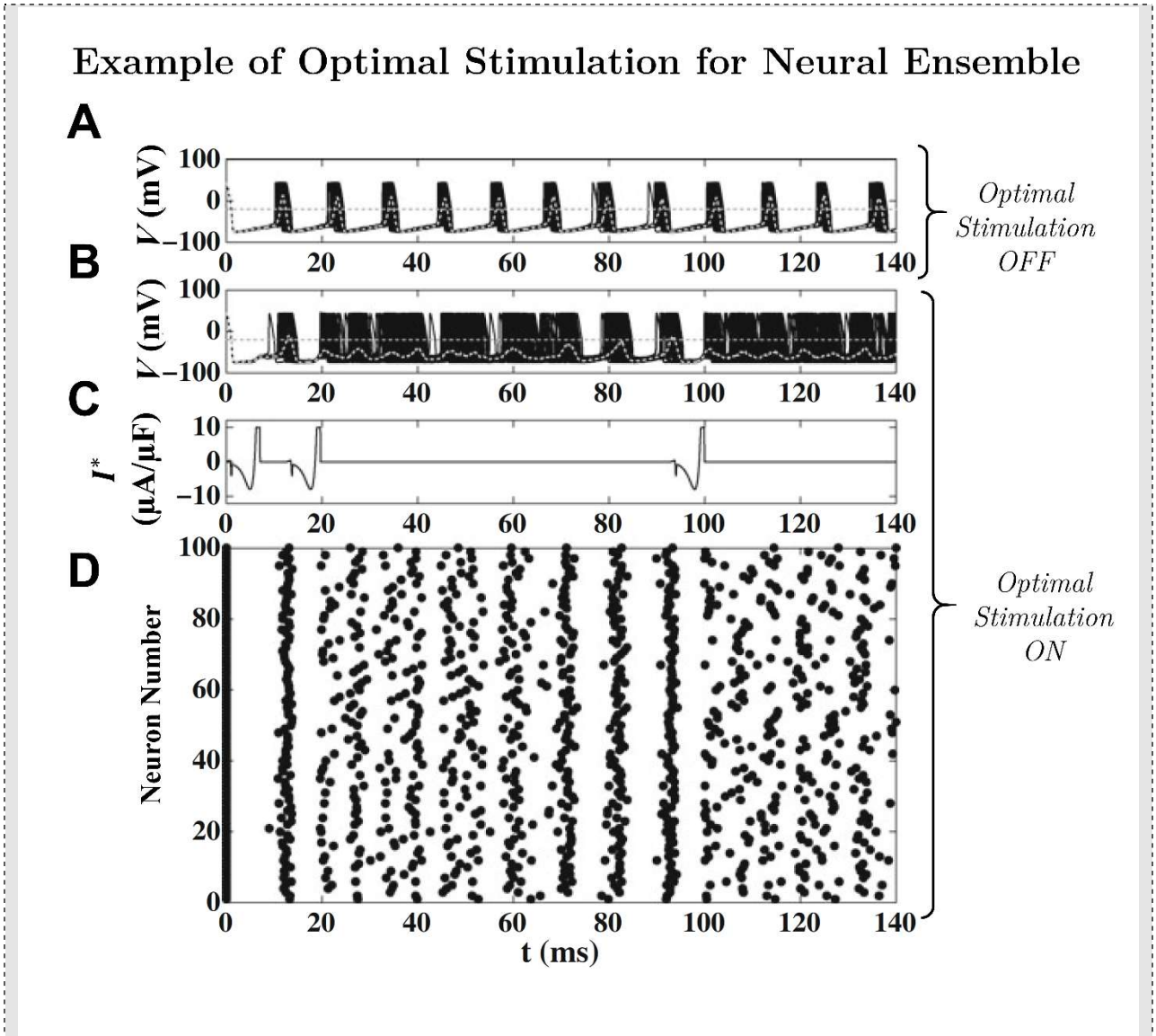

Figure 12. ***Optimal stimulation for ensemble desynchronization*.** Numerical example of optimal desynchronizing stimulation for an ensemble of 100 noisy, coupled neurons from (Nabi *et al*., 2013). **A-B)** Transmembrane voltage of the 100 neurons (*black lines*) and ensemble average $\bar{V}$ (*gray lines*) in the absence of optimal control (A) and when an event-based optimal stimulus $I^*(t)$ is applied (B). A *dotted* horizontal line in A-B) indicates the minimum value (i.e., -20 mV) that $\bar{V}$ must reach to trigger the stimulation. **C)** Event-based optimal stimulus $I^*(t)$ delivered to the ensemble in B) in response to $\bar{V}$ passing the assigned threshold. **D)** Raster plot of the neurons in B) during event-based optimal desynchronization, with one line per neuron. Desynchronization is noted following each stimulus. *Image reproduced with permission from* [129], *© 2013 Springer Nature.*

In this figure, an ensemble of 100 noisy, coupled neurons is simulated in the absence of stimulation (Fig. 12A) and when the optimal desynchronizing stimulus is applied (Fig. 12B). The optimal stimulus is applied according to an event-based policy (Fig. 12C), i.e., the stimulus is switched on when $\bar{V}(t)$ is away from the target unstable fixed point and switched off otherwise, and the shape of the optimal stimulus results in a rapid disruption of the collective firing pattern of the neurons in the ensemble (Fig. 12D).

4.3.1. *Ensemble Desynchronization Using Phase Representation*

A variation to the minimum energy problem for neural ensemble desynchronization is proposed

in refs. [127, 130-132]. In these studies, neurons are represented in the phase space according to (Eq. 8), i.e.,

$$\dot{\boldsymbol{z}}_n = \omega + Z(\boldsymbol{z}_n)I(t) \tag{14}$$

where $\boldsymbol{z}_n(t) \in [0, 2\pi[$ is the phase of the generic neuron n, with $1 \leq n \leq N$, and $Z(\cdot)$ is the phase response curve, which is assumed similar for all neurons. In this representation, neurons form a continuum of phase values across the ensemble, and the collective behavior of the neural population at any time t is captured by the probability distribution of the instantaneous phases $\boldsymbol{z}_n(t)$. The state of the ensemble is therefore described by tracking the mean value of the phase distribution, i.e., $\boldsymbol{z}(t) = \langle \boldsymbol{z}_n(t) \rangle$, and the PRC $Z(\cdot)$ is estimated from the mean value $\boldsymbol{z}(t)$ or a related measure of collective activity, e.g., see ref. [133] for details on PRC estimation from ensemble activity.

Refs. [127, 130] develop a phase model for the average variable $\boldsymbol{z}(t)$, i.e., a model like (Eq. 8) above, and then use the approach described in Section 3.3 to design a minimum energy stimulus for steering $\boldsymbol{z}(t)$ to the value $\boldsymbol{z} = 0$ over a finite time interval. In this formulation, $\boldsymbol{z} = 0$ corresponds to a reset condition for the entire ensemble. In refs. [131, 132], instead, the objective is to design a set of minimum energy stimuli that are applied to spatially segregated clusters of neurons within the ensemble and evoke a coordinated reset (CR) among the clusters [134].

Altogether, methods proposed in [127-132] are relevant because of their clinical potential, as neural desynchronization may mediate therapeutic outcomes in several applications, e.g., see section 5.2 for applications in DBS. Perhaps more importantly, these methods are appealing because of the simplistic models that are introduced to describe the ensemble's field activity. These models can be efficiently estimated from field measurements such as EEG, local field potentials, and multiunit recordings, with mild assumptions about the connectivity within the ensemble that are typically met both *in vivo* and *in vitro*. Also, differently than the robust and stochastic methods discussed in previous sections, these mean-field models retain the simplicity of the phase-based models discussed for single neurons in section 3 and therefore allow to extend the optimization tools presented for single neurons to the design of stimulation protocols for neural ensembles.

5. OPTIMAL STIMULATION IN CLINICAL APPLICATIONS

The optimization framework presented in section 3-4 has been applied to the design of neuromodulation therapies for a wide range of applications, including (i) DBS for movement disorders, psychiatric disorders, and epilepsy, (ii) sensory neuroprostheses for retinopathies, hearing loss, and brain-machine interfaces, and (iii) optogenetics for fundamental neuroscience investigation. However, the translation of optimal methods and solutions from the theoretical framework to *in vivo* and *in vitro* experiments has advanced slowly, and it is only recently that the translation has gained momentum. Two common challenges across many applications can explain the lag between theoretical developments and applications:

C1. ***Modeling gap.*** A significant gap exists between the simplistic models used to constrain the optimal solutions and the complex behavior of neural tissue over time. This gap has required the development of multivariate identification techniques to estimate relevant model parameters, which are often specific to single neurons (e.g., PRC and point process model parameters), from measurements of collective activity such as fluorescence calcium imaging or local field potentials. It is only recently that promising techniques, e.g., [133, 135, 136], have been proposed to significantly reduce this gap.

C2. ***Technological gap.*** Since several optimal solutions are in closed loop, a need exists for devices that can (i) stimulate neural tissue while gathering feedback measurements and (ii) reprogram the stimulation protocol in real time. Devices satisfying (i) have been intensively investigated for DBS applications, as numerous closed loop stimulation protocols have been proposed in recent years to modulate the DBS signal based on measurements of field potential, see a list in [137]. Devices satisfying (ii), instead, are critical to implement multi-site stimulation protocols for multielectrode arrays, non-square stimulus waveforms, and complex optimization formulas as those discussed in section 4.1-4.2.

Addressing challenges C1) and C2) has required an intense technology development, whose presentation is beyond the scope of this chapter, and has recently led to a new generation of neurostimulation devices. These devices can alternate the stimulation among multiple electrode contacts to create focused electric fields [44, 138-140], can record neural activity during stimulation with an adequate signal-to-noise ratio [92, 141], and have computational capabilities to handle complex algorithms implementing adaptive stimulation protocols [91]. The applications of optimal stimulation discussed in the following sections have been enabled by the development of these technological innovations.

5.1. Minimum Energy Stimulus Design for DBS Applications

An important problem in several neuromodulation therapies and especially DBS deals with the waveform of the electric pulses. Study [48] in section 3.2 provides a first attempt at using an optimization framework to find a waveform that is safe, effective in eliciting action potentials, and energy efficient. The problem defined in [48], though, critically assumes that neurons are quiet at rest and receive an injected current. These assumptions hardly hold for *in vivo* scenarios, where the electric pulses are delivered extracellularly, and neurons display ongoing spiking activity.

Despite the specific limitations of the embodiment presented in ref. [48], an optimization framework is appealing to solve the trade-off between safety and energy consumption because, as discussed in section 3.2, it can lead to exploring stimulus waveforms beyond those typically tested in clinical programming protocols [31]. Accordingly, study [47] reformulated the minimum energy problem with two major innovations:

- The charge-balanced optimal waveform $I^*(t)$ that minimizes the energy over the pulse waveform width T is now constrained by an upper bound, i.e., $|I^*(t)| \leq I_{thrd}$ determined by safety consideration [9, 10] and must activate a bundle of geometrically reconstructed mammalian axon models when applied extracellularly in a volume (see cost function in Table 3); and
- The solution $I^*(t)$ is determined numerically rather than analytically by combining an evolutionary algorithm (i.e., genetic algorithm) and numerical simulations of the model axons.

The result of this optimization process is reported in **Figure 13**. The optimal pulse waveforms were tested *in vivo* on a cat sciatic nerve and demonstrated superior energy efficiency and charge efficiency than conventional waveforms used in neural stimulation. Also, the study showed that an optimal pulse can have a Gaussian-like structure (Figure 13) with a smooth slope both for short and long widths, which is consistent with the solution provided by [48] and depicted in Figure 5.

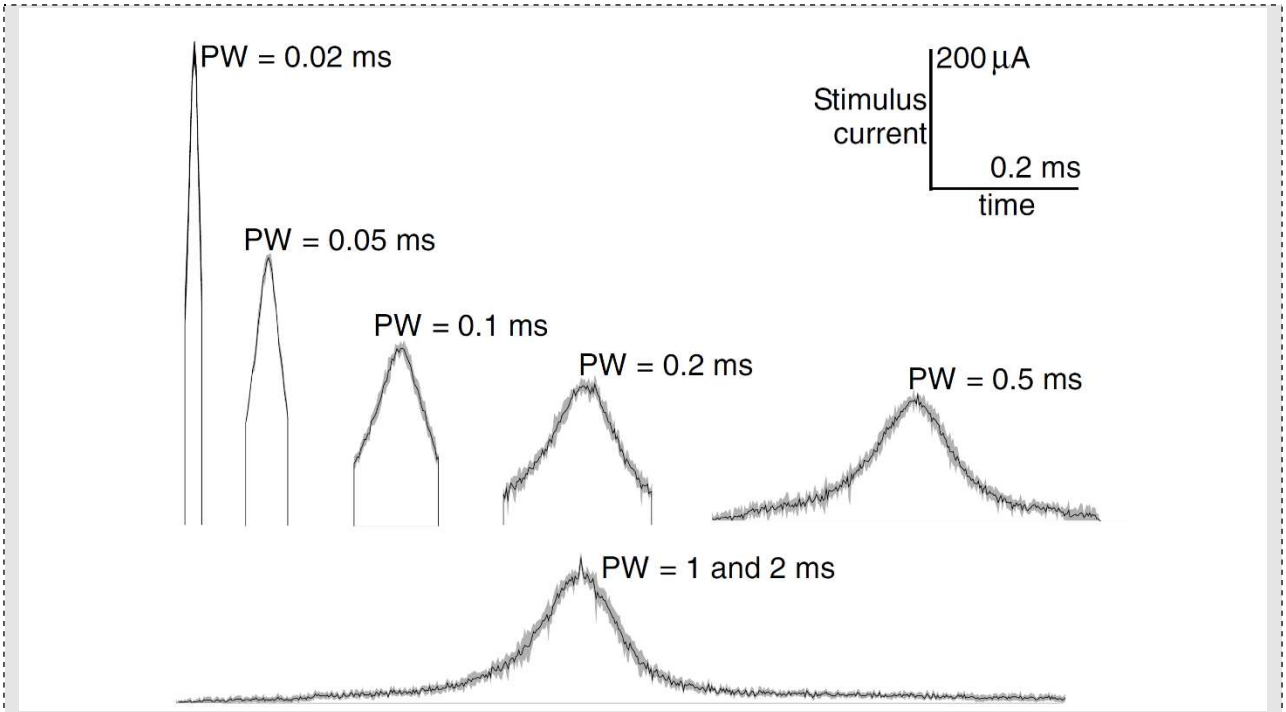

Figure 13. ***Examples of optimal stimulus waveforms for neural stimulation.*** Minimum energy stimulus waveforms for neural stimulation proposed by (Wongsarnpigoon & Grill, 2010) using a genetic algorithm. Waveforms are reported for different pulse widths (PW), ranging from 0.02ms to 2ms. Curves represent the means of the optimal waveforms across five trials of the genetic algorithm, and the gray regions define 95% confidence intervals. *Image reproduced with permission from* [47]. *© 2010 IOP Publishing Ltd.*

More recently, the waveform optimization problem has been solved in [49] using a stochastic search with extrema features, which is a gradient-based numerical approach that restricts the search space to the extrema (i.e., maxima and minima) of $I^*(t)$ instead of the entire waveform over the pulse width. The optimal solution in [49] confirmed traits seen in refs. [47, 48], i.e., the optimal waveform is not rectangular, with a wide hyperpolarizing component followed by a rapid depolarizing phase. More importantly, the study shows that the optimal solution depends on the phase of the neuron's spiking pattern at rest, which reflects the important fact that optimal waveforms are directly related to the type of ion channels present in the target neurons [142, 143].

5.2. Optimal DBS for Movement Disorders

The optimization framework presented in section 4 to control neural ensembles was primarily translated to develop DBS protocols for patients with severe movement disorders. A reason is that the desynchronization of neural ensembles is highly relevant to the treatment of Parkinson's disease (PD) via DBS, as exaggerated neural synchronization in the range 13-35 Hz (beta band) is a widely accepted biomarker of PD [120, 144], and the suppression of beta band oscillations in the subthalamic nucleus (STN), which is the preferred DBS target, is a known hallmark of therapeutic DBS [145]. Regarding the desynchronization of STN, two questions have been recently addressed:

Q1. ***When is the right time to deliver a DBS pulse?*** This question assumes that the waveform of the DBS pulse is set *a priori*. Hence, this question is complementary to the problem discussed in section 4.3, which focuses on finding a minimum energy desynchronizing stimulus.

Q2. ***Which DBS electrode should be activated?*** This question is motivated by the recent developments in DBS hardware, which have resulted in DBS leads with tens of electrode contacts.

In this case, the objective is to select the contact that may maximize the patient's motor improvement during stimulation.

An answer to question Q1) can be obtained by solving the problem:

$$\begin{gathered} \min \tau \\ \text{subject to} \quad \dot{\boldsymbol{z}}(t) = \omega + Z(\boldsymbol{z})\delta(t-\tau), \quad \boldsymbol{z}(\tau^+) = 0. \end{gathered} \tag{15}$$

This is a variation of the optimization problems discussed in section 4.3, with $\boldsymbol{z}(t)$ being the mean phase of the neural population targeted by the DBS input. The value $\boldsymbol{z}(t)$ can be estimated from field potential measurements around the DBS lead, while $Z(\boldsymbol{z})$ is the ensemble-averaged phase response curve, and τ is the time when a DBS pulse is delivered to desynchronize. In this formulation, it is assumed that the DBS pulses are strong enough to desynchronize the population (i.e., $\boldsymbol{z}(\tau^+) = 0$), and the solution to (Eq. 15) is the time τ^* when $Z(\cdot)$ is minimal, i.e., desynchronization is achieved by applying the DBS pulse at time τ^* such that $\boldsymbol{z}(\tau^*) = \boldsymbol{z}^*$ and $Z(\boldsymbol{z}^*) \leq Z(\boldsymbol{z})$ for all $\boldsymbol{z} \in [0,\ 2\pi[$.

This solution was first introduced in [133, 135], where a method was developed to estimate the ensemble-averaged phase response curve $Z(\boldsymbol{z})$ from STN oscillations in the beta frequency band, and an event-based algorithm was proposed to track the instantaneous phase, $\boldsymbol{z}(t)$, of the beta-band oscillation over time and apply DBS when it reaches the value $\boldsymbol{z}^*$. The relevance of the solution in refs. [133, 135] is that the prediction of a preferred phase $\boldsymbol{z}^*$, which is specific to the STN used to estimate $Z(\boldsymbol{z})$, was later demonstrated in a clinical study involving 10 PD patients who received STN stimulation during the DBS surgery study [146]. A patient-specific preferred phase was empirically determined from the STN local field potentials, where the preferred phase is the value that utmost ameliorates the PD motor symptoms. Also, it was shown that the deterioration of the motor symptoms increases with the lag between the preferred phase and the phase at which the stimulation is delivered, and the increment is consistent across patients, **Figure 14**.

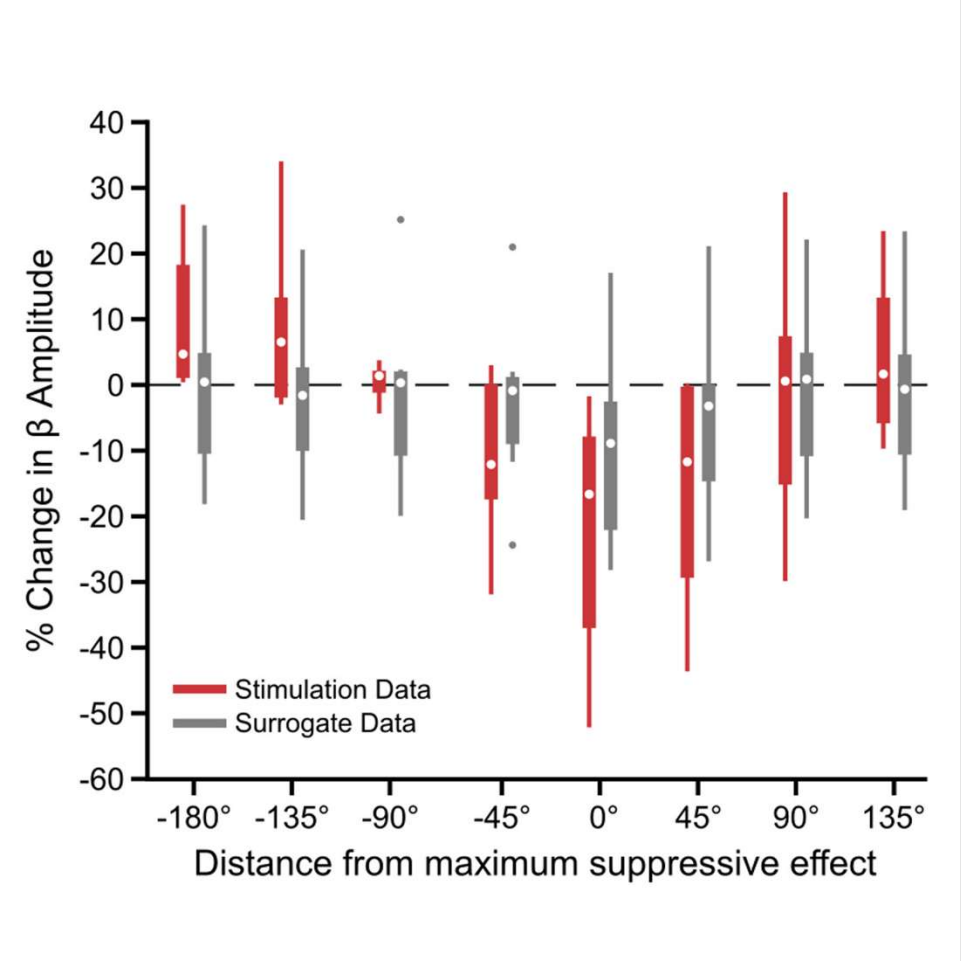

Figure 14. ***Phase-specific variation of pathological neural oscillations in response to phase-locked DBS for Parkinson's disease.*** Results presented in (Holt *et al*., 2019) showing a phase-dependent effect of DBS pulses on the amplitude of the subthalamic (STN) beta oscillation. *Red bars* denote the change in STN beta amplitude as a function of the relative phase lag of the DBS pulse from the preferred phase. *Gray bars* refer to surrogate data, i.e., pre-stimulation data that have been time-matched to the data used to compute the red bars. Data are from 10 Parkinson's disease patients and shown using a boxplot. For each boxplot, the central dot is the median, and box edges are the 25th and 75th percentiles. *Image reproduced from* [146] *under the terms of the Creative Commons Attribution 4.0 International License (CC-BY), © 2019 Society for Neuroscience.*

Finally, the phase-dependent DBS protocol that results from stimulating at the preferred phase requires fewer pulses per unit of time than regular DBS protocols [135], which can significantly improve the efficiency of the stimulation, the duration of the charge-based neural stimulators, and the long-term safety and tolerability of the DBS therapy, well beyond the theoretical improvements obtained with other closed-loop DBS protocols, e.g., protocols designed via adaptive control techniques [147-155] and Bayesian control techniques [156].

An alternative, more recent solution to question Q1) has been obtained by formulating the DBS pulse train as a sequence of K pulses, with $K > 1$, that are repeated periodically, and optimizing the resultant sequence of $K - 1$ inter-pulse intervals. This idea was investigated in refs. [35, 157, 158] using a computational approach similar to the one discussed in section 5.1, i.e., a cost function is defined to quantify the effect of a K-long DBS sequence on a computational model of neurons under PD conditions, and a genetic algorithm is used to search the space of all K-long sequences and find a sequence that minimizes the cost function. The optimal DBS sequences proposed in [35, 157, 158] demonstrated a therapeutic value close to the value of regular DBS protocols in PD patients as well as rodent models of PD but the optimal DBS sequences resulted in using

approximately 30% less power than regular DBS. Furthermore, the optimal DBS sequences are irregular and low frequency (i.e., less than 50 pulses per second, see Fig. 2A in section 1.1), which may have additional long-term positive effects on safety and tolerability of DBS therapies [159].

5.2.1. *Selection of Optimal DBS Electrode in Multi-Contact Leads*

Question Q2) is more recent because it follows the latest hardware developments for DBS applications [44, 92, 138]. Nonetheless, an established body of work has been developed to address this question. The general problem was first introduced in ref. [160] and further developed in following studies [50, 51, 161].

In these studies, authors integrated scan images from non-human primates and finite-element modeling to create a detailed 3-D model of the DBS lead, electrode contacts, and subject's neural tissue surrounding the DBS lead. The neural tissue considered in [160] was from the ventral thalamus. Moreover, the DBS model was paired with conductance-based models of afferent axons to the thalamus, and numerical simulations were used to estimate the response of these axons to the activation of the various contacts on the DBS lead. The combination of the axon models and the 3-D reconstruction of the DBS lead, contacts, and thalamic nuclei resulted in a sophisticated computational platform that allows to estimate the volume of activated tissue (VAT) that would be obtained in response to various configurations of the active electrode contacts. Specifically, for any combination $\mathbf{I} = (I_1, I_2, I_3, \dots, I_N)$ of currents applied to $N = 32$ contacts (i.e., one current for contact, with $I_j = 0$ for any $1 \leq j \leq N$ indicating that contact j is not activated), authors measured the fraction of axon fibers (AF) that were activated and used AF as a proxy for the VAT. Then, since the fraction AF depends on $\mathbf{I}$, i.e., $AF = AF(\mathbf{I})$, the following optimization problem was posed:

$$\begin{aligned} &\min_{\mathbf{I}} \mu\big(AF_{max} - AF(\mathbf{I})\big) \\ &\text{subject to} \quad \sum_{k=1}^{N} I_k = I_{tot}, \quad I_k \geq 0. \end{aligned} \tag{16}$$

The solution to the problem in (Eq. 16) is the optimal configuration of currents across the electrode contacts on the DBS lead (i.e., the problem is solved with respect to $\mathbf{I}$) and was obtained by combining the computational platform and a convex minimization algorithm [12]. In (Eq. 16), I_{tot} is the total current that can be delivered per charge phase, AF_{max} is the maximum number of axons that can be activated, and μ is a measure of the distance between the two amounts of fibers. Finally, a threshold-based rule was applied to the optimal solution to determine the electrode contacts to be activated. **Figure 15** reports the solution to the problem in (Eq. 16).

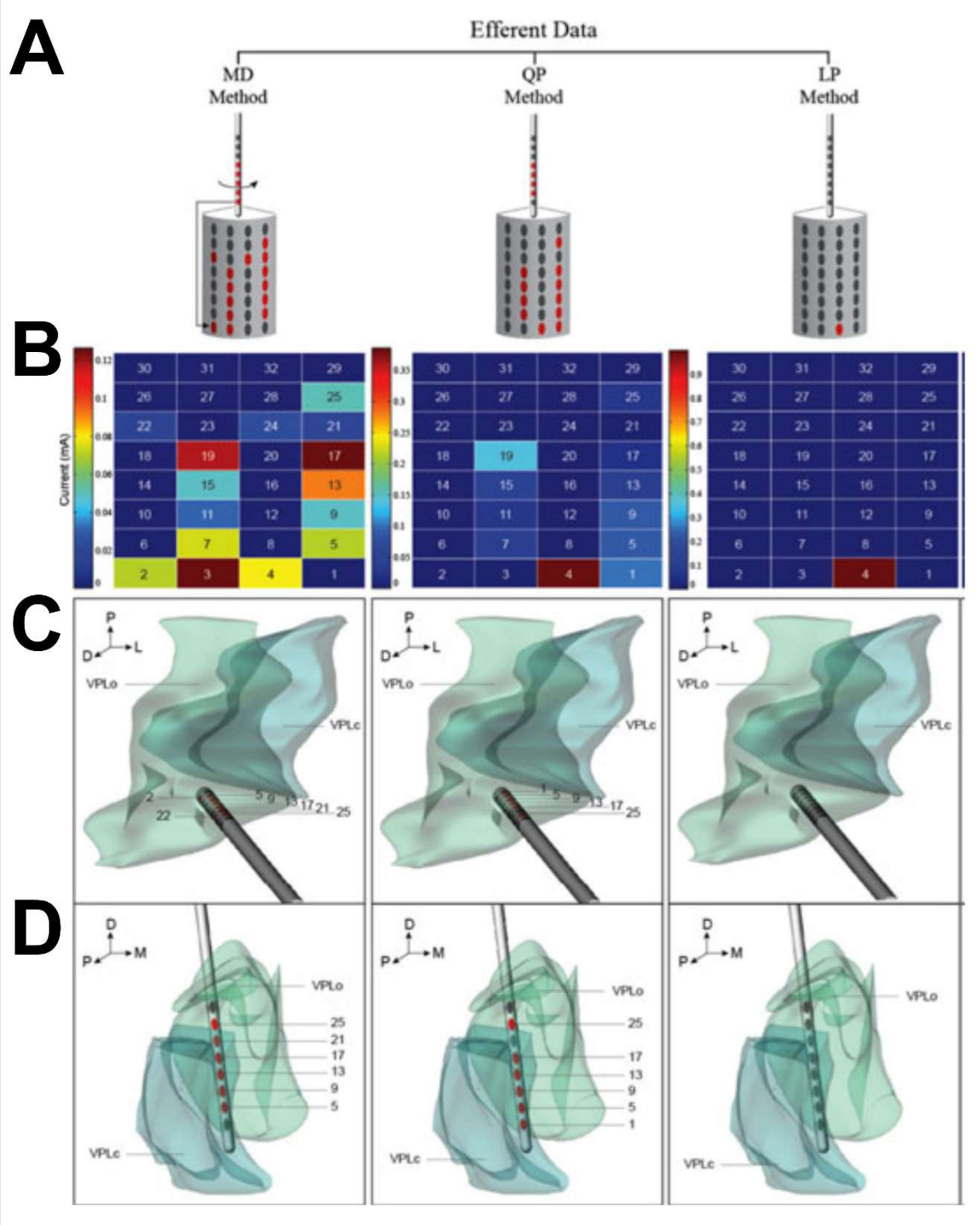

Figure 15. ***Example of optimal DBS contact selection.*** Results of the optimization procedure proposed in (Xiao *et al*., 2016) to select the optimal electrode contacts on a DBS lead. Three algorithm-generated electrode configurations are depicted to maximize the activation of the thalamic efferent axons. The *left*, *middle*, and *right* columns show outcomes from three distance functions $\mu(\cdot)$ in problem (Eq. 16), respectively. **A-B)** For each case, active contacts (A) are reported along with the precise amount of optimal current calculated by the algorithm (B). Active contacts (*red*) are contacts for which the optimal current is higher than 1μA. **C-D)** Axial views (C) and oblique views (D) of the oral and caudal ventral posterior lateral nuclei of thalamus (VLPo and VLPc, respectively), the DBS lead, and the active electrode contacts (*red*). *Image reproduced with permission from* [160], *© 2016 IEEE.*

Fig. 15A reports the solution for three different choices of the distance μ, along with the optimal currents (Fig. 15B), and the estimated 3D arrangement of the active contacts in the thalamus (Fig.

15C-D). As suggested by the results in the figure, two aspects of the approach proposed in ref. [160] are of particular interest here.

First, solving (Eq. 16) provides an efficient way to sample the N-dimensional space of electrode configurations within a finite amount of time. Although affected by the limitations of the computational platform and the choice of μ (see differences between columns in Fig. 15A and Fig. 15B), in fact, the optimal solution is expected to have a positive effect on neural tissue, nonetheless. The alternative would be an empirical, trial-and-error approach, which would be likely unfeasible for large values of N (e.g., $N = 32$ in this study).

Second, the optimal solution is obtained via a personalization process. Since the computational platform integrates bits of information that are specific to the subject, the solution to (Eq. 16) can be customized to individual subjects, i.e., PD patients, by simply updating the anatomical models used to constrain the problem.

Altogether, these studies demonstrate the feasibility of translating optimal design methodologies to clinical applications and provide proof-of-concept evidence of the positive impact that optimization methods can have in the design process for DBS protocols.

5.3. Optimal Stimulation for Epilepsy Surgery

The concept of optimal stimulation has been recently explored for diagnostics purposes. A challenging diagnostic problem, which is often faced during the epilepsy surgery, deals with designing electrical stimulation probing protocols to identify epileptogenic zones intraoperatively [162-164]. The idea of probing the brain electrically has been investigated over the past decade to estimate the functional networks involved in cognitive processes, e.g., see [165, 166], but it remains unclear how to choose a sequence of stimuli to retrieve a functional network of interest most effectively.

Studies [54, 167] have recently designed stimulation-based probing rules that address this issue. Perhaps more importantly, the rules derived in these studies were obtained by solving optimization problems. The general idea adopts established principles of network theory [99] and is stated as:

- Under the assumptions that (i) $N > 0$ electrodes are placed in the brain for stimulation and recording purposes and (ii) the electrodes are nodes in the brain functional network, the functional network is uniquely defined by the edges between the nodes and their intensity, which are gathered in a $N \times (N-1)$ vector $\hat{\boldsymbol{z}}$ (adjacency vector). Adjacency vector $\hat{\boldsymbol{z}}$ is a proxy for the brain functional network, is expected to be insensitive to probing pulses and can provide unique information to identify the epileptogenic zone. Vector $\hat{\boldsymbol{z}}$, though, is unknown and must be estimated through probing. Hence, the problem can be posed as:

> **Problem:** Find a sequence of $M > 1$ nodes, with M assigned, that maximizes the estimation of vector $\hat{\boldsymbol{z}}$ when the nodes are probed sequentially, i.e., one node at the time, one pulse per node.

This problem was mathematically formulated in ref. [54]: vector $\hat{\boldsymbol{z}}$ was considered an unknown state of the functional network, and the electric stimuli were considered as inputs that are applied to estimate $\hat{\boldsymbol{z}}$. Specifically, denoted with $\boldsymbol{z}_k$ an estimation of $\hat{\boldsymbol{z}}$ obtained after applying the k-th probing pulse, it is assumed that $\boldsymbol{z}_k$ evolves according to a random walk:

$$\begin{aligned} \boldsymbol{z}_{k+1} &= \boldsymbol{z}_k + \boldsymbol{w}_k \\ \boldsymbol{y}_k &= \mathbf{C}_k(\sigma_k)\boldsymbol{z}_k + \boldsymbol{v}_k \end{aligned} \tag{17}$$

where $\boldsymbol{y}_k$ is the vector of electrographic recordings (e.g., intracranial EEG) measured at the N electrodes, $\boldsymbol{w}_k$ and $\boldsymbol{v}_k$ are Gaussian random vectors (i.e., noise), and $\mathbf{C}_k(\sigma_k)$ is the state-to-output matrix [86]. By definition, $\mathbf{C}_k(\sigma_k)$ is a diagonal matrix, whose nonzero values depend on which node is probed at stage k, i.e., nonzero elements in $\mathbf{C}_k(\sigma_k)$ are those associated with nodes that are neighbor to the probed node. The information about which node is probed at stage k, instead, is expressed by the decision variable σ_k, where σ_k is a $N \times 1$ binary vector that has all zeros and a single 1 at the position of the probed node.

Although a precise derivation can be found in [54], it is important to note here that the notation introduced in (Eq. 17) implies that a refined estimation $\boldsymbol{z}_{k|k}$ of the true adjacency vector $\hat{\boldsymbol{z}}$ can be obtained from $\boldsymbol{z}_k$ by implementing a Kalman filter, and a sequence of M probing nodes is uniquely represented by a sequence of M decision vectors $\boldsymbol{\sigma} = (\sigma_1, \sigma_2, \sigma_3, \dots, \sigma_M)$. Altogether, the model in (Eq. 17) and the mathematical notations introduced thereafter result in an optimal probing policy, which is given by the solution $\boldsymbol{\sigma}^*$ to the optimization problem:

$$\min_{\boldsymbol{\sigma}} \frac{1}{M} \sum_{k=1}^{M} E\{\|\boldsymbol{z}_k(\sigma_k) - \boldsymbol{z}_{k|k}(\sigma_k)\|_2^2\} \quad \text{subject to} \quad \|\sigma_k\| = 1. \tag{18}$$

The solution to (Eq. 18) is constrained by the model in (Eq. 17) and the equations of the Kalman filter, and the optimal sequence $\boldsymbol{\sigma}^* = (\sigma_1^*, \sigma_2^*, \sigma_3^*, \dots, \sigma_M^*)$ determines the order according to which nodes must be probed to minimize the variance of the estimation of the adjacency vector $\hat{\boldsymbol{z}}$.

The optimization problem provided in [54] is relevant because it derives a precise round robin protocol that can be applied during the epilepsy surgery. More importantly, authors determined that, under mild assumptions that are generally satisfied by electrode grids during epilepsy surgeries, the optimal stimulation protocol identifies the functional network with at most one impulse per electrode, i.e., $M \leq N$, which means that the optimal stimulation protocol can significantly reduce the duration of the epilepsy surgery [168].

5.4. Optimal Stimulation for Seizure Control

The use of electrical stimulation to control seizures in patients with drug-resistant epilepsy has been investigated for several decades, and major embodiments are represented by VNS [16], cortical stimulation [169], and DBS of the anterior nucleus of thalamus [170]. Further embodiments for pre-clinical investigations have also involved optogenetic stimulation [171].

While clinical studies have primarily focused on demonstrating the safety and effectiveness of neuromodulation in seizure control, several preclinical studies have investigated the optimization of the stimulation protocol. Since seizures are phenomena with a repetitive, patient-specific evolution [172, 173] two main problems arise in seizure control, i.e., finding the most effective stimulation parameters and detecting the onset time of a seizure to maximize the impact of stimulation.

Studies [174-176] focus on the first problem, i.e., stimulus optimization, and propose methods for an unsupervised adaptation of the stimulation to control seizures over time. The motivation for this investigation is that the electrographic activity in the brain can follow different trajectories during the evolution towards a seizure [172, 173], which means that every seizure requires a different type of stimulation, depending on the trajectory and the phase of the trajectory at which the stimulation is delivered. Also, the type of stimulation must be determined in *real time*. The key

idea in [174-176] is that the evolution of the neural activity in response to pre-synaptic inputs and electrical stimulation can be subsumed in a Markov process [177], whose parameters can be estimated offline. A seizure is a state within the Markov process, and the goal of the stimulation is to prevent the brain from reaching the seizure state. This idea is paired with reinforcement learning in refs. [174, 175] to solve the trade-off between the probability of having a seizure and the energy of a pulse train, while it is paired with adaptive control in [176], see **Figure 16**.

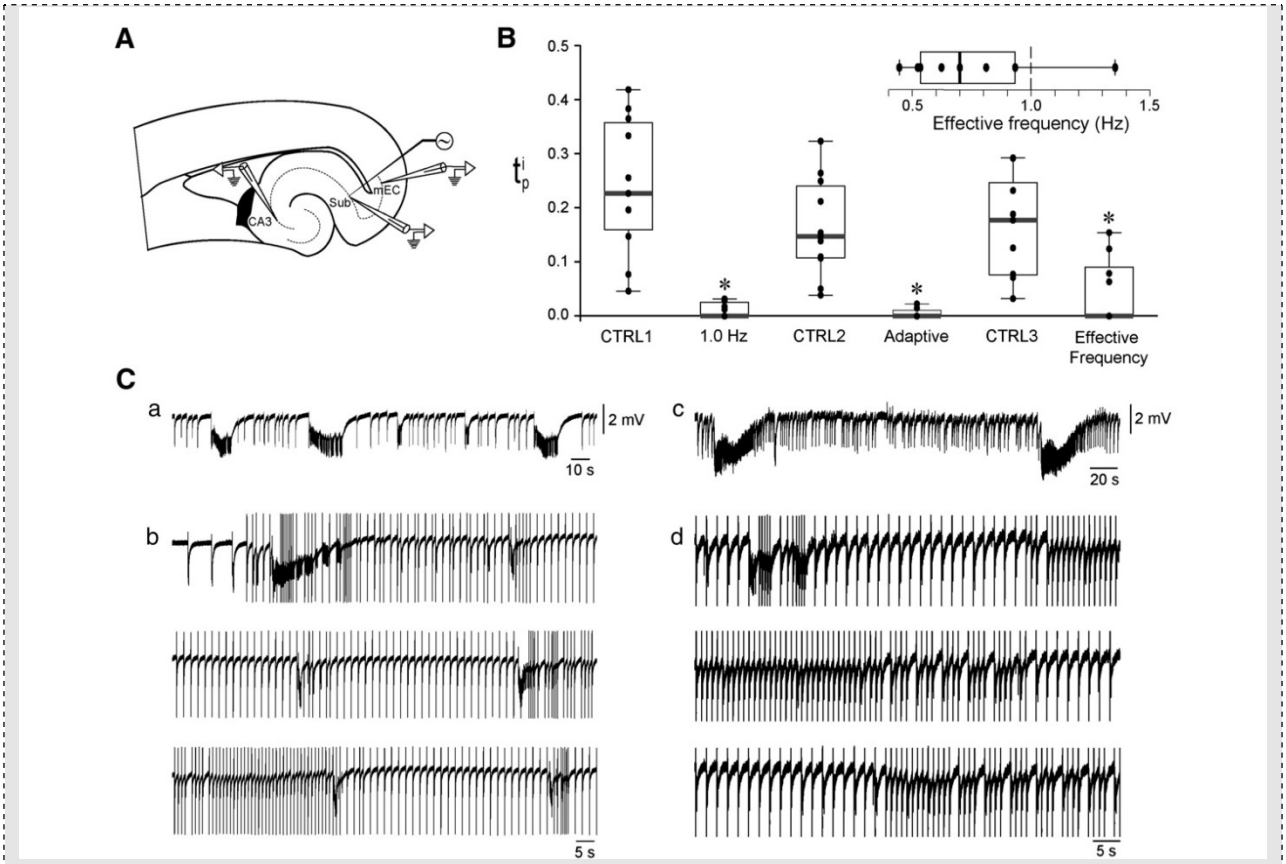

Figure 16. ***Adaptive stimulation for seizure control*.** Example of seizure control *in vitro* via adaptive stimulation from (Panuccio *et al*., 2013). **A)** Schematic of the brain slice and experimental preparation. **B)** Boxplots summarizing the performance of three stimulation protocols in terms of suppression of seizures as compared to their respective pre-stimulation control phases. Protocols are: 1-Hz periodic stimulation (*1.0 Hz*), adaptive stimulation (*Adaptive*), and periodic stimulation at the average frequency of the adaptive stimulation (*Effective Frequency*). *Inset*: Range of frequencies spanned by the *Adaptive* protocol. Each protocol decreased the seizure time (t_p^i) significantly (Asterisks: rank-sum test, *P*-value, $P < 0.05$), but the adaptive stimulation has the lowest variance and uses the least among of stimulation overall, as indicated by graph in the *Inset*. **C)** Recordings from the entorhinal cortex in two brain slices under adaptive stimulation. Panels a) and Panels c) report the control phases of the experiments in Panels b) and Panels d), respectively. *Image reproduced with permission from* [176], © *2013 Elsevier.*

An *in vitro* preparation (Fig. 16A) obtained from a rodent model of epilepsy was used, and the control algorithm in [176] was implemented at fixed intervals (stages), i.e., the calculation conducted at each stage aimed to determine the rate of the pulsatile stimulus that would be applied at the next stage. As reported in Fig. 16B, the optimal, adaptive solution outperformed periodic, non-optimal stimulation protocols and resulted in volleys of electric pulses (see example of volleys in Fig. 16C). These volleys were irregularly spaced, had different lengths, and included sequences of pulses with different time-varying rates (Fig. 16C, panel b and panel d), which ultimately disrupted the pattern observed during seizures (Fig. 16C, panel a and panel c).

Interestingly, these optimal sequences demonstrated high efficacy in seizure control and robustness against external perturbations despite the irregularity of the pulses, i.e., see the boxplots in

Fig. 16B. Furthermore, these optimal sequences delivered, on average, less stimulation to the tissue than existing, open-loop protocols, as indicated by the range of pulse rates that was used (*inset* in Fig. 16B), which was below the value used in regular open-loop protocols.

Studies [178-180], instead, focused on the second problem, i.e., seizure onset detection, and used Dynamic Programming. Specifically, the detection of the seizure onset time is formulated as a sequential decision problem, where the cost of each decision is a trade-off between the probability of future seizures, which grows as time passes, and the penalty for a false detection, which would result in an untimely stimulation of the brain. Interestingly, the optimal solution to this detection problem corresponds to the transition of the brain network to an unstable manifold, where the neuronal activity can avalanche towards seizure in response to small insults [181]. Moreover, it is shown that small, highly localized stimuli delivered to the brain at the time of this detection can divert the brain network from instability and therefore result in a suppression of the seizure, e.g., see [182-185].

6. DISCUSSION

Although well formalized in Operative Research, Computer Science, and Control Theory, the mathematical concept of "optimality" is still novel to the neuromodulation community and rapidly gaining momentum across an ample range of applications. The interest in pursuing "optimal" solutions is twofold.

First, an optimal solution satisfies a problem of interest while balancing additional, nontrivial, and often conflicting considerations, such as performance constraints, time limits, and energy savings. This is extremely appealing to the neuromodulation community because neurostimulation solutions via implantable devices are invasive, hard to titrate, and prone to side effects [4]. These aspects of neurostimulation therapies pose remarkable challenges that rarely reconcile each other. The optimization framework allows to systematically express these challenges and derive solutions that explicitly trade off concurrent requirements. Second, the theory of optimization offers an ample and mature body of mathematical methods, numerical algorithms, and theoretical tools that allows to conveniently explore the space of possible solutions to a problem and rapidly find the optimal one. Moreover, the results obtained for optimal stimulation strategies involving implantable devices can be easily generalized to neuromodulation modalities that use transcranial stimulation and ultrasound stimulation modalities, as recently shown in refs. [186, 187].

Altogether, these advantages promote a design paradigm where neuromodulation protocols are determined offline, i.e., using pilot data, numerical simulations, and mathematical derivations, instead of following an online trial-and-error paradigm, where the neuromodulation protocols must be determined empirically on test-subjects. This may dramatically shorten the design cycle of neuromodulation protocols while increasing safety and efficiency [188]. Furthermore, the integration of computational tools into the development of neural stimulation protocols can facilitate the personalization of the protocols to the patient's actual needs, as these needs can be tracked over time, analyzed using machine learning tools, and directly encompassed in the formulation of the optimization problem, rather than being addressed acutely during the testing phase. Finally, since cost functions and constraints can be linearly added to an optimization problem, novel solutions can be rapidly calculated with modest changes to the mathematical framework and tools used to solve the optimization problems.

Overall, these considerations reflect the important fact that the technological development of devices and probes for neural stimulation has rapidly outpaced the development of methodologies (i.e., algorithms and decision rules) to fully utilize the latest devices. This is of special interest in the case of implantable neurostimulation devices for chronic applications such as DBS and VNS, as the rapid multiplication of electrode contacts and stimulation modalities has not been paired by an equally rapid development of heuristic stimulation protocols. This is perhaps a reason for the rapid development of multi-objective optimization methods for neural stimulation and, specifically, for DBS applications, as exemplified in [35, 51, 135, 160]. This development has spanned both theoretical aspects and computational aspects, leading to a steady translation of methods from the theory to the clinical and preclinical domains.

7. FUTURE DIRECTIONS

While optimization methods are rapidly finding application in DBS and other neuromodulation therapies for chronic neurological diseases, there is an early but intensive investigation of optimal control as a novel and potentially transformative tool in the field of sensory rehabilitation, cognitive state decoding, and motor control [189, 190]. In recent applications for retina prostheses [191-193], in fact, optimal control problems have been formulated with the goal of design stimulation protocols that maximize the perception of the brightness of a phosphene and maximize the spatial resolution of the visual field. Optimization methods have also been used to design sequences of acoustic stimuli that maximally suppress tinnitus [194, 195].

Refs. [196, 197] also focus on tinnitus suppression and are of special interest here because they formulate the problem of suppressing tinnitus as a desynchronization problem. In these studies, an optimal solution is derived and eventually implemented via a coordinated resetting (CR) stimulation protocol (see ref. [198] for a definition of CR stimulation). Specifically, the objective of desynchronizing the auditory cortex was pursued through coordinated sequences of bilateral sounds and resulted in significant improvements for patients. In a clinical study [194], in fact, more than 60 patients with hearing loss up to 50 dB and chronic tonal tinnitus were treated with optimal CR stimulation over a 10-months period. Results demonstrated that up to 50% attenuation of tinnitus loudness and symptoms was achieved in over 75% of the patients, with a significant lowering of the tinnitus frequency and a stable long-term improvement over the 10-months period.

Overall, these studies indicate that the optimization framework discussed in this chapter can be translated to numerous applications beyond chronic deep brain stimulation. Furthermore, although the array of targeted systems has been limited thus far, these studies demonstrate that an ever-growing interest is devoted to the development of optimal, nonelectrical neuromodulation tools. Finally, these studies show the extent to which optimization methods and an optimal control framework may assist with improving the performance of prostheses for the restoration of impaired sensory functions and neural rehabilitation.

CONCLUSIONS

The mathematical concept of optimality has been recently introduced in neuromodulation as a paradigm shift in the design of neurostimulation therapies. Optimal design methodologies have gained momentum across an ample range of clinical applications involving implantable neurostimulation devices, e.g., from deep brain stimulation for movement disorders to intraoperative

electrical probing of the brain during epilepsy surgery, from controlling neural oscillations in psychiatric disorders to sensory rehabilitation and brain-machine interface. Optimization-based design methodologies allow neural engineers to address the pressing need of balancing multiple nontrivial (and often conflicting) considerations when neuromodulation protocols are designed. Optimization methods and tools also help shorten the design cycle of new neuromodulation therapies while increasing safety and efficiency of the stimulation and provide a unifying framework through which the design process can be personalized to the patient's needs and clinical data, while seemingly integrating computational and data analytics resources into the prototyping and testing stages.

ACKNOWLEDGEMENTS

This work was partly supported by the CT Institute for the Brain and Cognitive Sciences IBRAiN Fellowship (to X.Z.) and the US National Science Foundation CAREER Award 1845348 (to S.S.).

REFERENCES

[1] M. C. H. Li, M. J. Cook: Deep Brain Stimulation for Drug-Resistant Epilepsy, Epilepsia **59**, 273-290 (2018)

[2] C. A. Wathen, L. A. Frizon, T. K. Maiti, K. B. Baker, A. G. Machado: Deep Brain Stimulation of the Cerebellum for Poststroke Motor Rehabilitation: From Laboratory to Clinical Trial, Neurosurg Focus **45**, E13 (2018)

[3] H. A. Roy, A. L. Green, T. Z. Aziz: State of the Art: Novel Applications for Deep Brain Stimulation, Neuromodulation **21**, 126-134 (2018)

[4] A. M. Lozano, N. Lipsman, H. Bergman, P. Brown, S. Chabardes, J. W. Chang, K. Matthews, C. C. McIntyre, T. E. Schlaepfer, M. Schulder, Y. Temel, J. Volkmann, J. K. Krauss: Deep Brain Stimulation: Current Challenges and Future Directions, Nat Rev Neurol **15**, 148-160 (2019)

[5] M. I. Hariz, P. Blomstedt, L. Zrinzo: Deep Brain Stimulation between 1947 and 1987: The Untold Story, Neurosurg Focus **29**, E1 (2010)

[6] S. Little, A. Pogosyan, S. Neal, B. Zavala, L. Zrinzo, M. Hariz, T. Foltynie, P. Limousin, K. Ashkan, J. FitzGerald, A. L. Green, T. Z. Aziz, P. Brown: Adaptive Deep Brain Stimulation in Advanced Parkinson Disease, Ann Neurol **74**, 449-457 (2013)

[7] D. T. Brocker, B. D. Swan, D. A. Turner, R. E. Gross, S. B. Tatter, M. M. Koop, H. Bronte-Stewart, W. M. Grill: Improved Efficacy of Temporally Non-Regular Deep Brain Stimulation in Parkinson's Disease, Exp Neurol **239**, 60-67 (2013)

[8] H. Cagnan, D. Pedrosa, S. Little, A. Pogosyan, B. Cheeran, T. Aziz, A. Green, J. Fitzgerald, T. Foltynie, P. Limousin, L. Zrinzo, M. Hariz, K. J. Friston, T. Denison, P. Brown: Stimulating at the Right Time: Phase-Specific Deep Brain Stimulation, Brain **140**, 132-145 (2017)

[9] D. B. McCreery, W. F. Agnew, T. G. Yuen, L. A. Bullara: Comparison of Neural Damage Induced by Electrical Stimulation with Faradaic and Capacitor Electrodes, Ann Biomed Eng **16**, 463-481 (1988)

[10] D. B. McCreery, W. F. Agnew, T. G. Yuen, L. Bullara: Charge Density and Charge Per Phase as Cofactors in Neural Injury Induced by Electrical Stimulation, IEEE Trans Biomed Eng **37**, 996-1001 (1990)

[11] S. Santaniello, J. T. Gale, S. V. Sarma: Systems Approaches to Optimizing Deep Brain Stimulation Therapies in Parkinson's Disease, Wiley Interdiscip Rev Syst Biol Med, doi:10.1002/wsbm.1421e1421 (2018)

[12] S. P. Boyd, L. Vandenberghe: *Convex Optimization*, (Cambridge University Press, Cambridge, UK ; New York 2004)

[13] C. N. Shealy, J. T. Mortimer, J. B. Reswick: Electrical Inhibition of Pain by Stimulation of the Dorsal Columns: Preliminary Clinical Report, Anesth Analg **46**, 489-491 (1967)

[14] J. T. Mortimer, C. N. Shealy, C. Wheeler: Experimental Nondestructive Electrical Stimulation of the Brain and Spinal Cord, J Neurosurg **32**, 553-559 (1970)

[15] S. Miocinovic, S. Somayajula, S. Chitnis, J. L. Vitek: History, Applications, and Mechanisms of Deep Brain Stimulation, JAMA Neurol **70**, 163-171 (2013)

[16] D. J. Englot, E. F. Chang, K. I. Auguste: Vagus Nerve Stimulation for Epilepsy: A Meta-Analysis of Efficacy and Predictors of Response, J Neurosurg **115**, 1248-1255 (2011)

[17] S. W. Siegel, F. Catanzaro, H. E. Dijkema, M. M. Elhilali, C. J. Fowler, J. B. Gajewski, M. M. Hassouna, R. A. Janknegt, U. Jonas, P. E. van Kerrebroeck, A. A. Lycklama a Nijeholt, K. A. Oleson, R. A. Schmidt: Long-Term Results of a Multicenter Study on Sacral Nerve Stimulation for Treatment of Urinary Urge Incontinence, Urgency-Frequency, and Retention, Urology **56**, 87-91 (2000)

[18] P. E. van Kerrebroeck, A. C. van Voskuilen, J. P. Heesakkers, A. A. Lycklama a Nijholt, S. Siegel, U. Jonas, C. J. Fowler, M. Fall, J. B. Gajewski, M. M. Hassouna, F. Cappellano, M. M. Elhilali, D. F. Milam, A. K. Das, H. E. Dijkema, U. van den Hombergh: Results of Sacral Neuromodulation Therapy for Urinary Voiding Dysfunction: Outcomes of a Prospective, Worldwide Clinical Study, J Urol **178**, 2029-2034 (2007)

[19] D. Kumsa, G. K. Steinke, G. F. Molnar, E. M. Hudak, F. W. Montague, S. C. Kelley, D. F. Untereker, A. Shi, B. P. Hahn, C. Condit, H. Lee, D. Bardot, J. A. Centeno, V. Krauthamer, P. A. Takmakov: Public Regulatory Databases as a Source of Insight for Neuromodulation Devices Stimulation Parameters, Neuromodulation **21**, 117-125 (2018)

[20] S. F. Cogan, K. A. Ludwig, C. G. Welle, P. Takmakov: Tissue Damage Thresholds During Therapeutic Electrical Stimulation, J Neural Eng **13**, 021001 (2016)

[21] J. B. Ranck: Which Elements Are Excited in Electrical Stimulation of Mammalian Central Nervous System: A Review, Brain Res **98**, 417 417-440 (1975)

[22] L. Garcia, J. Audin, G. D'Alessandro, B. Bioulac, C. Hammond: Dual Effect of High-Frequency Stimulation on Subthalamic Neuron Activity, J Neurosci **23**, 8743-8751 (2003)

[23] A. L. Jensen, D. M. Durand: High Frequency Stimulation Can Block Axonal Conduction, Exp Neurol **220**, 57-70 (2009)

[24] I. Bar-Gad, S. Elias, E. Vaadia, H. Bergman: Complex Locking Rather Than Complete Cessation of Neuronal Activity in the Globus Pallidus of a 1-Methyl-4-Phenyl-1,2,3,6-Tetrahydropyridine-Treated Primate in Response to Pallidal Microstimulation, J Neurosci **24**, 7410-7419 (2004)

[25] S. Chiken, A. Nambu: High-Frequency Pallidal Stimulation Disrupts Information Flow through the Pallidum by Gabaergic Inhibition, J Neurosci **33**, 2268-2280 (2013)

[26] P. C. Klink, B. Dagnino, M. A. Gariel-Mathis, P. R. Roelfsema: Distinct Feedforward and Feedback Effects of Microstimulation in Visual Cortex Reveal Neural Mechanisms of Texture Segregation, Neuron **95**, 209-220 e203 (2017)

[27] T. Koeglsperger, C. Palleis, F. Hell, J. H. Mehrkens, K. Botzel: Deep Brain Stimulation Programming for Movement Disorders: Current Concepts and Evidence-Based Strategies, Front Neurol **10**, 410 (2019)

[28] J. Volkmann, J. Herzog, F. Kopper, G. Deuschl: Introduction to the Programming of Deep Brain Stimulators, Mov Disord **17 Suppl 3**, S181-187 (2002)

[29] D. De Ridder, S. Vanneste, M. Plazier, E. van der Loo, T. Menovsky: Burst Spinal Cord Stimulation: Toward Paresthesia-Free Pain Suppression, Neurosurgery **66**, 986-990 (2010)

[30] E. Moro, R. J. Esselink, J. Xie, M. Hommel, A. L. Benabid, P. Pollak: The Impact on Parkinson's Disease of Electrical Parameter Settings in Stn Stimulation, Neurology **59**, 706-713 (2002)

[31] J. Volkmann, E. Moro, R. Pahwa: Basic Algorithms for the Programming of Deep Brain Stimulation in Parkinson's Disease, Mov Disord **21 Suppl 14**, S284-289 (2006)

[32] A. Velisar, J. Syrkin-Nikolau, Z. Blumenfeld, M. H. Trager, M. F. Afzal, V. Prabhakar, H. Bronte-Stewart: Dual Threshold Neural Closed Loop Deep Brain Stimulation in Parkinson Disease Patients, Brain Stimul **12**, 868-876 (2019)

[33] S. Little, M. Beudel, L. Zrinzo, T. Foltynie, P. Limousin, M. Hariz, S. Neal, B. Cheeran, H. Cagnan, J. Gratwicke, T. Z. Aziz, A. Pogosyan, P. Brown: Bilateral Adaptive Deep Brain Stimulation Is Effective in Parkinson's Disease, J Neurol Neurosurg Psychiatry **87**, 717-721 (2016)

[34] A. Amon, F. Alesch: Systems for Deep Brain Stimulation: Review of Technical Features, J Neural Transm (Vienna) **124**, 1083-1091 (2017)

[35] D. T. Brocker, B. D. Swan, R. Q. So, D. A. Turner, R. E. Gross, W. M. Grill: Optimized Temporal Pattern of Brain Stimulation Designed by Computational Evolution, Sci Transl Med **9**, (2017)

[36] B. D. Swan, D. T. Brocker, R. E. Gross, D. A. Turner, W. M. Grill: Effects of Ramped-Frequency Thalamic Deep Brain Stimulation on Tremor and Activity of Modeled Neurons, Clin Neurophysiol **131**, 625-634 (2020)

[37] H. Cagnan, J. S. Brittain, S. Little, T. Foltynie, P. Limousin, L. Zrinzo, M. Hariz, C. Joint, J. Fitzgerald, A. L. Green, T. Aziz, P. Brown: Phase Dependent Modulation of Tremor Amplitude in Essential Tremor through Thalamic Stimulation, Brain **136**, 3062-3075 (2013)

[38] N. C. Swann, C. de Hemptinne, M. C. Thompson, S. Miocinovic, A. M. Miller, R. Gilron, J. L. Ostrem, H. J. Chizeck, P. A. Starr: Adaptive Deep Brain Stimulation for Parkinson's Disease Using Motor Cortex Sensing, J Neural Eng **15**, 046006 (2018)

[39] A. M. Kuncel, W. M. Grill: Selection of Stimulus Parameters for Deep Brain Stimulation, Clin Neurophysiol **115**, 2431-2441 (2004)

[40] P. E. O'Suilleabhain, W. Frawley, C. Giller, R. B. Dewey, Jr.: Tremor Response to Polarity, Voltage, Pulsewidth and Frequency of Thalamic Stimulation, Neurology **60**, 786-790 (2003)

[41] T. Van Havenbergh, T. Vancamp, P. Van Looy, S. Vanneste, D. De Ridder: Spinal Cord Stimulation for the Treatment of Chronic Back Pain Patients: 500-Hz Vs. 1000-Hz Burst Stimulation, Neuromodulation **18**, 9-12; discussion 12 (2015)

[42] A. Fasano, S. Appel-Cresswell, M. Jog, M. Zurowkski, S. Duff-Canning, M. Cohn, M. Picillo, C. R. Honey, M. Panisset, R. P. Munhoz: Medical Management of Parkinson's Disease after Initiation of Deep Brain Stimulation, Can J Neurol Sci **43**, 626-634 (2016)

[43] L. Timmermann, R. Jain, L. Chen, M. Maarouf, M. T. Barbe, N. Allert, T. Brucke, I. Kaiser, S. Beirer, F. Sejio, E. Suarez, B. Lozano, C. Haegelen, M. Verin, M. Porta, D. Servello, S. Gill, A. Whone, N. Van Dyck, F. Alesch: Multiple-Source Current Steering in Subthalamic Nucleus Deep Brain Stimulation for Parkinson's Disease (the Vantage Study): A Non-Randomised, Prospective, Multicentre, Open-Label Study, Lancet Neurol **14**, 693-701 (2015)

[44] A. Willsie, A. Dorval: Fabrication and Initial Testing of the Mudbs: A Novel Deep Brain Stimulation Electrode with Thousands of Individually Controllable Contacts, Biomed Microdevices **17**, 9961 (2015)

[45] D. N. Anderson, C. Anderson, N. Lanka, R. Sharma, C. R. Butson, B. W. Baker, A. D. Dorval: The Mudbs: Multiresolution, Directional Deep Brain Stimulation for Improved Targeting of Small Diameter Fibers, Front Neurosci **13**, 1152 (2019)

[46] A. H. Marblestone, G. Wayne, K. P. Kording: Toward an Integration of Deep Learning and Neuroscience, Front Comput Neurosci **10**, 94 (2016)

[47] A. Wongsarnpigoon, W. M. Grill: Energy-Efficient Waveform Shapes for Neural Stimulation Revealed with a Genetic Algorithm, J Neural Eng **7**, 046009 (2010)

[48] J. Chang, D. Paydarfar: Switching Neuronal State: Optimal Stimuli Revealed Using a Stochastically-Seeded Gradient Algorithm, J Comput Neurosci **37**, 569-582 (2014)

[49] J. Chang, D. Paydarfar: Evolution of Extrema Features Reveals Optimal Stimuli for Biological State Transitions, Sci Rep **8**, 3403 (2018)

[50] E. Pena, S. Zhang, S. Deyo, Y. Xiao, M. D. Johnson: Particle Swarm Optimization for Programming Deep Brain Stimulation Arrays, J Neural Eng **14**, 016014 (2017)

[51] E. Pena, S. Zhang, R. Patriat, J. E. Aman, J. L. Vitek, N. Harel, M. D. Johnson: Multi-Objective Particle Swarm Optimization for Postoperative Deep Brain Stimulation Targeting of Subthalamic Nucleus Pathways, J Neural Eng **15**, 066020 (2018)

[52] A. Zlotnik, J. S. Li: Optimal Entrainment of Neural Oscillator Ensembles, J Neural Eng **9**, 046015 (2012)

[53] A. Nabi, T. Stigen, J. Moehlis, T. Netoff: Minimum Energy Control for in Vitro Neurons, J Neural Eng **10**, 036005 (2013)

[54] M. Kafashan, S. Ching: Optimal Stimulus Scheduling for Active Estimation of Evoked Brain Networks, J Neural Eng **12**, 066011 (2015)

[55] J.-S. Li, I. Dasanayake, J. Ruths: Control and Synchronization of Neuron Ensembles, IEEE Transactions on Automatic Control **58**, 1919 1919-1930 (2013)

[56] D. P. Bertsekas: *Dynamic Programming and Optimal Control*, (Athena Scientific, Belmont, MA 1995)

[57] R. Horst, P. M. Pardalos, N. V. Thoai: *Introduction to Global Optimization*, 2nd ed., Nonconvex Optimization and Its Applications, 48 (Kluwer Academic Publishers, Dordrecht ; Boston 2000)

[58] A. S. Boger, N. Bhadra, K. J. Gustafson: High Frequency Sacral Root Nerve Block Allows Bladder Voiding, Neurourol Urodyn **31**, 677-682 (2012)

[59] N. Bhadra, N. Bhadra, K. Kilgore, K. J. Gustafson: High Frequency Electrical Conduction Block of the Pudendal Nerve, J Neural Eng **3**, 180-187 (2006)

[60] Y. Guan, P. W. Wacnik, F. Yang, A. F. Carteret, C. Y. Chung, R. A. Meyer, S. N. Raja: Spinal Cord Stimulation-Induced Analgesia: Electrical Stimulation of Dorsal Column and Dorsal Roots Attenuates Dorsal Horn Neuronal Excitability in Neuropathic Rats, Anesthesiology **113**, 1392-1405 (2010)

[61] J. Gervain, M. N. Geffen: Efficient Neural Coding in Auditory and Speech Perception, Trends Neurosci **42**, 56-65 (2019)

[62] J. Green, A. Adachi, K. K. Shah, J. D. Hirokawa, P. S. Magani, G. Maimon: A Neural Circuit Architecture for Angular Integration in Drosophila, Nature **546**, 101-106 (2017)

[63] A. D. Reyes, E. W. Rubel, W. J. Spain: In Vitro Analysis of Optimal Stimuli for Phase-Locking and Time-Delayed Modulation of Firing in Avian Nucleus Laminaris Neurons, J Neurosci **16**, 993-1007 (1996)

[64] J. J. Briguglio, M. Aizenberg, V. Balasubramanian, M. N. Geffen: Cortical Neural Activity Predicts Sensory Acuity under Optogenetic Manipulation, J Neurosci **38**, 2094-2105 (2018)

[65] M. F. Bolus, A. A. Willats, C. J. Whitmire, C. J. Rozell, G. B. Stanley: Design Strategies for Dynamic Closed-Loop Optogenetic Neurocontrol in Vivo, J Neural Eng **15**, 026011 (2018)

[66] G. Doron, M. von Heimendahl, P. Schlattmann, A. R. Houweling, M. Brecht: Spiking Irregularity and Frequency Modulate the Behavioral Report of Single-Neuron Stimulation, Neuron **81**, 653-663 (2014)

[67] D. M. Brandman, S. S. Cash, L. R. Hochberg: Review: Human Intracortical Recording and Neural Decoding for Brain-Computer Interfaces, IEEE Trans Neural Syst Rehabil Eng **25**, 1687-1696 (2017)

[68] J. Feng, H. C. Tuckwell: Optimal Control of Neuronal Activity, Phys Rev Lett **91**, 018101 (2003)

[69] S. Kirischuk, R. Grantyn: Inter-Bouton Variability of Synaptic Strength Correlates with Heterogeneity of Presynaptic Ca(2+) Signals, J Neurophysiol **88**, 2172-2176 (2002)

[70] A. Neishabouri, A. A. Faisal: Axonal Noise as a Source of Synaptic Variability, PLoS Comput Biol **10**, e1003615 (2014)

[71] I. Segev, J. Rinzel, G. M. Shepherd (eds): *The Theoretical Foundation of Dendritic Function : The Collected Papers of Wilfrid Rall with Commentaries*, Computational Neuroscience Series, (The MIT Press, Cambridge, MA 2003)

[72] A. Richard, P. Orio, E. Tanre: An Integrate-and-Fire Model to Generate Spike Trains with Long-Range Dependence, J Comput Neurosci **44**, 297-312 (2018)

[73] H. C. Tuckwell: *Introduction to Theoretical Neurobiology*, Cambridge Studies in Mathematical Biology, (Cambridge University Press, Cambridge ; New York 2006)

[74] J. Moehlis, E. Shea-Brown, H. Rabitz: Optimal Inputs for Phase Models of Spiking Neurons, Journal of Computational and Nonlinear Dynamics **1**, 358 358-367 (2006)

[75] P. Danzl, A. Nabi, J. Moehlis: Charge-Balanced Spike Timing Control for Phase Models of Spiking Neurons, Discrete & Continuous Dynamical Systems - A **28**, 1413 1413-1435 (2010)

[76] A. T. Winfree: *The Geometry of Biological Time*, 2nd ed., Interdisciplinary Applied Mathematics, 12 (Springer, New York 2001)

[77] D. Wilson, A. B. Holt, T. I. Netoff, J. Moehlis: Optimal Entrainment of Heterogeneous Noisy Neurons, Front Neurosci **9**, 192 (2015)

[78] A. Nabi, J. Moehlis: Time Optimal Control of Spiking Neurons, J Math Biol **64**, 981-1004 (2012)

[79] I. S. Dasanayake, J. S. Li: Design of Charge-Balanced Time-Optimal Stimuli for Spiking Neuron Oscillators, Neural Comput **26**, 2223-2246 (2014)

[80] J. Wang, W. Costello, J. E. Rubin: Tailoring Inputs to Achieve Maximal Neuronal Firing, J Math Neurosci **1**, 3 (2011)

[81] W. Truccolo, U. T. Eden, M. R. Fellows, J. P. Donoghue, E. N. Brown: A Point Process Framework for Relating Neural Spiking Activity to Spiking History, Neural Ensemble, and Extrinsic Covariate Effects, J Neurophysiol **93**, 1074-1089 (2005)

[82] E. Brown, R. Barbieri, U. Eden, L. Frank: Likelihood Methods for Neural Spike Train Data Analysis. In: *Computational Neuroscience*, Chapman & Hall/Crc Mathematical & Computational Biology, doi:10.1201/9780203494462.ch9, ed. by J. Feng (Chapman and Hall/CRC, London, UK 2003), pp. 253-289

[83] Y. Ahmadian, A. M. Packer, R. Yuste, L. Paninski: Designing Optimal Stimuli to Control Neuronal Spike Timing, J Neurophysiol **106**, 1038-1053 (2011)

[84] S. Koyama, L. Paninski: Efficient Computation of the Maximum a Posteriori Path and Parameter Estimation in Integrate-and-Fire and More General State-Space Models, J Comput Neurosci **29**, 89-105 (2010)

[85] A. Iolov, S. Ditlevsen, A. Longtin: Stochastic Optimal Control of Single Neuron Spike Trains, J Neural Eng **11**, 046004 (2014)

[86] T. Kailath: *Linear Systems*, Prentice-Hall Information and System Science Series, (Prentice-Hall, Englewood Cliffs, N.J. 1980)

[87] I. Dasanayake, J. S. Li: Optimal Design of Minimum-Power Stimuli for Phase Models of Neuron Oscillators, Phys Rev E Stat Nonlin Soft Matter Phys **83**, 061916 (2011)

[88] I. S. Dasanayake, J.-S. Li: Constrained Charge-Balanced Minimum-Power Controls for Spiking Neuron Oscillators, Systems & Control Letters **75**, 124 124-130 (2015)

[89] K. N. O'Connor, C. I. Petkov, M. L. Sutter: Adaptive Stimulus Optimization for Auditory Cortical Neurons, J Neurophysiol **94**, 4051-4067 (2005)

[90] J. P. Newman, M. F. Fong, D. C. Millard, C. J. Whitmire, G. B. Stanley, S. M. Potter: Optogenetic Feedback Control of Neural Activity, Elife **4**, e07192 (2015)

[91] Y. Yang, A. T. Connolly, M. M. Shanechi: A Control-Theoretic System Identification Framework and a Real-Time Closed-Loop Clinical Simulation Testbed for Electrical Brain Stimulation, J Neural Eng **15**, 066007 (2018)

[92] S. Stanslaski, P. Afshar, P. Cong, J. Giftakis, P. Stypulkowski, D. Carlson, D. Linde, D. Ullestad, A. T. Avestruz, T. Denison: Design and Validation of a Fully Implantable, Chronic, Closed-Loop Neuromodulation Device with Concurrent Sensing and Stimulation, IEEE Trans Neural Syst Rehabil Eng **20**, 410-421 (2012)

[93] O. Miranda-Dominguez, J. Gonia, T. I. Netoff: Firing Rate Control of a Neuron Using a Linear Proportional-Integral Controller, J Neural Eng **7**, 066004 (2010)

[94] T. Stigen, P. Danzl, J. Moehlis, T. Netoff: Controlling Spike Timing and Synchrony in Oscillatory Neurons, J Neurophysiol **105**, 2074-2082 (2011)

[95] L. Li, I. M. Park, A. Brockmeier, B. Chen, S. Seth, J. T. Francis, J. C. Sanchez, J. C. Principe: Adaptive Inverse Control of Neural Spatiotemporal Spike Patterns with a Reproducing Kernel Hilbert Space (Rkhs) Framework, IEEE Trans Neural Syst Rehabil Eng **21**, 532-543 (2013)

[96] S. Ching, J. T. Ritt: Control Strategies for Underactuated Neural Ensembles Driven by Optogenetic Stimulation, Front Neural Circuits **7**, 54 (2013)

[97] A. Nandi, H. Schattler, J. T. Ritt, S. Ching: Fundamental Limits of Forced Asynchronous Spiking with Integrate and Fire Dynamics, J Math Neurosci **7**, 11 (2017)

[98] Y. Tang, H. Gao, W. Du, J. Lu, A. V. Vasilakos, J. Kurths: Robust Multiobjective Controllability of Complex Neuronal Networks, IEEE/ACM Trans Comput Biol Bioinform **13**, 778-791 (2016)

[99] M. E. J. Newman: *Networks : An Introduction*, (Oxford University Press, Oxford ; New York 2010)

[100] K. Zhou, J. C. Doyle, K. Glover: *Robust and Optimal Control*, (Prentice Hall, Upper Saddle River, N.J. 1996)

[101] M. E. Newman: Modularity and Community Structure in Networks, Proc Natl Acad Sci U S A **103**, 8577-8582 (2006)

[102] Y. Tang, Z. Wang, H. Gao, S. Swift, J. Kurths: A Constrained Evolutionary Computation Method for Detecting Controlling Regions of Cortical Networks, IEEE/ACM Trans Comput Biol Bioinform **9**, 1569-1581 (2012)

[103] Y. Tang, H. Gao, J. Kurths: Multiobjective Identification of Controlling Areas in Neuronal Networks, IEEE/ACM Trans Comput Biol Bioinform **10**, 708-720 (2013)

[104] J. Lu, J. Kurths, J. Cao, N. Mahdavi, C. Huang: Synchronization Control for Nonlinear Stochastic Dynamical Networks: Pinning Impulsive Strategy, IEEE Trans Neural Netw Learn Syst **23**, 285-292 (2012)

[105] W. Yu, P. DeLellis, G. Chen, M. di Bernardo, J. Kurths: Distributed Adaptive Control of Synchronization in Complex Networks, IEEE Transactions on Automatic Control **57**, 2153 2153-2158 (2012)

[106] Y. Tang, W. K. Wong: Distributed Synchronization of Coupled Neural Networks Via Randomly Occurring Control, IEEE Trans Neural Netw Learn Syst **24**, 435-447 (2013)

[107] Y. Tang, H. Gao, J. Lu, J. K. Kurths: Pinning Distributed Synchronization of Stochastic Dynamical Networks: A Mixed Optimization Approach, IEEE Trans Neural Netw Learn Syst **25**, 1804-1815 (2014)

[108] Y. Tang, H. Gao, J. Kurths: Distributed Robust Synchronization of Dynamical Networks with Stochastic Coupling, IEEE Transactions on Circuits and Systems I: Regular Papers **61**, 1508 1508-1519 (2014)

[109] Y. Tang, Z. Wang, H. Gao, H. Qiao, J. Kurths: On Controllability of Neuronal Networks with Constraints on the Average of Control Gains, IEEE Trans Cybern **44**, 2670-2681 (2014)

[110] L. Z. Wang, R. Q. Su, Z. G. Huang, X. Wang, W. X. Wang, C. Grebogi, Y. C. Lai: A Geometrical Approach to Control and Controllability of Nonlinear Dynamical Networks, Nat Commun **7**, 11323 (2016)

[111] Z. Yuan, C. Zhao, Z. Di, W. X. Wang, Y. C. Lai: Exact Controllability of Complex Networks, Nat Commun **4**, 2447 (2013)

[112] H. K. Khalil: *Nonlinear Control*, (Pearson, Boston 2015)

[113] H. Lorach, R. Benosman, O. Marre, S. H. Ieng, J. A. Sahel, S. Picaud: Artificial Retina: The Multichannel Processing of the Mammalian Retina Achieved with a Neuromorphic Asynchronous Light Acquisition Device, J Neural Eng **9**, 066004 (2012)

[114] M. Feng, H. Qu, Z. Yi, X. Xie, J. Kurths: Evolving Scale-Free Networks by Poisson Process: Modeling and Degree Distribution, IEEE Trans Cybern **46**, 1144-1155 (2016)

[115] A. Nandi, M. Kafashan, S. Ching: Control Analysis and Design for Statistical Models of Spiking Networks, IEEE Trans Control Netw Syst **5**, 1146-1156 (2018)

[116] Z. Chen, D. F. Putrino, S. Ghosh, R. Barbieri, E. N. Brown: Statistical Inference for Assessing Functional Connectivity of Neuronal Ensembles with Sparse Spiking Data, IEEE Trans Neural Syst Rehabil Eng **19**, 121-135 (2011)

[117] J. W. Pillow, J. Shlens, L. Paninski, A. Sher, A. M. Litke, E. J. Chichilnisky, E. P. Simoncelli: Spatio-Temporal Correlations and Visual Signalling in a Complete Neuronal Population, Nature **454**, 995-999 (2008)

[118] Y. Ahmadian, J. W. Pillow, L. Paninski: Efficient Markov Chain Monte Carlo Methods for Decoding Neural Spike Trains, Neural Comput **23**, 46-96 (2011)

[119] A. R. Paiva, I. Park, J. C. Principe: A Reproducing Kernel Hilbert Space Framework for Spike Train Signal Processing, Neural Comput **21**, 424-449 (2009)

[120] J. F. Marsden, P. Limousin-Dowsey, P. Ashby, P. Pollak, P. Brown: Subthalamic Nucleus, Sensorimotor Cortex and Muscle Interrelationships in Parkinson's Disease, Brain **124**, 378-388 (2001)

[121] A. Pogosyan, F. Yoshida, C. C. Chen, I. Martinez-Torres, T. Foltynie, P. Limousin, L. Zrinzo, M. I. Hariz, P. Brown: Parkinsonian Impairment Correlates with Spatially Extensive Subthalamic Oscillatory Synchronization, Neuroscience **171**, 245-257 (2010)

[122] R. B. Yaffe, P. Borger, P. Megevand, D. M. Groppe, M. A. Kramer, C. J. Chu, S. Santaniello, C. Meisel, A. D. Mehta, S. V. Sarma: Physiology of Functional and Effective Networks in Epilepsy, Clin Neurophysiol **126**, 227-236 (2015)

[123] X. Zhang, S. Santaniello: Role of Cerebellar Gabaergic Dysfunctions in the Origins of Essential Tremor, Proc Natl Acad Sci U S A **116**, 13592-13601 (2019)

[124] J. P. Lachaux, E. Rodriguez, J. Martinerie, F. J. Varela: Measuring Phase Synchrony in Brain Signals, Hum Brain Mapp **8**, 194-208 (1999)

[125] C. Zhou, J. Kurths, I. Z. Kiss, J. L. Hudson: Noise-Enhanced Phase Synchronization of Chaotic Oscillators, Phys Rev Lett **89**, 014101 (2002)

[126] A. Zlotnik, R. Nagao, I. Z. Kiss, J. S. Li: Phase-Selective Entrainment of Nonlinear Oscillator Ensembles, Nat Commun **7**, 10788 (2016)

[127] D. Wilson, J. Moehlis: Locally Optimal Extracellular Stimulation for Chaotic Desynchronization of Neural Populations, J Comput Neurosci **37**, 243-257 (2014)

[128] P. Danzl, J. Hespanha, J. Moehlis: Event-Based Minimum-Time Control of Oscillatory Neuron Models: Phase Randomization, Maximal Spike Rate Increase, and Desynchronization, Biol Cybern **101**, 387-399 (2009)

[129] A. Nabi, M. Mirzadeh, F. Gibou, J. Moehlis: Minimum Energy Desynchronizing Control for Coupled Neurons, J Comput Neurosci **34**, 259-271 (2013)

[130] D. Wilson, J. Moehlis: Optimal Chaotic Desynchronization for Neural Populations, SIAM Journal on Applied Dynamical Systems **13**, 276-305 (2014)

[131] T. D. Matchen, J. Moehlis: Phase Model-Based Neuron Stabilization into Arbitrary Clusters, J Comput Neurosci **44**, 363-378 (2018)

[132] S. Kubota, J. E. Rubin: Numerical Optimization of Coordinated Reset Stimulation for Desynchronizing Neuronal Network Dynamics, J Comput Neurosci **45**, 45-58 (2018)

[133] A. B. Holt, T. I. Netoff: Origins and Suppression of Oscillations in a Computational Model of Parkinson's Disease, J Comput Neurosci **37**, 505-521 (2014)

[134] P. A. Tass: A Model of Desynchronizing Deep Brain Stimulation with a Demand-Controlled Coordinated Reset of Neural Subpopulations, Biol Cybern **89**, 81-88 (2003)

[135] A. B. Holt, D. Wilson, M. Shinn, J. Moehlis, T. I. Netoff: Phasic Burst Stimulation: A Closed-Loop Approach to Tuning Deep Brain Stimulation Parameters for Parkinson's Disease, PLoS Comput Biol **12**, e1005011 (2016)

[136] J. T. Vogelstein, A. M. Packer, T. A. Machado, T. Sippy, B. Babadi, R. Yuste, L. Paninski: Fast Nonnegative Deconvolution for Spike Train Inference from Population Calcium Imaging, J Neurophysiol **104**, 3691-3704 (2010)

[137] A. Priori, G. Foffani, L. Rossi, S. Marceglia: Adaptive Deep Brain Stimulation (Adbs) Controlled by Local Field Potential Oscillations, Exp Neurol **245**, 77-86 (2013)

[138] C. Pollo, A. Kaelin-Lang, M. F. Oertel, L. Stieglitz, E. Taub, P. Fuhr, A. M. Lozano, A. Raabe, M. Schupbach: Directional Deep Brain Stimulation: An Intraoperative Double-Blind Pilot Study, Brain **137**, 2015-2026 (2014)

[139] J. P. Slopsema, E. Pena, R. Patriat, L. J. Lehto, O. Grohn, S. Mangia, N. Harel, S. Michaeli, M. D. Johnson: Clinical Deep Brain Stimulation Strategies for Orientation-Selective Pathway Activation, J Neural Eng **15**, 056029 (2018)

[140] B. A. Teplitzky, L. M. Zitella, Y. Xiao, M. D. Johnson: Model-Based Comparison of Deep Brain Stimulation Array Functionality with Varying Number of Radial Electrodes and Machine Learning Feature Sets, Front Comput Neurosci **10**, 58 (2016)

[141] A. Zhou, S. R. Santacruz, B. C. Johnson, G. Alexandrov, A. Moin, F. L. Burghardt, J. M. Rabaey, J. M. Carmena, R. Muller: A Wireless and Artefact-Free 128-Channel Neuromodulation Device for Closed-Loop Stimulation and Recording in Non-Human Primates, Nat Biomed Eng **3**, 15-26 (2019)

[142] J. R. Clay, D. B. Forger, D. Paydarfar: Ionic Mechanism Underlying Optimal Stimuli for Neuronal Excitation: Role of Na+ Channel Inactivation, PLoS One **7**, e45983 (2012)

[143] D. B. Forger, D. Paydarfar, J. R. Clay: Optimal Stimulus Shapes for Neuronal Excitation, PLoS Comput Biol **7**, e1002089 (2011)

[144] G. Tinkhauser, A. Pogosyan, H. Tan, D. M. Herz, A. A. Kuhn, P. Brown: Beta Burst Dynamics in Parkinson's Disease Off and on Dopaminergic Medication, Brain **140**, 2968-2981 (2017)

[145] A. A. Kuhn, F. Kempf, C. Brucke, L. Gaynor Doyle, I. Martinez-Torres, A. Pogosyan, T. Trottenberg, A. Kupsch, G. H. Schneider, M. I. Hariz, W. Vandenberghe, B. Nuttin, P. Brown: High-Frequency Stimulation of the Subthalamic Nucleus Suppresses Oscillatory Beta Activity in Patients with Parkinson's Disease in Parallel with Improvement in Motor Performance, J Neurosci **28**, 6165-6173 (2008)

[146] A. B. Holt, E. Kormann, A. Gulberti, M. Potter-Nerger, C. G. McNamara, H. Cagnan, M. K. Baaske, S. Little, J. A. Koppen, C. Buhmann, M. Westphal, C. Gerloff, A. K. Engel, P. Brown, W. Hamel, C. K. E. Moll, A. Sharott: Phase-Dependent Suppression of Beta Oscillations in Parkinson's Disease Patients, J Neurosci **39**, 1119-1134 (2019)

[147] S. Santaniello, G. Fiengo, L. Glielmo, W. M. Grill: Closed-Loop Control of Deep Brain Stimulation: A Simulation Study, IEEE Trans Neural Syst Rehabil Eng **19**, 15-24 (2011)

[148] P. Gorzelic, S. J. Schiff, A. Sinha: Model-Based Rational Feedback Controller Design for Closed-Loop Deep Brain Stimulation of Parkinson's Disease, J Neural Eng **10**, 026016 (2013)

[149] F. Su, J. Wang, B. Deng, X. L. Wei, Y. Y. Chen, C. Liu, H. Y. Li: Adaptive Control of Parkinson's State Based on a Nonlinear Computational Model with Unknown Parameters, Int J Neural Syst **25**, 1450030 (2015)

[150] H. D. Huang, S. Santaniello: Closed-Loop Low-Frequency Dbs Restores Thalamocortical Relay Fidelity in a Computational Model of the Motor Loop, Annu Int Conf IEEE Eng Med Biol Soc **2017**, 1954-1957 (2017)

[151] O. V. Popovych, B. Lysyansky, P. A. Tass: Closed-Loop Deep Brain Stimulation by Pulsatile Delayed Feedback with Increased Gap between Pulse Phases, Sci Rep **7**, 1033 (2017)

[152] F. Su, J. Wang, S. Niu, H. Li, B. Deng, C. Liu, X. Wei: Nonlinear Predictive Control for Adaptive Adjustments of Deep Brain Stimulation Parameters in Basal Ganglia-Thalamic Network, Neural Netw **98**, 283-295 (2018)

[153] F. Su, K. Kumaravelu, J. Wang, W. M. Grill: Model-Based Evaluation of Closed-Loop Deep Brain Stimulation Controller to Adapt to Dynamic Changes in Reference Signal, Front Neurosci **13**, 956 (2019)

[154] J. E. Fleming, J. Orlowski, M. M. Lowery, A. Chaillet: Self-Tuning Deep Brain Stimulation Controller for Suppression of Beta Oscillations: Analytical Derivation and Numerical Validation, Front Neurosci **14**, 639 (2020)

[155] J. E. Fleming, E. Dunn, M. M. Lowery: Simulation of Closed-Loop Deep Brain Stimulation Control Schemes for Suppression of Pathological Beta Oscillations in Parkinson's Disease, Front Neurosci **14**, 166 (2020)

[156] L. L. Grado, M. D. Johnson, T. I. Netoff: Bayesian Adaptive Dual Control of Deep Brain Stimulation in a Computational Model of Parkinson's Disease, PLoS Comput Biol **14**, e1006606 (2018)

[157] X. J. Feng, E. Shea-Brown, B. Greenwald, R. Kosut, H. Rabitz: Optimal Deep Brain Stimulation of the Subthalamic Nucleus--a Computational Study, J Comput Neurosci **23**, 265-282 (2007)

[158] I. R. Cassar, N. D. Titus, W. M. Grill: An Improved Genetic Algorithm for Designing Optimal Temporal Patterns of Neural Stimulation, J Neural Eng **14**, 066013 (2017)

[159] M. C. Rodriguez-Oroz, E. Moro, P. Krack: Long-Term Outcomes of Surgical Therapies for Parkinson's Disease, Mov Disord **27**, 1718-1728 (2012)

[160] Y. Xiao, E. Pena, M. D. Johnson: Theoretical Optimization of Stimulation Strategies for a Directionally Segmented Deep Brain Stimulation Electrode Array, IEEE Trans Biomed Eng **63**, 359-371 (2016)

[161] D. N. Anderson, B. Osting, J. Vorwerk, A. D. Dorval, C. R. Butson: Optimized Programming Algorithm for Cylindrical and Directional Deep Brain Stimulation Electrodes, J Neural Eng **15**, 026005 (2018)

[162] A. Valentin, G. Alarcon, M. Honavar, J. J. Garcia Seoane, R. P. Selway, C. E. Polkey, C. D. Binnie: Single Pulse Electrical Stimulation for Identification of Structural Abnormalities and Prediction of Seizure Outcome after Epilepsy Surgery: A Prospective Study, Lancet Neurol **4**, 718-726 (2005)

[163] P. M. Murphy, A. J. von Paternos, S. Santaniello: A Novel Hfo-Based Method for Unsupervised Localization of the Seizure Onset Zone in Drug-Resistant Epilepsy, Conf Proc IEEE Eng Med Biol Soc **2017**, 1054-1057 (2017)

[164] S. L. Sumsky, S. Santaniello: Decision Support System for Seizure Onset Zone Localization Based on Channel Ranking and High-Frequency Eeg Activity, IEEE J Biomed Health Inform **23**, 1535-1545 (2019)

[165] C. J. Keller, S. Bickel, L. Entz, I. Ulbert, M. P. Milham, C. Kelly, A. D. Mehta: Intrinsic Functional Architecture Predicts Electrically Evoked Responses in the Human Brain, Proc Natl Acad Sci U S A **108**, 10308-10313 (2011)

[166] R. Matsumoto, D. R. Nair, E. LaPresto, W. Bingaman, H. Shibasaki, H. O. Luders: Functional Connectivity in Human Cortical Motor System: A Cortico-Cortical Evoked Potential Study, Brain **130**, 181-197 (2007)

[167] K. Q. Lepage, S. Ching, M. A. Kramer: Inferring Evoked Brain Connectivity through Adaptive Perturbation, J Comput Neurosci **34**, 303-318 (2013)

[168] S. U. Schuele, H. O. Luders: Intractable Epilepsy: Management and Therapeutic Alternatives, Lancet Neurol **7**, 514-524 (2008)

[169] M. J. Morrell, R. N. S. S. i. E. S. Group: Responsive Cortical Stimulation for the Treatment of Medically Intractable Partial Epilepsy, Neurology **77**, 1295-1304 (2011)

[170] R. Fisher, V. Salanova, T. Witt, R. Worth, T. Henry, R. Gross, K. Oommen, I. Osorio, J. Nazzaro, D. Labar, M. Kaplitt, M. Sperling, E. Sandok, J. Neal, A. Handforth, J. Stern, A. DeSalles, S. Chung, A. Shetter, D. Bergen, R. Bakay, J. Henderson, J. French, G. Baltuch, W. Rosenfeld, A. Youkilis, W. Marks, P. Garcia, N. Barbaro, N. Fountain, C. Bazil, R. Goodman, G. McKhann, K. Babu Krishnamurthy, S. Papavassiliou, C. Epstein, J. Pollard, L. Tonder, J. Grebin, R. Coffey, N. Graves, S. S. Group: Electrical Stimulation of the Anterior Nucleus of Thalamus for Treatment of Refractory Epilepsy, Epilepsia **51**, 899-908 (2010)

[171] J. T. Paz, T. J. Davidson, E. S. Frechette, B. Delord, I. Parada, K. Peng, K. Deisseroth, J. R. Huguenard: Closed-Loop Optogenetic Control of Thalamus as a Tool for Interrupting Seizures after Cortical Injury, Nat Neurosci **16**, 64-70 (2013)

[172] S. P. Burns, S. Santaniello, R. B. Yaffe, C. C. Jouny, N. E. Crone, G. K. Bergey, W. S. Anderson, S. V. Sarma: Network Dynamics of the Brain and Influence of the Epileptic Seizure Onset Zone, Proc Natl Acad Sci U S A **111**, E5321-5330 (2014)

[173] M. A. Kramer, U. T. Eden, E. D. Kolaczyk, R. Zepeda, E. N. Eskandar, S. S. Cash: Coalescence and Fragmentation of Cortical Networks During Focal Seizures, J Neurosci **30**, 10076-10085 (2010)

[174] V. Nagaraj, A. Lamperski, T. I. Netoff: Seizure Control in a Computational Model Using a Reinforcement Learning Stimulation Paradigm, Int J Neural Syst **27**, 1750012 (2017)

[175] J. Pineau, A. Guez, R. Vincent, G. Panuccio, M. Avoli: Treating Epilepsy Via Adaptive Neurostimulation: A Reinforcement Learning Approach, Int J Neural Syst **19**, 227-240 (2009)

[176] G. Panuccio, A. Guez, R. Vincent, M. Avoli, J. Pineau: Adaptive Control of Epileptiform Excitability in an in Vitro Model of Limbic Seizures, Exp Neurol **241**, 179-183 (2013)

[177] J. G. Kemeny, J. L. Snell: *Finite Markov Chains*, The University Series in Undergraduate Mathematics, (Van Nostrand, Princeton, N.J., 1960)

[178] S. Santaniello, S. P. Burns, A. J. Golby, J. M. Singer, W. S. Anderson, S. V. Sarma: Quickest Detection of Drug-Resistant Seizures: An Optimal Control Approach, Epilepsy Behav **22 Suppl 1**, S49-60 (2011)

[179] S. Santaniello, D. L. Sherman, N. V. Thakor, E. N. Eskandar, S. V. Sarma: Optimal Control-Based Bayesian Detection of Clinical and Behavioral State Transitions, IEEE Trans Neural Syst Rehabil Eng **20**, 708-719 (2012)

[180] S. Santaniello, S. P. Burns, W. S. Anderson, S. V. Sarma: An Optimal Control Approach to Seizure Detection in Drug-Resistant Epilepsy. In: *A Systems Theoretic Approach to Systems and Synthetic Biology I: Models and System Characterizations*, doi:10.1007/978-94-017-9041-3_6, ed. by V. V. Kulkarni, G.-B. Stan, K. Raman (Springer Netherlands, 2014), pp. 153-178

[181] D. Sritharan, S. V. Sarma: Fragility in Dynamic Networks: Application to Neural Networks in the Epileptic Cortex, Neural Comput **26**, 2294-2327 (2014)

[182] D. Ehrens, D. Sritharan, S. V. Sarma: Closed-Loop Control of a Fragile Network: Application to Seizure-Like Dynamics of an Epilepsy Model, Front Neurosci **9**, 58 (2015)

[183] Y. Schiller, Y. Bankirer: Cellular Mechanisms Underlying Antiepileptic Effects of Low- and High-Frequency Electrical Stimulation in Acute Epilepsy in Neocortical Brain Slices in Vitro, J Neurophysiol **97**, 1887-1902 (2007)

[184] L. B. Good, S. Sabesan, S. T. Marsh, K. Tsakalis, D. Treiman, L. Iasemidis: Control of Synchronization of Brain Dynamics Leads to Control of Epileptic Seizures in Rodents, Int J Neural Syst **19**, 173-196 (2009)

[185] B. Beverlin Ii, T. I. Netoff: Dynamic Control of Modeled Tonic-Clonic Seizure States with Closed-Loop Stimulation, Front Neural Circuits **6**, 126 (2012)

[186] A. Baltus, S. Wagner, C. H. Wolters, C. S. Herrmann: Optimized Auditory Transcranial Alternating Current Stimulation Improves Individual Auditory Temporal Resolution, Brain Stimul **11**, 118-124 (2018)

[187] R. Lorenz, L. E. Simmons, R. P. Monti, J. L. Arthur, S. Limal, I. Laakso, R. Leech, I. R. Violante: Efficiently Searching through Large Tacs Parameter Spaces Using Closed-Loop Bayesian Optimization, Brain Stimul **12**, 1484-1489 (2019)

[188] M. Picillo, A. M. Lozano, N. Kou, R. Puppi Munhoz, A. Fasano: Programming Deep Brain Stimulation for Parkinson's Disease: The Toronto Western Hospital Algorithms, Brain Stimul **9**, 425-437 (2016)

[189] X. Kang, S. V. Sarma, S. Santaniello, M. Schieber, N. V. Thakor: Task-Independent Cognitive State Transition Detection from Cortical Neurons During 3-D Reach-to-Grasp Movements, IEEE Trans Neural Syst Rehabil Eng **23**, 676-682 (2015)

[190] S. L. Sumsky, M. H. Schieber, N. V. Thakor, S. V. Sarma, S. Santaniello: Decoding Kinematics Using Task-Independent Movement-Phase-Specific Encoding Models, IEEE Trans Neural Syst Rehabil Eng **25**, 2122-2132 (2017)

[191] C. O. Savage, D. B. Grayden, H. Meffin, A. N. Burkitt: Optimized Single Pulse Stimulation Strategy for Retinal Implants, J Neural Eng **10**, 016003 (2013)

[192] J. I. Lee, M. Im: Optimal Electric Stimulus Amplitude Improves the Selectivity between Responses of on Versus Off Types of Retinal Ganglion Cells, IEEE Trans Neural Syst Rehabil Eng **27**, 2015-2024 (2019)

[193] T. Flores, G. Goetz, X. Lei, D. Palanker: Optimization of Return Electrodes in Neurostimulating Arrays, J Neural Eng **13**, 036010 (2016)

[194] P. A. Tass, I. Adamchic, H. J. Freund, T. von Stackelberg, C. Hauptmann: Counteracting Tinnitus by Acoustic Coordinated Reset Neuromodulation, Restor Neurol Neurosci **30**, 137-159 (2012)

[195] R. A. Arts, E. L. George, M. N. Chenault, R. J. Stokroos: Optimizing Intracochlear Electrical Stimulation to Suppress Tinnitus, Ear Hear **36**, 125-135 (2015)

[196] P. A. Tass, O. V. Popovych: Unlearning Tinnitus-Related Cerebral Synchrony with Acoustic Coordinated Reset Stimulation: Theoretical Concept and Modelling, Biol Cybern **106**, 27-36 (2012)

[197] L. Lucken, S. Yanchuk, O. V. Popovych, P. A. Tass: Desynchronization Boost by Non-Uniform Coordinated Reset Stimulation in Ensembles of Pulse-Coupled Neurons, Front Comput Neurosci **7**, 63 (2013)

[198] I. Adamchic, C. Hauptmann, U. B. Barnikol, N. Pawelczyk, O. Popovych, T. T. Barnikol, A. Silchenko, J. Volkmann, G. Deuschl, W. G. Meissner, M. Maarouf, V. Sturm, H. J. Freund, P. A. Tass: Coordinated Reset Neuromodulation for Parkinson's Disease: Proof-of-Concept Study, Mov Disord **29**, 1679-1684 (2014)

INDEX